POTABLE WATER PRODUCTION FROM ATMOSPHERIC VAPOUR USING AN EJECTOR EVACUATED SOLAR POWERED REFRIGERATION SYSTEM

by

JOHN HENRY CAWOOD

Student number: 213282909

Submitted in fulfilment of the requirements for the degree of

MAGISTER TECHNOLOGIAE: ENGINEERING: MECHANICAL

in the

FACULTY OF ENGINEERING

at the

NELSON MANDELA UNIVERSITY

Supervisor: Prof. Russell Phillips

2018

DECLARATION

I, JOHN HENRY CAWOOD, Student Number 213282909 , hereby declare that the dissertation for a Masters in Mechanical Engineering is my own work and that it has not previously been submitted for assessment to another University or for another qualification.

I declare that this dissertation is my own, unaided work. This dissertation is submitted for the degree of Master of Technology: Engineering: Mechanical at the Nelson Mandela University. It has not been submitted before for any degree or examination at any other tertiary institution.

The copy of this dissertation has been supplied on condition that it is understood that the copyright rests with the author and that no information from it may be published without the consent of the author.

John Henry Cawood

…13/03/2018…….

Date:

DEDICATION

I wish to thank the following for their support during the execution of this project:

- Mr. Dennis da Silva of Middle East Engineering and Marine Services for his patient assistance to of manufacture strange and tiny components.
- Mr. Monaem Hijazi of Bucheery Contracting for his excellent fabrication of stainless steel components and timeous completion of work.
- My wife for her contribution of personal time and endless patience, also for her minimal opposition to the installation of a machine shop in the home study.
- To my supervisor Prof. Russell Phillips for his patience and support over the years to bring this project to completion. The progress was halted for some time between 2015 and 2016 due to more pressing issues but was happily restarted in June 2016 and to date.

SUMMARY /ABSTRACT

This research project explores the possibility of using solar radiation energy to produce safe liquid water through the condensation of atmospheric water vapour for human consumption, livestock watering and also for small scale high value crop irrigation.

The research activities are comprised of a literature study, comparison of similar devices in use, a design and prototyping exercise, a measure of development work to enhance the performance of the prototype and testing in Al-Batinah province in the Sultanate of Oman, where the author is currently on a work assignment.

This dissertation describes the research activities performed to answer the following question:

'Is it possible to economically produce sufficient quantities of liquid

water from atmospheric vapour using only heat energy from the sun?'

This question poses a further two questions which need to be answered in the literature study. These are: 'What is an economical price for clean drinking water?' and 'What is a sufficient quantity of water?'

The purpose of producing liquid water from atmospheric water vapour is an attempt to develop the technology to harvest an alternative and almost inexhaustible water source. The reason for requiring a new source of water is due to the fact that the available fresh water resources of the world are diminishing due to pollution, extensive utilisation and salination. Several references indicate that the problem is compounding itself due the increasing demand on a diminishing resource, with deepening negative effects on agriculture[1], health[2], economy[3], industry and lifestyle[4]. Many future scenarios depict clean water as a scarce and expensive commodity, unaffordable to many.

The condensation of atmospheric vapour is not a new concept. The literature study explores historical attempts to achieve this, as well as detailing the shortcomings of contemporary vapour condensation units as the modern state of the art. This survey covers the spectrum from large versions deployed by military and remote area

construction operations to produce water for all purposes, to small desktop electrical water producing machines.

The focus of the research is on a more environmentally conscious process, attempting to use a simple ejector driven device with sunshine as the energy source and water as the refrigerant. A further environmental enhancement of the concept is that of designing the machine to last for an extremely long working life, thereby diluting the carbon footprint of manufacture over a great number of years.

A portion of the research is devoted to the development of a basic model which takes into account the climatic and meteorological variables to accurately predict a water harvest. The development of the model is then used to optimise the process, narrow the variability of assumptions and assist with the design. The model also serves to predict the performance of the unit in other locations under different prevailing climatic conditions.

A design specification and a prototype are produced and tested. Finally the design is scrutinised using value engineering principles to reduce cost, effort and environmental impact and also to reduce the overall cost to provide a more economically viable appliance.

The prototype device used in this study will use a collector area of 1 square meter, roughly equivalent to 1000 Watts of solar power under ideal conditions.

Keywords: solar powered refrigeration, water from air, ejector performance, water as refrigerant.

TABLE OF CONTENTS

Page

CHAPTER 3

LITERATURE STUDY

CHAPTER 4

CONCEPTUAL PROCESS

CHAPTER 5

MODELLING

CHAPTER 6

NOTES FROM THE PROTOTYPE DESIGN, MANUFACTURE AND DEVELOPMENT

CHAPTER 7

FINAL COMPONENT TESTING AND ASSEMBLY

CHAPTER 8

PRODUCTION TESTING

LIST OF FIGURES

Page

LIST OF ATTACHMENTS

Page

NOMENCLATURE

Condenser

A heat exchanging device designed to remove heat from a vapour to cause condensation of that vapour to a liquid state.

Choked Flow

The state of flow achieved when the gas mass flow and velocity through a restriction remains unchanged despite a reduction in the downstream pressure.

Convergent – Divergent Nozzle

A device whose cross sectional area reduces and again increases in relation to the distance from the inlet, in order to promote fluid speeds in excess of the speed of sound in that medium.

Ejector

A device which uses a nozzle to accelerate a fluid in order to produce a low pressure area beyond the nozzle outlet, usually with the intention of entraining another fluid. Ejectors may have convergent and divergent nozzles as well as chokes or diffusers to regain pressure energy from kinetic energy.

Evaporator

A heat exchanging device designed to change the state of a liquid to the vapour phase, by means of heat addition or pressure reduction, or a combination of both heat addition and pressure variation.

Mach Number

A ratio which reflects the ratio of an actual fluid velocity to the speed of sound in that fluid under identical conditions (Pressure, Temperature and Density).

Motive Evaporator

The evaporation device used to provide pressurised vapour for the purpose of doing work elsewhere in the system and which is operated by the addition of heat.

Refrigerant

A fluid which absorbs or rejects latent heat of evaporation from its surroundings for the purpose of changing its phase i.e. to evaporate or condense.

Refrigeration Evaporator

The evaporation device used to draw heat from the surroundings as a result of pressure induced evaporation of a refrigerant fluid.

Supersonic Flow

A fluid flow whose velocity exceeds the speed of sound in that fluid i.e. Mach numbers of unity and greater, beyond the trans-sonic boundary.

CHAPTER 1

INTRODUCTION

1.1 THE CONCEPT

Evident from the literature study during this project, is the fact that the production of liquid water from atmospheric water vapour using cooling derived from vapour compression refrigeration is an established and commercially active technology. Some commercially available equipment is shown in Attachment 1. The main drawback of this technology is the relatively high energy consumption per kilogram of water produced and the reliance of these devices on electrical or fossil fuelled prime movers. In most instances the electrically powered option would be dependent on a fossil fuelled power plant, which in turn attaches a pollutant and carbon cost to every drop of water produced. A further drawback of this technology is the use of a variety of refrigerant gases which are, at best, less damaging to the environment than the original Freon® products.

The obvious solution to the energy conundrum would be to use renewable energy; yet the conversion of any energy source into another form comes at the cost of efficiency losses and waste.

Cooling systems that use solar heat and ejector devices are well researched, but despite the 'free' raw energy supply, the conversion of solar energy to another form requires equipment which carries a capital cost and maintenance cost. The manufacture of the equipment and the materials from which it is made, also require industrial processes and conventional energy which contribute to the carbon burden on the environment. Hence the seemingly ideal solution may eventually not be feasible due to the physical scale of the equipment and the accompanying capital costs.

This project explores the possibility of adapting previous work on solar-ejector cooling systems, with integrated motive and refrigerant circuits, as the cooling mechanism to condense atmospheric water vapour. This concept is notably absent in the definitive summary of ejector driven systems by El-Dessouky et al[5], which indicates that the

combination of the method and purpose stated above may well be novel and hence carries several new challenges in producing a working cooling system with integrated power and water condensation systems. The chosen refrigerant compound is R718 or pure water. The notion of water as a refrigerant becomes quite practical if the application is appreciably above freezing point, but has its own challenges insofar the extremely low pressure requirements as well as the inordinately high specific volume of vapour for saturation, at or below air dew point temperatures.

The ideal refrigeration application would be capable of functioning satisfactorily at low energy levels, have few moving or wearing parts, a long working life, be simple to manufacture and be commercially and environmentally acceptable.

The inefficiency of the conversion of heat to mechanical energy is theoretically offset by the refrigeration Co-efficient of Performance, so that in an ideal system, the value of heat absorbed in the refrigeration cycle would match the quantity of heat absorbed by the solar collector i.e. unity.

It is anticipated that, should the physical and economic performance of the concept prove satisfactory, the device will find uses in any area where surface water or ground water is scarce, polluted or non-existent, provided that the resources of solar energy and ambient humidity are available. The applications of a successful device are numerous, for example drinking water for developing nations, refugee camps, remote settlements, desert wells, animal watering and irrigation. On a larger and much more ambitious scale, the device may be used to convert arid lands to agricultural land and even halt or reverse the growth of deserts by creating strategically placed oasis-type green spaces across the path of an advancing desert.

1.2 PROBLEM STATEMENT

Fresh water resources constitute only around 2,5% of the world's water, of which 68,7% is held in the polar ice caps. [1] These fresh water resources worldwide are under pressure from pollution and overutilization, as industry and agriculture encroach on the natural water sources. Natural water resources are also under threat from past and present pollution. A further effect is the salination of the polar water stocks as global warming diminishes the pure frozen resources.

Furthermore, already some 18% of the population of the world does not have access to clean drinking water.[2] The various institutions monitoring climate change, concur that the single greatest resource under threat at this time is clean drinking water.

It is estimated that by 2025 two-thirds of the world's population will be facing severe drinking water stress. [3]

Already, during year 2005 the contaminated water disease diarrhoea was the cause of 17% of all child deaths under 5 years, worldwide. [4]

The problem is aggravated by population growth as increasing population densities are required to share the diminishing fresh water resources.

CHAPTER 2

METHODOLOGY

2.1 PLANNED STAGES OF THE RESEARCH

To successfully answer the hypothesis, a methodology along the following lines is pursued:

2.1.1 Conduct Literature Survey

A thorough literature study is undertaken to determine the current state of the art in the fields of ejector–induced refrigeration and commercially available water-from-air devices, with particular focus on costs, productivity and energy consumption.

2.1.2 Develop the Process and Process Model

A process design exercise is conducted to establish a Process Circuit, showing each step of the process, what equipment is required to perform that step and what the expected outcome of each step is. The output of this exercise is a Process Diagram (PD).

From the PD a basic mathematical model is written to define the process at each step and to produce the predicted outcomes roughly in line with the expectations on the PD. The PD is refined to show equipment, appliances and instrumentation as well as to define the piping and attachments. The second design document is produced with all of the above incorporated into one drawing which is the Piping and Instrumentation Drawing (P&ID).

The model shares the dependencies and results that govern the PD. It also incorporates some aspects of the P&ID to simulate changes more closely i.e. pressure drops in long tube lengths. The model is used initially to simulate the basic process. The optimised process yields the required dimensions such as the areas and heat exchange properties to produce a working prototype design.

The model will provide the means to produce a prediction of the water gathering performance of the specified process under the input conditions of air temperature, relative humidity and solar radiation intensity. Later the refined model may be used to predict performance of the device for use at a different geographical location.

2.1.3 Mechanical Design

The above numerical exercises provide the basis for a mechanical design. From estimated process values, the individual components are designed and drawn up. Standardised items such as gears are selected from the catalogue and ordered. Tubing and valves and any special parts are ordered for delivery to coincide with the assembly dates. The prototype is intended to represent a 'cross-sectional' scale model of the final device, i.e. the prototype can be treated as a module. To extend the capacity, more modules are placed in parallel. The final size of the module may change as a result of the conclusions of commercial analysis and physical test results. The desired attributes or performance objectives for each component is produced from the model. A detailed mechanical and thermal design is done to describe the attributes of each component and the manufacture of the satisfactory designs is approved by the author. The components are tested individually to confirm design accuracy after which the prototype is assembled and preliminary testing is started.

2.1.4 Testing and Instrumentation Requirements

A basic performance test plan is derived from the Model, which indicates the nature (pressure, temperature etc.), the magnitude and the number of instruments required for later testing. These are ordered to coincide with the assembly phase.

For the prototype testing, extensive instrumentation is used to cover all aspects of the design and to allow sufficient data to be available for comparison with the model.

2.1.5 Manufacture of System Components

Once the design is completed, the individual components are manufactured and checked for suitability. Basic pressure testing is done for leaks in heat exchangers and air tests are done on the ejector circuit to simulate vapour flow. There then follows a set of performance tests to establish the specific qualities of each component.

2.1.6 Assembly and Preparation

The device is assembled at the test site, aligned and secured. Access to the site is restricted to the author and assistant. The refrigerant is introduced and the complete machine pressure is tested. The device is exposed to sunlight and any operational problems resolved. A vacuum retention test is performed to ensure that no air ingress. The test instrumentation is attached and the device is ready for operation.

2.1.7 Production Testing and Verification

The test procedure is drawn up. Test instruments are calibrated and verified. Background values such as humidity and temperatures are compared against data from the nearby weather station. Test data is recorded and variations on the design are tested and quantified. Any further controls or verifications that are required are implemented to achieve a set of field results.

Extensive testing over several months is performed to produce many sets of relevant data. The data is cross referenced with the local weather station to confirm the consistency of results and the consistent performance of the prototype.

2.1.8 Data Processing and Analysis

The data that has been acquired is converted to engineering units and stored. The results are compared to the model outputs. The variations are quantified and the reasons for variations are resolved. The model is updated to replace any assumptions or estimated values with factual values that have been experimentally obtained and ratified.

2.1.9 Evaluation of Changes

This step is a development exercise. Having established a baseline performance and parallel predictive model performance, the model is then used to predict the effects of various enhancements of the basic prototype. Where possible, the actual change is effected and the results are measured against the baseline performance to monitor improvement or otherwise.

Changes to the device are conceived based on perceived performance shortfalls or to boost performance or efficiency. Should a change produce negative results, it will be reversed.

2.1.10 Finalise Specification

A detailed costing exercise is undertaken along with a value engineering exercise, under the assumptions of specific production volumes and the predicted life of the device. Based on the above results, the Hypothesis is answered. A final specification is drawn up according to good engineering practises.

2.1.11 Compile Dissertation

A draft dissertation is started early in the process and it is updated at the conclusion of each phase of the work. The draft is also presented to the supervisor for comment and guidance.

The prototype design is evaluated from local fabrication experience and costs to determine its feasibility as an economical, low technology solution for the production of safe water for use in the developing world.

The final dissertation and associated documentation is submitted for scrutiny and evaluation to the Faculty.

CHAPTER 3

LITERATURE STUDY

3.1 HISTORICAL ATTEMPTS AT HARVESTING ATMOSPHERIC VAPOUR

The concept of producing water from atmospheric vapour is not a new idea; throughout history many references are made to the production of water from air wells and other devices which were said to produce water. One example is the pyres of stones discovered in 1900 near present day Feodosia, Ukraine. The discovery of these pyres coincides with the discovery of the remains of clay pipes and which led their discoverer, an engineer named Zibold, to believe that the constructions were built as air wells to provide water to the ancient city of Theodosiya, around the sixth century BC. To prove his theory, he constructed a replica air well that did produce water, although no record of the production quantities exists.[6]

Several other scientists and engineers created experimental constructions during the early 19th Century, some of which still stand. Unfortunately none were known to be successful and the production figures are sketchy or non-existent. One must consider that, had these structures performed as intended then they would not have faded quietly into history as they indeed have.

Every one of these devices relied on a large mass which would give up heat during the cool nights and then act as a sink to absorb the latent heat from airborne moisture and cause condensation during the day. The concept at first appears to be good but there are several shortcomings, for example in the massive design found at Trans-en-Provence, France.[7]

- The temperature required to condense vapour from the air needs to be at or below dew point for the air condition at the time. Since the cooling effort is supplied from the night air, the device is required to also produce dewfall during the daytime. A large mass of rock cooled overnight would generate at least a little condensation until it warms to the daytime dew point temperature. For this

process to be continuous, it requires consistently cold dry nights and warm humid days. Water will only be produced under these weather conditions.

- The amount of heat that can be sunk is finite. Similar to the Trans-en-Provence centre column, consider a large limestone pillar of 8 metres diameter and 10 metres tall, volume 500 cubic metres and mass around 1250 metric tons. Should the pillar be cooled through to 10 degrees below dew point during a cold night, a sink exists with the potential to absorb 1125 MJ of heat energy. By sinking all of the available heat potential, the latent heat absorbed from airborne vapour would allow only around 490 kg of water to condense per daily cycle.

- The above mass of water produced would be further limited by the fact that the heat sink is warming proportionally as it absorbs heat i.e. it is not cooled through. The effects of convective heat exchange on the surface would create a temperature profile across the pillar whereby the core remains cool and the contact surface is at a temperature approaching the air temperature, reaching and surpassing dew point temperature and reducing the surface-to-air convective heat transfer to a value which matches the diminishing differential temperature. Even assuming a day and night temperature differential of 10 degrees Celsius, the column would experience the same heat exchange challenges during cooling as for heating.

If we are to improve on the historical approach, it is clear that some form of applied cooling is required to maintain a predictable and controllable temperature profile across the heat exchange surfaces.

3.2 CONTEMPORARY COMMERCIAL VARIANTS

Attachment 1 contains sample brochures of commercial products available and a tabulated comparison of cost, power consumption and yield. This table provides the backdrop for the expected performance of an alternative water condenser.

3.2.1 Vapour Compression Refrigeration Devices

The production of air sourced water for home and office use, has met with some popularity in the USA. The array of commercially available machines range from

desktop models to produce clean drinking water for the office or apartment, including refrigerator sized models for larger domestic requirements and up to large diesel driven machines housed in packaging containers or models that are permanently mounted on large truck chassis that are utilised for water supply at remote military sites and also for civil emergency services.

These models all share some common design and operational attributes.

- All are driven by a prime mover which is energised by either the electrical grid or carbon fuelled internal combustion engines.
- All use commercial fluorocarbon refrigerants.
- All use a vapour compression refrigeration cycle to achieve their cooling effect.

Performance evaluation of these commercial offerings is difficult to compare, due to differing (usually undisclosed) climatic conditions at the time of testing and also due to performance claims without proof. Power consumption and water production are often expressed in monetary terms, which serve advertising ends but do not provide much scientific data. A table of comparisons of the smaller scale equipment on offer is included in Attachment 1.

An example of one of these offerings is the Air Juicer 4010 ® from Watair, USA, which is a domestic appliance retailing for $999-00 (USD, 2015). This manufacturer produces electrically powered equipment with outputs ranging between 24 and 7500 litres per day.

The electrical power usage is specified for both water production and also the total power absorbed which includes other services such as cooling and pumping. The power absorbed by this machine for water condensation duties alone is stated as 495 Watts. The total power usage is stated at 2400 Watt-hour per US Gallon or 635 Watt-hour per kilogram of condensed water. Given that the latent heat of evaporation of water is 2437kJ/kg at sea level and ambient temperature is within the 26.7°C range as stated by Watair, the above relationship implies a 24 hour production capacity of 0.78 kg of water per hour, (18.72 kg/day) absorbed latent heat of 528 W and a COP of 1.067:: 1.

If this machine is used as a benchmark, the target production for an alternative machine should average at least 0.78 kg/hour or 18.72 kg/day. The use of solar power allows an effective 6 to 8 hours of production daily, dependent on geographical location, so that the dimensional scale of the machine would be a factor of between 3 and 4 times greater in order to meet the daily production rate of 18.72 kg/day within a solar day. This type of machine uses grid power, so that every kilogram of water comes with a hidden environmental impact in carbon.

A final note concerning domestic and office machines is the fact that their effectiveness is directly proportional to Relative Humidity. Many of these machines are designed to work inside homes and offices where the climate control and air conditioning systems reduce ambient humidity to a fraction of the natural outdoor value.

3.2.2 Absorption Mechanisms using Desiccants

A system advertised simply as A2WH (see listing in Attachment 1) claimed that its desiccant system, using solar power for air circulation and some heating, can produce water volumes between 4 litres and 76 cubic metres per day dependent on the size of the appliance that has been selected. The company claims a water production cost of between (ZAR) R0.78/kg-day to R0.02/kg-day, dependent on the size of the machine. Later claims are that of a drastically reduced capital cost, simplified mechanism and an estimated production of 0.67 US Gallon (2.5 kg) per day, per square metre of solar collector area. With this relationship it is apparent that the 76 m^3/day model must then cover a solar energy footprint of around 3 hectares at an insolation rate of 1000 W/m^2.

The environmental requirements specify a 20°C night time temperature and a 60% RH for at least two hours at night to realise the advertised production rates. There is also a rider that states that production volumes may vary according to prevailing conditions. A product review by the website Environmental Expert [www.environmental-expert.com/products/original-a2wh-product-436123] states that the working mechanism is water absorption at night and the rejection of water vapour from the desiccant using daytime sunshine, whereupon the vapour condenses inside the ambient cooled casing and the liquid water so obtained, flows to an external storage tank.

The system is then similar to the original historical attempts outlined in Paragraph 3.1, with some refinements.

A novel application of the device is found in its use for tree sapling irrigation in hostile climates, where the casing takes on the form of a plastic envelope with an air inlet flap and where the collected water drains into the ground via a buried plastic tube. Once the sapling is deemed independent of external water supplies, the device is moved to another plant. Yet at the listed price of around USD 3500-00 per unit, the options of the pumping or trucking of irrigation water become more feasible.

The company does not appear to have experienced much initial growth since their first published advertisements in 2008, with the same advertising page with factual and spelling errors still posted on their website by 2014, yet the basic A2WH system appears in many searches in different configurations and carries many testimonials on the internet in 2017.

A more credible sorption-type collector is provided by Sanakvo, a Swiss non-profit organisation [www.sanakvo.org]. The system is discussed freely on their website and the process described in some detail. A hygroscopic mixture of Glycerol and water is exposed to the air, whereby the glycerol forms water hydrates in contact with atmospheric water vapour. The vapour is driven off by solar heating and water vapour is released through a membrane and condensed against a surface cooled by ambient air. Despite the similarities with the above desiccant system, Sanakvo admits that its theoretical collection rate is 14.4 litres per sunshine day, per square metre of solar radiation, but that in practise the real yield is around 5 litres per sunshine day, per square metre of solar exposure.

Using the North American average sunshine day analogy being an average of 700 Watt/m^2 for 6 effective hours in the southern states, one square metre of sunshine would yield in the region of 15.12 MJ/day, which sets the energy standard for this type of machine at a theoretical 3024 kJ/kg water produced, equating to a COP of 0.805::1.

In comparison to the vapour compression types, this system appears to be less effective, but continues to operate predictably at very low relative humidity levels whereas the compression machine has a low temperature limitation which reduces the production at low dew point temperatures. The other advantage of this system is the

direct use of sunshine for driving the moisture from the desiccant solution. The Sanakvo system is not for sale but instead it is donated to needy communities by the organisation.

3.2.3 Solar Stills and Solar Desalination

These devices do not draw water from the air, but are included because their operating cycle requires the condensation of a vapour. These devices utilise solar heating to evaporate water using sunshine as the energy source and sourcing water from a moisture rich medium such as damp earth, as demonstrated by the A2WH sapling irrigation device. Alternative sources of liquid water feedstock are contaminated ground water or seawater. The solar energy generates a humid atmosphere which is then exposed to a cooler surface and which promotes pure water vapour to form liquid water.

Yet other specialised versions derive moisture only from seawater and these designs usually incorporate a forced cooling facility for enhancing the condensation process. The process then becomes evaporative desalination.

Due to the high specific heat capacity of water and latent heat of evaporation, large amounts of energy are required to achieve the evaporation. Despite the beneficial effects of the Co-efficient of Performance of refrigeration cycles, even more energy must then be expended to create cooling in order to condense the humid vapour.

A simple energy balance of a typical solar still shows that 1 kg of moisture at 20°C requires approximately 42 kJ of sensible heat and 2430 kJ of latent heat to evaporate at 30°Celsius. To effectively condense this vapour back to 20°C using a conventional refrigeration system, the typical COP would be 3:: 1, so that the input energy required to produce the requisite refrigeration effect would be 2472 kJ/3 or 824 kJ. The energy usage of the still will be 3296 kJ/kg of water produced. The refrigeration process with COP of 3:: 1 is only part of the cycle, causing the overall COP to be 0.75:: 1. This option utilises renewable energy for heating but requires some form of conventional energy for the refrigeration process. The advantage of this system for large scale water production, lies in the fact that the humidity feed source is constant and controllable and not a random natural phenomenon. This system is suitable for areas which have a generous solar energy resource, a warm water source and the availability of an

economical electrical power supply for refrigeration. One location that fits this profile well is the coastline of the Sultanate of Oman, [8] which is soon to be see the development of a second sea-to-irrigation system and the first of its kind from the Australian supplier SolarDrop.

3.2.4 Condensation Devices

To overcome the temperature differential between ambient and dew point, many devices have been conceived to condense water vapour directly by using the earth as a heat sink. The latest device on the market is the Waterseer from VICI Labs. This is a well-like device that is wind powered. A vertical axis wind turbine pumps humid air into an underground cavity where the moisture condenses on the walls of an underground reservoir. The dry air is displaced by the incoming flow of wet air. Water collects in the reservoir and is accessed by a tube and hand pump on the surface. The device prompts some questions as to the cleanliness of the water and cleaning dust and algae from the reservoir but the most astonishing aspect is the price, announced on the internet [Tree-Hugger.com] at USD 134-00.

3.3 SOLAR REFRIGERATION VARIANTS USING EJECTOR DEVICES

A great deal of research has evolved from the concept of producing cooling from sunshine. Pridasawas and Lindqvist[9] have produced a proliferation of papers on various aspects of this subject, especially pertaining to ejector operated devices. Pridasawas[10] specifically does not recommend water as a refrigerant due to its high specific volume at low pressures. Others, Kilicarslan and Muller[11] recommend the use of water due to its high latent enthalpy and acceptability for uses above freezing temperatures.

The basic cycle concept is similar to the original Steam Jet Refrigeration concept[12] with a few notable deviations:

- The vapour is supplied at low temperatures achievable from a simple vapour generator i.e. flat panel solar collector and evaporation vessel.

- The motive vapour supplied has little or no superheat and is invariably a wet vapour.

- Pressures are aligned with steam table saturation pressures (Psat) for sub-atmospheric pressures.
- The refrigeration effect is used as a sink to condense atmospheric humidity.
- The condenser is air cooled.
- The scale of the installation is small in comparison with industrial refrigeration installations.

The source of the heat is a solar water heater. Where low boiling point refrigerants or volatile hydrocarbons are used instead of water, higher pressures are achieved compared to water vapour, vapour volumetric flows are significantly less than water vapour and mass flows are greater than water mass flow due to the lower latent enthalpies. The inherent properties of water demand that the water refrigeration equipment be somewhat different to a hydrocarbon installation i.r.o. piping dimensions, surface areas for heat exchange and robustness of design for very low pressures.

Insofar as circuit design is concerned, examples of the many variations of the basic refrigeration circuit are:

- Zhengshu et al[13] 2012 proposed a R134a pump-less system which periodically equalised the pressure across the Rankine system and balanced the levels between generator and condensate tank. This causes a small loss in production during the pressure equalisation and recovery interval. The pump-less solution appears to be adequate although the ejector functionality was not favourable and resulted in low entrainment ratios.
- Huang, Hu et al [14] utilised two vapour generators using R141b refrigerant which doubled as condensers, described as Multi-Function Generators (MFG) i.e. when one unit is in service as a steam generator, the other acts as a condenser. The flow circuitry operated on actuated valves for the change-over. An interval in production was evident at the change-over and the system functioned as a ‘pump-less’ Rankine cycle.

- Huang, Chang et al[15] (1998) developed a high performance R141b cooling system which included, in the basic circuitry, a feed heating regenerator which recycled ejector exhaust heat. The system circulated fluid through the collector using a venturi on the collector inlet and a feed pump.

- Shen et al [16] produced numerical models to evaluate a Rankine system that is comprised of two ejectors, one of which served as a feed pump.

- Pridasawas and Lindqvist [9] produced a numerical study, an 'exergy analysis', on the boundaries of an ejector driven Butane cooling system that is powered by solar heat. The study concluded that ejector losses reduced inversely proportional to motive temperature and dominates the total losses.

One recurring thread through all of the above literature and many other papers on the subject is that, despite the many variations of the apparatus and arrangement of the components, the main contributor to the success of every device, is the ejector design.

Elhub et al [17] reviewed ejector geometry and the state of that art. He concluded that the purpose designed ejector systems are effective in one narrow range and variable input energy systems (such as solar powered heat systems) would benefit from variable area geometry such as that proposed by Pereira et al[18] from both numerical and experimental studies.

A variable area ejector system would compensate for the changing energy input that is provided by solar heating, but would require boundary limits for especially the throat area as well as the convergent section of the primary nozzle. These boundaries can be determined by Computational Flow Dynamics methods as described by Scott[19]. The variable area ejector would require actuation to adapt to the changing conditions and it is a potentially complex project by itself. Yet an obvious solution to the variable energy input conundrum that is posed by solar powered devices, is the use of a choked flow device which allows a constant energy flow that is less than the available source and which is supplemented by a heat storage capacity to extend the operational hours beyond the solar day.

For a definitive design of a choked flow ejector system, a manual method of determining the basic ejector dimensions can be found in the evaluation methods

proposed by El-Dessouky[1], whose semi empirical correlations allow for the calculation of ideal shapes for the limiting conditions. A very useful ejector dimensioning method is to be found in the doctoral thesis of Pridasawas[10] with a flowchart for the design procedure. These latter resources were used extensively in the design and development of the ejector system for this project.

CHAPTER 4

CONCEPTUAL PROCESS

4.1 RATIONALE

The envisaged process resembles a traditional Steam Jet8 refrigeration system working at sub-atmospheric pressures, with the refrigeration evaporator external surfaces doing duty as a humidity condenser. Using Figure 4.1 as reference, the process consists of a motive cycle (G'AB'F'F) marked in red, which utilises a solar heat source and an atmospheric cooling sink to produce the work potential that is required to run the second system which is the refrigeration cycle (G'GHEF'F) marked in blue. The common circuit between the two cycles is the condensation process that is marked in green. The refrigeration cycle provides the necessary heat sink in order to cool the atmospheric air to a temperature at or below the prevailing ambient dew point in order to condense the airborne vapour.

Typically, the system will be subject to a minimum of 700W/ m^2 of solar insolation. The absorbed heat is employed as sensible and latent heat to generate steam at a low pressure. The steam is then expanded into the condenser via an ejector system to convert part of its energy into mechanical effort in order to drive the refrigeration process.

The temperature boundaries are limited to ambient temperature and solar heater stagnation temperature and typically these would be 40°C and 85°C respectively.

Figure 4.1: Basic TS Diagram of Steam Jet Refrigeration System

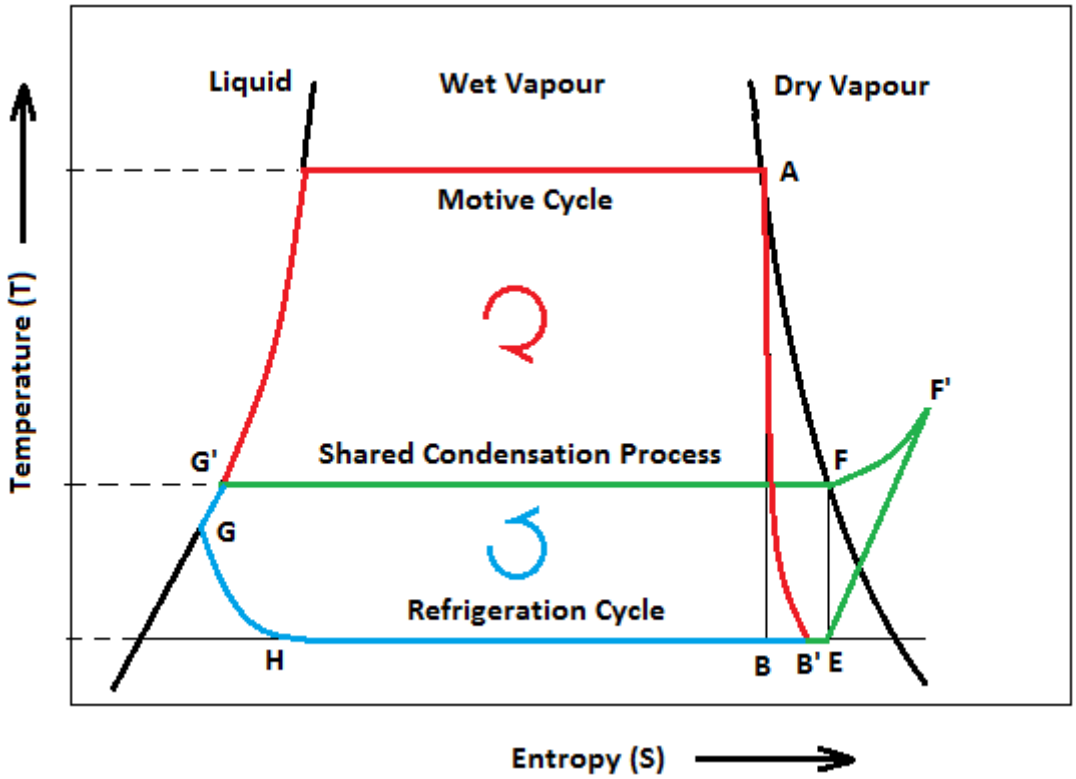

The hot vapour is expanded to realise this mechanical work in the form of a supersonic flow through an ejector nozzle which then creates a low pressure for refrigeration purposes. The refrigeration temperature boundaries are at dew point, typically between 8°C and 25°C, and condenser temperature, again typically between 30°C and 40°C for an air cooled design. The refrigeration COP would ideally mirror the work-from-heat equation with a theoretical 1:: 1 or potentially a minimum 700 J/s of refrigeration. This result would naturally be less in practise, due to imperfect expansions, heat losses and friction losses.

For condensation, the condenser is expected to sink the latent heat that was originally absorbed in the solar heater, plus the heat energy gleaned from the refrigeration process. For the above ideal example, this value would be 1400 J/s.

The amount of water condensed from the atmosphere depends on the atmospheric pressure, humidity and temperature. An indication of the latent heat that is absorbed at the above condition is around 2400 kJ/kg. Assuming that we absorb only latent heat, the maximum mass of water condensed will be:

Equation 4.1

Water Harvest $m_w = 3600 \times Q_R / Q_L$ *kg/h*

- where m_w is water production, Q_R is refrigeration effect and Q_L is total heat of condensation of atmospheric humidity.

Given a COP of 1:: 0 and a perfect condensation cycle, this equates to an ideal water harvest of 1.05 kg/h or 6.3 kg per sunshine day (6 hours per day), per square metre of sunlight averaging 700 W/m^2, similarly 1.5 kg/h would be harvested at a constant 1000 W/m^2 input energy.
The energy consumption would be the latent heat provided at around 2400 kJ/kg water produced.
With losses, the COP reduces below unity and the energy consumption exceeds the latent heat per kilogram of water harvested.
Other researchers have published COP figures varying from 0.8:: 1[9] down to 0.28:: 1[10]. By the above analogy, their refrigeration cycles would require an input energy of between 875 W and 2500 W to produce a 1.05 kg/h water harvest.

The refrigerant medium that has been selected is water, which has the ASHRAE refrigerant identity of R718. The main reason for this choice is the fact that the envisaged process will mix the refrigerant with the motive vapour to avoid the complexity, cost and inefficiencies of non-contact heat exchangers. Other reasons for choosing water as refrigerant are:

- Water is a naturally occurring substance and it has none of the environmentally hazardous properties of other refrigerants.

- The application requires cooling only to dew point temperature and which is above freezing temperature of water across the range of operation.

- Water has a very high specific heat capacity and amongst natural compounds, the propensity for storing and releasing heat, is second only to ammonia. The high heat capacity results in smaller mass flows for the same energy transfer.

The disadvantage of water vapour as a refrigerant is the extremely low vapour pressures that are required for operation within the range of ambient temperatures and the very high specific volumes at those pressures.

4.1.1 The Motive Cycle or Power Circuit

The motive cycle consists of a Rankine power cycle. Input energy is absorbed through the use of a solar collector to generate vapour at or above the saturation temperature. The pressurised vapour then passes through an ejector system, which entrains vapour from the refrigeration evaporator. The ejector discharges the mixed vapour at a partially recovered pressure to a condenser where the combined vapour stream is condensed. The liquid condensate is returned to the collector by means of a pressure boosting or equalisation device. The work done by this cycle is invested in the entrainment and partial pressurisation of the entrained vapour from the refrigeration evaporator. The heat energy that is required to do this work is sourced from sunshine and the sink for the heat is the atmospheric air around the condenser.

4.1.2 The Refrigeration Circuit

The refrigeration cycle exists as a secondary process loop within the above Rankine cycle and takes the form of a reversed Rankine cycle where energy is expended to create a low pressure environment in order to promote evaporation and thereby remove heat from the refrigeration water reservoir. The chilled water absorbs the latent heat of evaporation from the atmospheric air around the refrigeration evaporator.

The two cycles share a common condensation circuit between the ejector mixer and the condenser hot well, so that on the Temperature/Entropy (TS) diagram, the two cycles are linked across the condensing process pressure line. The work done by each process is indicated by the area that is enclosed by the cycle on a PV diagram. The ratio of the areas of refrigeration and motive cycles will yield the actual COP. The inverse of the COP will be the overall efficiency. Due to the fact that we are using more heat energy to do the work required to remove a lesser amount of heat energy, the COP will necessarily be less than 1:: 1. The inverse, cycle efficiency, will notably be 1 or greater than 1. This is possible as we are sinking more heat than the heat that is absorbed from the sun so that the system efficiency will appear to be greater than 100%.

A part of the total condensate flow is bled off to the refrigeration evaporator from the condenser hot well to maintain a working level in this vessel. Condensate evaporates readily in the low pressure environment created by the ejector entrainment port and the resident water is chilled which then draws heat from the evaporator surfaces by conduction. An internal baffle ensures that chilled water rises along the vessel walls as it warms and the cooler water below the evaporation surface sinks to the lower level of the vessel to maintain the circulation. Warm vapour is entrained by the ejector as stated above and it is drawn to the condenser where all vapours condense.

The walls of the refrigeration evaporator are exposed to the ambient air. The humid air is cooled to form condensation on the heat exchange surfaces, which merge to form rivulets that flow through the means of gravity, into a storage basin. The external walls of the evaporator are roughened by sandblasting and treated with a hydrophobic coating to ensure small droplet runoff and to keep the heat exchange surface as unobstructed as possible.

4.1.3 Rankine Cycle Practical Requirements

In industrial Rankine power cycle's various issues, require a constant monitoring of the power fluids (water and steam) and their chemical contents. An online chemical analysis is done to mainly control conductivity, p_h and dissolved oxygen in order to control corrosion which would otherwise be accelerated under the influence of elevated temperatures and pressures. Another typical power cycle malady is the ingress of air and the accumulation of incondensable gases that are drawn in from the atmosphere through gaskets, thread interfaces, pump glands or any other seal with the atmosphere. These gases blanket heat exchange surfaces and greatly reduce the heat transfer rates. All of these issues do not apply to the proposed test device as it will be hermetically sealed as with a conventional refrigerator circuit and no moving seal interfaces exist between the atmosphere and the internals. The refrigerant fluid will be oversupplied and the system will be thoroughly vented to exclude as much oxygen as possible. The venting procedure will be repeated after some hours of running time to reduce any final air quantities which were previously trapped in the system. Any remaining oxygen will react with an iron coupon which will be placed in the dead space of the refrigeration evaporator and captured as FeO2 (Haematite), after which the corrosion would become dormant due to a lack of free oxygen. A trace

of Nitrogen is expected to remain in the circuit as it is inert but of such a small quantity that it would not have a negligible effect on the process.

The main difference between this device and a commercial air conditioner is that the air conditioner is designed to cool a captive volume of air to a low temperature, usually below dew point, to blend with the air in a room and thereby reduce the ambient temperature of a room, after which the same air is re-circulated through the cooler. The vapour is gleaned constantly from the circulating air which causes the humidity in the room to be gradually reduced. Alternately, the water harvesting device constantly cools a large volume of fresh, humid air to dew point. Any cooling below this point (sub-cooling) is a waste of cooling effort and represents a reduced water yield per unit of input energy. The cooled air after condensation is exhausted to atmosphere, no longer a raw material as it has given up its inherent moisture content and the cooling is merely a wasted by-product. Yet the dry and cool exhaust air may still be useful as a heat sink to boost the performance of the condenser and improve the overall performance of the device. This would require the spent dry air to be re-heated by passing it across the condenser heat exchange surfaces.

4.2 RELATIONSHIP BETWEEN BAROMETRIC PRESSURE, RELATIVE HUMIDITY AND DEW POINT TEMPERATURE

The successful operation of the device depends on the physical properties of water and water vapour in the atmosphere.

To accurately predict the performance of the device under a combination of conditions affecting the dew point requires a good understanding of the inter-relationships between those factors which dictate the onset of condensation, i.e. pressure, temperature and humidity.

The system is powered by solar energy and cooled by ambient air. The relationship between these two properties is not fixed since a sunny day usually produces warmer ambient air conditions but other factors will skew any attempt at a rigidly fixed relationship. Despite this fact, the design simplicity requires that the machine dimensions are fixed, i.e. the ejector throat and expansion areas and the condenser convection area.

Barometric pressure plays a very small role in this design due to the small normal variation in pressure of around 10 hPa at the test site. This does not affect the internal, hermetically sealed process in any way.

Humidity is important as a contributor to the amount of water which can be produced, but it is part of the given environment and cannot be manipulated. The amount of humidity condensed, is a function jointly of the amount of latent heat which can be absorbed by the refrigeration process and the volume of humid air in contact with the cooled surfaces.

It is imperative that a temperature below dew point be reached by the Refrigeration Evaporator surfaces, without which no condensation of humidity is possible. Refrigeration at a temperature above dew point will result in zero condensation. Inversely, refrigeration at any temperature significantly below dew point will not increase the production but merely waste refrigeration effort. Despite the above statement, sufficient refrigeration for the exposed condensation areas will result in a largely self-regulating system which follows the rules of heat conduction, meaning that any heat imbalance creates a larger temperature differential which in turn increases the heat flux to the heat sink.

The relationship between the dew point temperature (T) and the saturation pressure is:

Equation 4.2.1

Dew Point Temperature $$T = \frac{B\left(ln\frac{e}{C}\right)}{A-\left(ln\frac{e}{C}\right)}$$

Where the operators are:

A = 17,635 ; B = 243,04°C ; C = 610,94 Pa and '***e***' represents the saturation pressure at dry bulb temperature.

The above equation relates dew point temperature to the saturation pressure, which is accurate to within 0.6%.

The saturation pressure may be estimated with a high degree of accuracy, around 0.3%, by another empirical equation.

Equation 4.2.2

Saturation Pressure $$e = C.10^{\left[\frac{AT}{(B+T)}\right]}$$

In this case the operators are:

In A = 7,5 ; B = 237,3°C ; C = 610,94 kPa with ***'e'*** the saturation pressure, leaving ***T*** as the only variable.

Using equations 4.2.1 and 4.2.2, the relationship between the dry bulb atmospheric temperature and the dew point can be estimated. The variability of this method requires that the error be compensated for by marginal overcooling by say 0.5 degree Celsius. A small loss of productivity may be experienced but this loss is quite acceptable when faced with the alternative total loss of production due to the dew point temperature control being set too high.

4.3 METHODS OF MOTIVE FLUID RECIRCULATION

In a Rankine-type condensing vapour cycle, condensate needs to be recycled to the evaporator or boiler, in order to perpetuate the cycle.

For the refrigeration cycle, a reversed Rankine cycle is employed whereby the vapour pressure is lower than the condensate pressure, so that the fluid passes naturally into the refrigeration evaporator without external effort.

For the motive Rankine cycle, an external effort is required to recirculate the condensate. Methods of performing this pumping duty are discussed below:

4.3.1 Gravity Method

Due to the density differences, the head pressure of a vapour column is in the order of hundreds of times less than the pressure under a liquid column of the same height. By constructing the ejector and condensing equipment at a level equivalent to the top of the vapour column, the condensate may be re-introduced into the motive evaporator without external assistance such as a pump as described by Kilicarslan[11] and Khurmi[12]

due to the nett head i.e. the hydrostatic head offset against the condenser pressure, provided that the system is tall enough. The differential pressure and resultant fluid flow, represents the work done to feed liquid back to the evaporator.

The disadvantages of such a system are the physical dimensions of the apparatus. A device using water as refrigerant would require the condenser to be mounted around 10m above the steam generator for every 100 kPa of vapour pressure. A device using methanol as refrigerant and achieving 93 degrees Celsius vapour temperature would generate in excess of 300 kPa of vapour pressure and require a head of around 24m. The concept lends itself to tall buildings and mountainous areas where such a head may be achieved by utilising existing structures or natural features.

4.3.2 Feed Pump Method

For a compact device without a tall structure, some form of mechanical pump is required to return liquid condensate to the Motive Evaporator and to perpetuate the Rankine cycle.

Although many means exist to drive the pump, for the sake of simplicity a small vapour bleed using the pressure differential between the motive evaporator and the condenser, will produce sufficient energy to drive the pump.

The pump is an auxiliary device hence the selection criteria would be small energy consumption, high effectivity and reliability for a very long life expectancy.

Considering that the fluid mass flow to be pumped, should at least match the motive vapour mass generated, the liquid volumetric flow rate is very small.

The device may also be rotating or reciprocating. The following discussion presents the common pump mechanisms and their properties:

4.3.2.1 Centrifugal Machines

A centrifugal impeller, which is capable of meeting the pressure between Condenser and Motive Evaporator, requires a very high rotational speed and hence it leads to large energy losses due to fluid friction or alternatively a lower rotational speed with

an oversized impeller diameter, producing high energy losses due to large wetted surfaces in motion.

An example solution to the above problem is a direct drive micro-turbine with an etched pump impeller wheel. The unit would run at many thousands of revolutions per minute and generate a constant pressure against a level control valve, but friction losses would be high and the device would consume several times the theoretical amount of energy required to pump the condensate.

A multistage impeller solution may reduce the rotational speed requirement, but adds complexity.

Rotating prime movers of small dimensions such as micro turbines are necessarily complex to design in order to achieve good performance and it is costly due to the level of precision work required in manufacture.

4.3.2.2 Reciprocating Machines

Reciprocating pumps of a very small scale are simpler than rotating types. To provide a radically extended operating life, the minimum of working parts are required and a minimum of sliding wearable surfaces are desirable. Simplistic designs use a displacer instead of a piston and ball type check valves which use their own weight to ensure closure.

4.3.2.3 Direct Contact Pulse Pumps

This concept meets the criteria for the ideal system. The analogy is that of a reciprocating batch pump using vapour pressure as the piston[12]. A feed chamber of suitable volume is placed at a position above the evaporator operating level. A level operated valve inside the evaporator admits a dose of pressurised vapour to the flooded chamber. The chamber is bounded by check valves, which all face in the same flow direction i.e. one in and one out. The inlet valve is connected to the condenser hot well and the outlet valve is connected to the collector feed tube. The vapour cools and collapses, drawing in liquid from the condenser hot well and again flooding the chamber. As the evaporator level reduces, the level operated valve snaps open and a

fresh dose of vapour is introduced into the feed chamber, equalising the chamber pressure to that of the collector pressure and allowing fluid to flow to the collector.

The challenge with this concept is the control of the dosage and the activation of the pulse. A further complexity is that the vapour pressure theoretically just equals the required head of condensate[13], so that the device is to be mounted above the Motive Evaporator at a height calculated to overcome any system flow resistances.

4.3.2.4 Positive Displacement Gear Pump

Another rotating type of pump, which can achieve very high pressures at low rotational speeds and which lends itself to small applications, is a gear pump. The pump is protected from reversing by means of a discharge check valve. The actuation of the gear set can be achieved by a second set of gears that act as a pneumatic motor and which is powered by refrigerant vapour.

The actuator is not a turbine device as the heat, expansion and velocity of the vapour is not utilised, merely the pressure differential. The gears in mesh act as a rotary piston and the motive vapour used to drive the gears, expands only on exiting the tooth-to-casing voids while it is ducted to the condenser. A small quantity of vapour is expected to leak forwards through the gear clearances.

The actuating gears may be of a larger diameter than the pump gears and this provides a mechanical advantage to overcome static head, flow friction and the opening pressure of the discharge check valve at the cost of increased vapour consumption per unit of condensate pumped. Only one of the actuating gears is required to share an axle with the pump gear set since both gears are in mesh with each other, hence the secondary gear set may have a different gear modulus.

If no control is in place, this type of pump will drain the entire circuit into the collector and flood the motive evaporator and vapour ducting until no more vapour exists to drive it.

The flow restriction control of a positive displacement pump is not usually practised since the result in larger scale devices is often a catastrophic failure due to overpressure. In this application, the motive torque is limited so that the risk of such a

failure is not possible, yet the throttling of the liquid feed flow stresses the components and this is not ideal.

Other control means are the torque or speed control of a gear pump. The restriction of motive vapour is a suitable method of flow control. Further, should the control be linked to the liquid level of the motive evaporator, then a synergetic and elegant solution exists to both pump and level control requirements.

The vapour driving the feed pump is supplied directly from a float valve device inside of the motive evaporator. The valve port is sized to oversupply the pump requirement i.e. allow it to pump more than the evaporation rate when the float is at a low level and to close off tightly at high level, effectively stopping the pump. In between these levels, it is conceivable that some level of equilibrium will prevail at a steady state and the pump will react to step changes in level due to the effect caused by the difference between the static and sliding friction in the bearing seals.

As the gear dimensions are known, the measurement of the rotation of the gear may be used with a factor or volumetric constant in order to measure condensate flow, assuming zero leakage. Similarly, as the gears are linked by one common shaft and hence rotations of each set are identical, vapour consumption of the pump can also be calculated using the volumetric displacement of the actuator gears and the condition of the vapour supplied from the motive evaporator. Again, the assumption is for zero leakage.

At steady state conditions, condensate mass flow equals vapour mass flow (including pump vapour consumption) so that the motive evaporator vapour mass flow is also measurable.

Measurement of the pump rotation may prove to be challenging. One concept is the placement of a powerful micro-magnet in the flange of the gear and measuring the magnetic pulsations with a magnetic pulse detector attached to the pump casing, with a timer comparator to relate revolutions to time.

This solution rather takes care of the level control, pump actuation, pump directional control, short circuit losses to condenser, reversal of flow, self-starting capability, pump discharge flow, capability to perform, energy effectivity, vapour mass flow

measurement. This solution also promises operational longevity and reliability, based on the historical dependability of this type of machine.

From the above discussion, both the gear type and the pulse type of mechanism will be considered in the design stage although either of these systems would require substantial development attention to produce a reliable appliance. For the working prototype, an electrical feed pump is considered to set up a working system.

4.4 EVAPORATION OF REFRIGERANT FOR COOLING DUTY

The evaporating fluid molecules rely on their own inherent heat and the heat conducted from the surrounding fluid molecules to provide the latent energy to overcome the surface tension and to evaporate. By the evaporation of some molecules, the remaining molecules are left poorer in heat content and are thus cooler. This low temperature of the contents of the container draws heat from the surroundings and causes the walls of the container to become cooled.

For optimal evaporation, the design of the Refrigeration Evaporator should meet certain criteria.

- The evaporation surface area should be adequate.
- There should be a sufficient depth to create a thermo-siphon between the warmed fluid up the inner walls of the vessel and the chilled centre column of water.
- A flow path for effective extraction or passage of vapour.
- A ready supply of liquid refrigerant for evaporation.
- A large external surface area to maximise the heat flow to the flash water.

The design becomes complex when we try to optimise the surface area of the evaporator. Too large an area may smother the cooling effort yet too small may represent a loss in potential productivity. Of these extremes the former is untenable. The design will cater for a variable external surface area where the unwanted area may be insulated to ensure that some water production will take place during low energy periods.

Another aspect of the exterior of the evaporator is the orientation of finning, if this is to be added. It is undesirable to have horizontal surfaces as this does not promote water run-off and disrupts airflow. The ideal profile is a vertical finning which presents a very small profile to the airflow and ensures all condensation surfaces are vertical.

Most importantly, the external surface finish and composition material of the finned heat exchange areas needs to be carefully considered. A hydrophilic surface will coat with water and flood the air-to-surface interface. A fully hydrophobic surface will cause difficulties with heat exchange since most hydrophobic materials are not good conductors of heat due to their non-polar structures. A hydrophobic surface that is created by virtue of its surface texture may allow good heat exchange, but the final surface must be designed with some care. A smooth hydrophobic surface will allow heat exchange through the footprint area of a droplet. A super-hydrophobic surface such as the Cassie Baxter[20] model will allow droplets to run off as they are formed but heat exchange will be hindered by the gas voids in the contact surface, i.e. the surface area for heat transfer will be a small fraction of the droplet footprint area that is discussed above. A compromise is required as described for the Wentzel[21] state, a droplet is in intimate contact with a rough surface, actually increasing the projected surface area. In spite of this near-perfect contact, the droplet maintains the liquid-to-solid surface tension so that the surface is not wetted, thus allowing the droplet to roll away as soon as it has matured and hence maintaining a clear air-to-surface interface. The surface coating needs to be carefully selected and the surface texture manufacturing method needs to be well-defined[22.]

4.5 CONDENSATION OF VAPOURS

As both motive and refrigerant fluids are water, the streams of motive vapour and evaporated refrigerant may mix in the ejector mixing tube and flow into the condenser.

The mixture of motive vapour and entrained vapour are combined in a wet state after the mixing tube shock wave. The steam flows in at one end of the condenser and expands along its length, creating intimate contact with the walls of the vessel. The condenser has the ability to extract the latent heat from the steam mixture by radiation as well as a combination of conduction and convection. The pressure of the mixture reduces as it enters the condenser and spontaneous condensation occurs on the walls

of the vessel. Condensate flows to the lowest point and drains to the feed water vessel via a check valve.

4.6 THE EJECTOR DEVICE

The success of the ejector will determine the success or failure of the project. This section describes the design rationale that has been used to design the ejector device for this project. Numerical solutions to the rationale are provided in Attachment 4, Part C - Ejector Design.

For the purpose of achieving a satisfactory design without an extended excursion into an ejector gas flow theory, extensive use is made of various papers such as the semi-empirical ejector design method of El-Dessouky et al[10]. The ejector device adheres to the principle of the conservation of energy, but above sonic vapour speed the compressibility effects become significant as the vapour density change is proportional to the square of the Mach number. The best performance of the device is a compromise, i.e. low refrigeration temperatures can be achieved at the cost of a loss in entrainment mass flow. Alternately, high entrainment flow rates may be achieved but at the cost of entrainment vapour pressure, with the resultant higher refrigeration temperatures. In between these extremes lies a best fit operating point, where evaporation pressures can be achieved by utilising the available volume of motive gas.

The design target will be the dew point temperature of water vapour in air across a range of atmospheric conditions, which primarily sets this device apart from a conventional air conditioner. The cooling of wet air well below the existing dew point will not enhance the water harvest and constitutes a potential loss of production and also a waste of cooling capacity resources. The dew point temperature is dependent mainly on a combination of ambient temperature and barometric pressure, both of which are capable of changing with no regard to the other; hence the range of the dew point temperatures may be estimated based on a matrix of historical barometric pressures applied against a range of possible dew point temperatures.

To ensure a consistent performance across a variety of climatic conditions, the ejector is designed to be a choked flow unit, which means that between the operability limits of the system, the gas flow through the ejector throat does not vary appreciably with a

change in differential pressure across the nozzle and hence this removes one variable from the array.

The basic ejector device is comprised of three basic components namely:

- The Expansion Nozzle to expand the motive vapour.
- The Mixing Chamber to introduce low pressure entrainment vapour.
- The Expansion Chamber to expand the flow and recover static pressure.

The double choked ejector design requires that the high pressure vapour passing through it will:

- Enter with a minimum of friction loss.
- Accelerate from low velocity to throat velocity with minimal turbulence.
- Expand and exit the nozzle with the shock wave within a predictable range in the second choke tube.

To achieve these objectives, the components are designed to dimensions derived by the characteristics of the vapour itself.

4.6.1 Expansion Nozzle

The following features define the dimensions, the shape and the surface finish of the expansion nozzle.

The gas velocity and density at the approach point produce a Reynolds's number well below 2300, so are laminar.

The gas entry is shaped with a spherical contra flexure to accelerate the low velocity vapour to the throat in a uniformly radial flow pattern and without an energy-sapping swirl. The entry to the nozzle is concentrically precision bored to further ensure a balanced radial entry flow from all directions. To ensure that the transition is as smooth as possible, the inlet is polished circumferentially so as to promote a boundary layer very early in the entry flow and to reduce the losses through the throat.

The required or estimated gas flow is known so that the bore of the nozzle is calculated to suit the flow rate of motive gas. The boring of precision holes of arbitrary diameter is difficult and nearly impossible to measure with any degree of accuracy, so the above estimate is used only to approximate the hole size and to ensure that a precision drill bit size is chosen to produce a rounded-off exact hole size. The performance calculations use the exact bore size.

Knowing the expected pressure profile, heat constants and estimated nozzle velocity, the divergence of the nozzle should ideally be machined to produce a conical approximation of the ratio of the adiabatic curve of the expanding gas to the local velocity. This shape is approximated with a conical shape since the curvature of the walls is negligible at this scale and the cone angle is quite small.

As previously stated, the ejector is designed to be choked, i.e. the flow through the throat is always less than the potential evaporation rate. The pressure differential is by design chosen to be in excess of 1, 8:: 1 so that the flow is still supersonic in the mixing zone. This is achieved by designing the nozzle dimensions to meet the highest possible energy throughput (1050 Joule/sec) and ensuring that the choked flow conditions are still met at the lowest energy condition (700 Joule/sec). This combination ensures a consistent entrainment ratio and the lowest possible entrainment pressures across the input energy range. The diameter of the nozzle exit is then a function of the adiabatic expansion curve and the length of the divergent section. As the gas expansion pattern now follows the shape of the divergence, the exit shock at the primary nozzle exit is much reduced. There will be shock and energy losses if the nozzle is operated at a flow or pressure differential which differs significantly from design estimates.

4.6.2 Mixing Chamber and Divergent Nozzle

The area directly after the expansion nozzle exit comprises the mixing chamber. This chamber is in communication with the entrainment port which allows the entry of low pressure gas for mixing. The length limit of the mixing chamber varies from one design to the next. For the purpose of this design, the ratios of mixing chamber length to second choke entry diameter were estimated from commercial steam ejector dimensions.

The length of the mixing chamber is dependent on two factors, inertial energy losses and the expansion pattern of the motive gas. The chamber is to be as short as practically possible, as the flow through the chamber is dependent on motive gas inertia. The longer the chamber, the more inertial energy is lost and hence a long mixing chamber will experience more energy losses while being reduced in effectivity.

From the observations of the CFG-derived ejector flow patterns by others, the motive gas experiences inertial flow at a very high velocity in a cylindrical flow pattern after leaving the divergent nozzle, very similar in diameter to the nozzle exit. The surrounding gas is borne along with the low pressure jet stream and the whole flow, including the entrained vapour, is drawn into the entrance to the convergent section of the mixing chamber. Heat loss and pressure fluctuations causes a shock wave within the mixing tube, which acts as a kinetic compressor and converts some kinetic energy back into pressure energy. The area ratio of the convergent entry to the expansion nozzle outlet determines the maximum possible flow rate of induced gas. An overly short mixing chamber, whilst conserving momentum, also may be too short to produce the desired shock wave and may create problems with the condensation process.

In the exhaust nozzle, after the shock wave, the gas is moving at a subsonic speed again and slows down due to the enlarged area, i.e. compressibility or density change is negligible, being proportional to the square of the under-unity Mach number and hence the expelled gas experiences a further pressure increase in line with the laws of the conservation of energy. This final pressure is the eventual condenser pressure where the combined mixed vapour stream is cooled to the liquid state.

4.7 COLLECTING RADIATED HEAT

The solar collector envisaged for this application is required to absorb as much as possible of the solar insolation in the square metre aperture and to convert the radiation to heat and then transferring this heat effectively to the fluid within before releasing a minimum of the absorbed energy by re-radiation or other heat losses. The prototype will be a minimal design to set a benchmark. Improvements to the basic design will then be made and the performance changes will be measured.

The collector construction is similar to the standard rooftop domestic water heater, with a few pertinent differences. Both collector types are designed to effectively absorb

insolation and to convert this energy to heat energy. The collector for this project differs from a commercial solar water heater in the following ways:

- **Orientation**. The collector will be angled according to the local azimuth to collect a maximum of heat before midday at the test location. This aspect allows the machine performance to peak earlier in the day to harvest the highest humidity which peaks at around noon and rapidly drops off in the early afternoon. The collector angle is deemed to be the ideal at 24 degrees from the horizontal and this initial setting is chosen for this latitude for the target optimum operational time of day throughout the year.

- Tracking systems of any description are excluded during this exercise but they may well be a later improvement dependent on cost and complexity.

- **Collector type**. In a steady state, this application relies on the change in density between hot and cold legs to provide the differential pressure for a circulation by thermosiphon. The presence of vapour in the hot leg will further reduce the density of the hot leg and increase the pressure differential across the collector. This collector type serves the purpose of both feed water heater and boiler.

- **Motive Evaporator.** This is a steam generator, fed with hot water by the collector. The design uses existing flash tank design methods for volumetric sizing.

- Fluid is delivered to the motive evaporator at or above the boiling point corresponding to the vapour pressure, so that any pressure drop through vapour demand allows the refrigerant to evaporate spontaneously and accelerates the vapour production rate. The evaporator level is controlled to maintain a vapour/water interface area to allow the vapour to vent. A more detailed description follows in Paragraph 4.8.

- **Recirculation Loop.** Similar to the operation of the Refrigeration Evaporator described in Paragraph 4.4, evaporating water molecules absorb latent heat of vaporisation from neighbouring water molecules, leaving behind a lower energy state of neighbouring water molecules. The heat of vaporisation is supplied

from below and conducted through the upper layers of water which causes the lower layers of water to be at a lower energy state, cooler than those above. To maintain the heat supply to the liquid surface, the cooler water is allowed to descend from the lower end of the evaporator and to return to the collector for re-heating. The hot water is supplied just below the surface of the liquid-to-vapour interface to promote circulation across the evaporation area.

4.7.1 Level Control in Collector

The collector is designed to be permanently flooded. The level control occurs in the Motive Evaporator downstream of the collector plate. The collector outlet and recirculation tubes are oversized to allow a maximum circulation flow from very small pressure variations.

4.8 EVAPORATION FOR MOTIVE DUTY

With the purpose of receiving saturated water and evaporating it, the motive evaporator's shape and function is similar to a steam boiler drum. The device is fabricated from a seamless tube with flat plate ends welded after the appurtenances have been attached, also by welding. The riser or inlet from the collector is introduced from one end, entering centrally and just below the minimum control level in the side wall.

The recirculation port is in the vessel floor. The motive vapour outlet tube passes through the vessel roof and connects to the ejector steam inlet. The velocity in the tube is low so that any condensate that has been collected will drain back to the evaporator.

The feed pump vapour line is inserted adjacent to the motive vapour outlet tube. The vapour line is fitted with a snap-type valve and float arrangement with a tight shut off capability. The line provides an equalising steam to the feed water vessel at low evaporator levels. The valve has a mechanical détente which ensures an operational hysteresis: the valve opens late to ensure a full flow of steam without simmering, likewise the valve is held open against a rising level and released to close positively again without simmering. Trials with a differential gear pump proved wasteful as the

internal leakage of the gears was excessive for gases and vapours and such a device would be useful for more viscous fluids such as oils or water.

The above collector and evaporator devices are intended to operate well above ambient temperature and so they are insulated and covered for the sake of the conservation of heat as well as personnel safety from burns through contact. Steam temperatures exceeding 100° Celsius are possible.

CHAPTER 5

MODELLING

5.1 THE BASIC MODEL

A basic mathematical model is required to map the predicted performance of a humidity condensing device. The model assumes physical attributes which are to be confirmed through later prototype testing. The model uses a range of solar radiation values and cross-references a practical range of relative humidity to predict a yield mass of condensate.

The structure of the model follows a logical design sequence. The model is built in Microsoft Excel, with a front page which displays a schematic diagram with environmental inputs and predicted calculated values, linked to a calculation page where the inputs are calculated to produce predicted outputs, some of which are developed further to produce more predicted outputs along with their variations.

The model is written in a spread sheet format and it uses expressions in place of data arrays for calculations. Steam and psychometric quantities are calculated using accepted equations and constants.

The output of the model is the schematic diagram of the circuit, populated by the predicted outcomes of the values of pressure, temperature, flow and others, at each stage, under specified input conditions of air temperature, relative humidity and solar radiation intensity.

5.2 PHILOSOPHY OF THE MODEL PROCESS

The model calculates each process stage and mimics the design journey. The various waypoints in the process are denoted by the letters A through H portrayed on the TS diagram in Figure 5.2.

Figure 5.2: Detailed TS Diagram of Steam Jet Refrigeration Cycle

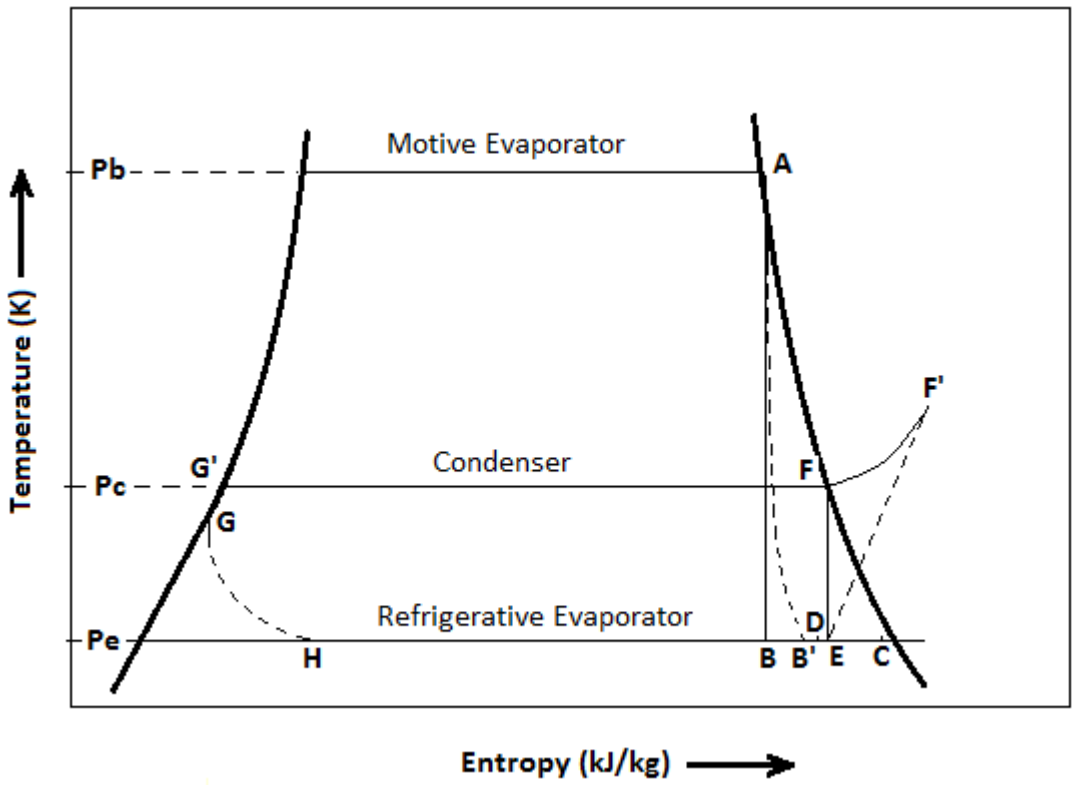

The calculations are entered into an Excel spread sheet, a transcript of which appears in Attachment 5.

The initial calculation attempts to predict the amount of available heat energy that is absorbed by the collector by using the inputs of solar radiation and ambient air temperature, represented by the lines G' – A and which represents both sensible and latent heat of evaporation. The calculation produces a water outlet temperature after losses and properties of steam at point A of enthalpy, entropy and dryness.

Using generic efficiencies for Nozzle efficiency, Entrainment Efficiency and Mixing efficiency, calculations are made to predict conditions at point B (theoretical adiabatic nozzle outlet), B' (estimated polytropic nozzle outlet), D(pre-mix condition), E (pre-shock condition), F (adiabatic compression at shock) and F' (polytropic condition after shock). This is followed by the calculation of entrainment G – H and further evaporation H – D. Heat values at these points allow for the calculation of the entrainment ratio, mass of steam produced, mass of entrainment and the condition of the vapours at every point. At this stage the steady state temperature of the refrigeration evaporator is known, hence the COP and refrigeration effects can be calculated.

The Mach numbers through the fixed nozzles are calculated, followed by the condensing mechanism and the psychometric calculation to estimate the water harvest.

5.2.1 Using the Model

For once off evaluations or snapshots, the four defining climatic condition data are entered i.e. air temperature, relative humidity, barometric pressure and a value for the insolation or solar radiation is entered.

All variables are calculated and the results linked from the calculation sheet, are displayed on the schematic diagram.

For simplicity, a two minimum (am and pm) and maximum (midday) condition are entered and the results are tabulated using Standard Deviation methods which returns a median production estimate for the day.

5.2.2 Updating the Model

The accuracy of the model is required to make meaningful predictions of machine performance in order to evaluate the modifications and changes to the machine which may be too time consuming or costly to implement physically during the term of this research. More importantly, a model which predicts the device performance reliably, will be an invaluable tool to determine the effectiveness of the device in various locations around the world, given only the annual climatic profile of the area.

Many variables are used in the initial model which may not be accurate. Physical data will undoubtedly show discrepancies in results between the actual and predicted data. A good degree of accuracy can be achieved by updating the model from experimental data. Variables which are listed in various publications yet are accurate only through experimental data are for example the emissivity of steel and glass, heat transfer co-efficient for various materials and heat conduction constants for various materials and fluids.

5.2.3 Energy Feasibility

The solar radiation intensity and daily durations are relatively well researched around the world. The objective of this exercise is to accurately predict the effective quantity of liquid water that can be reduced from the air under various conditions.

5.3 DESIGN CERTAINTY

This objective requires a detailed thermodynamic and mechanical design exercise to specify a device capable of performing the task at optimal energy efficiency. Various design challenges are to be addressed such as a highly effective heat absorbent surface and a thermally powered feed pump to circulate the distillate. (The output is a P&ID)

CHAPTER 6

NOTES FROM THE PROTOTYPE DESIGN, MANUFACTURE AND DEVELOPMENT

The notes below are provided to demonstrate the philosophy and development stages involved with the various components.

6.1 MECHANICAL DESIGN NOTES

6.1.1 Ejector Design

Using the design guidelines from Pridasawas[10], the ejector basic dimensions were obtained for a single choke system. The initial ejector housing was a fabricated T-piece from 20mm mild steel plate and the primary nozzle machined from a stainless steel M12 bolt which screwed into position. Various positions were tested using compressed air as a motive fluid but it was soon apparent that a double choke system would be required. A new housing was manufactured from an aluminium round stock to provide the second choke of a considerably larger diameter. The same primary nozzle was used in this variant but it proved to be ineffective. Temporary nozzles were machined from PVC rod and the outlet angle decreased in stages until an acceptable performance was reached. The final shape was machined from the more durable brass threaded rod with a view for making the permanent nozzle from stainless steel should there be no more need to change the shape. The final ejector assembly were comprised of four flanged aluminium sections with the primary nozzle positioned in the first section.

6.1.2 Solar Collector Design

The collector consists of a frame, a collector plate with tubing, a backing insulation and a glass cover.

The first frame was made using a composite wooden board, milled with internal slots to receive the cover, tube plate and backing board. This material did not stand up to the weather extremes and disintegrated before the performance tests could be

completed. This first model used a serpentine tube design which appeared to work well enough during the initial tests but it later proved to be inadequate. In keeping with the low-tech intent of this project, the collector plate was initially coated with a commercial synthetic enamel matt paint with the coating being applied by roller. This coating was later stripped off and the author's proprietary selective surface coating was applied.

A second frame was manufactured from extruded aluminium window sections and it was extensively tested under a variety of conditions. The clear result was the failure of the tube system to provide a sufficient flow to absorb the available heat. The small thermosiphon flow was restricted by the fluid friction of the single long tube, with the result that the terminal temperature was almost reached in the first few metres of tubing and the heat transfer in the greater part of the collector was stagnant. This fact was proven by a short series of tests that were performed with the use of a circulating pump at various flows. The heater produced good efficiency under forced flow conditions and collection figures at flows significantly above those possible by thermosiphon alone. Whilst investigating the possibility of using larger bore tubing, it was discovered that the contract manufacturer of the tube plate had used a smaller tube than specified, which aggravated the restricted flow condition.

A third prototype was fabricated using a system of two headers and interconnecting absorber tubes and this was also done under glass. This variant performed well, producing heat absorption figures very close to calculated expectations by thermosiphon alone. Unfortunately, the available materials for this design were FerroCopper tubing with soldered joints. Under extreme vacuum at elevated temperatures, the joints were found to shift and many weeks were lost trying to stem the leaks and re-soldering the joints several times.

It was finally decided to revert to the original serpentine system with oversized tube bore and no joints; this configuration proved highly successful for both performance and reliability aspects.

For brevity, only the final prototype design is laid out in the Attachments.

6.1.3 Motive Evaporator Design

The basic design is a vessel made from piping that is shut at both ends. Various tubes are welded through the body to provide flow to and from the vessel. The vessel is insulated to reduce heat loss. A parallel vessel employs a float valve to open at a given level and to provide pressure equalising steam to a separate feed water vessel at a higher elevation. The vessel then discharges into the evaporator and the rising level closes the float valve, similar to the Rankine feed system employed by Zengshu [13]. Steam in the feed water vessel cools and condenses and draws in fresh feed water from the condensing system and remains in this state until the steam float valve again drops open and the process is repeated.

The float valve requires a hysteresis to avoid the simmering and failure of the feed function. No such valve was available commercially and a prototype was developed and tested, a standard float valve body was modified to provide a détente for actuation of the float. The seat area was reduced by means of a pressed insert to meet the requirements of sealing under vacuum whilst still holding the valve shut until the weight of the float exceeds the vacuum force on the slide. A float was fabricated from PVC piping fittings and the mass was calibrated to allow enough gravitational force to overcome the pressure differential. The concept proved to work well but it was not reliable. Boil-off testing resulted in the violent vibration of the actuator float and audible shocks to the heavy valve system, which eventually led to the catastrophic failure of the valve. On several occasions the system was dismantled to service the valve, the soft sealing face became detached many times, the float developed leaks and was eventually filled with foam and the mass recalibrated. In June of 2016, the valve failed again catastrophically. Having proven the basic concept of the pump-less system to be workable, feed water duty was assigned to an external DC powered feed pump and flow switch for the testing phase with the power being derived from a separate 10W PV panel and surge battery.

A further improvement was the separation of the level control and evaporation functions. This was achieved by adding a dedicated evaporation vessel (boiler drum principle) connected in parallel with the float level control vessel at the steam and water sides by means of water and steam balance lines. This system allows the violent boiling which is required to produce large volumes of steam but prevents damage to

the valve system whilst maintaining liquid levels. This change also drastically improves evaporation area.

6.1.4 Condenser Design

The initial thought was to use a large open vessel as a combined plenum chamber, condenser and vacuum reservoir. The plenum chamber concept was used to allow high speed vapour to slow and increase pressure still further. The rarefied vapour requires some exhaust volume to initiate cooling and density increase, also to collect and drain water droplets in the exhaust so that the condenser receives only vapour. In series with the plenum chamber, an automotive air conditioning condenser was tested for heat rejection with hot water and proved to sink heat very effectively. Yet the inlet port size of the condenser was way too small to admit the large volumes of steam that its surface area could condense. Some experimental work was done using an automotive radiator but the unit was not robust enough to cope with very low pressures.

A final solution was found in the connection of the ejector outlet through a large plenum chamber and then into the condenser scrubber column while modifying the condenser internal passages to create a single pass unit.

6.1.5 Refrigeration Evaporator Design

To provide a high surface area, the evaporator was fabricated from piping, similar to the motive evaporator, but having welded fins around the periphery. The area was made arbitrarily large, with the thought that, should the surface need to be reduced then this could be done by insulating a part of the area. The fact that the co-efficient of performance is less than unity as well as the various losses along the way, resulted in a much smaller area than required. A second refrigeration evaporator was developed to reduce the area to within acceptable limits and to reduce the mass of refrigerant water to make the system more responsive. The second evaporator retained the length of the first for reasons of head and pressure but has a much reduced diameter. A new float valve was manufactured to ensure a bleed of make-up water.

6.1.6 Level Control in Refrigeration Evaporator

The refrigeration evaporator loses water mass by evaporation from its surface, hence the level is reduced. Effective cooling of the outer surfaces requires a constant high water level. A float valve was fabricated similar to the motive evaporator float to admit feed water and this valve connected to the plenum chamber outlet, this source being at a similar pressure and at a slightly higher elevation. Reliability issues also plagued this valve function and the passing seal allowed water to be drawn into the ejector and to flow through the ejector body, flooding the plenum chamber. In the process the aluminium secondary choke was damaged and it had to be re-machined, causing a minor variation to the design dimensions.

CHAPTER 7

FINAL COMPONENT TESTING AND ASSEMBLY

7.1 TESTING OF INDIVIDUAL COMPONENTS

The core of the device is the heat source, the solar collector.

7.1.1 Emissivity Test

The first test to be performed was the emissivity test. The final version collector plate was set up dry with backing insulation in place, in near windless conditions on 5th October 2016. Data from this test is provided in Attachment 7 Table 7.1.1. The solar insolation was measured simultaneously with the temperature of the collector plate over a period of time with gradually changing ambient conditions. The equation below was used to test whether the emissivity assumptions that were made are accurate, proving that

energy in (Q_I) equals energy absorbed (Q_t) plus losses

$$Q_I = Q_t + losses$$

$$Q_t = \epsilon \Theta A T^4 \qquad [Eq. 7.1.1.1]$$

$$Q_I > \epsilon \Theta A T^4 \qquad [Eq. 7.1.1.2]$$

Where Q_I is the measured radiated energy, ϵ is emissivity of the surface, Θ is the Boltzmann constant for solar radiation, A is the exposed area and T is the absolute temperature.

On 5th October 2016 the above test was performed in the period spanning 12 noon. The atmospheric conditions were hot and hazy, cloudless and windless. The test was done using a Titan 369HTL infrared temperature gauge and a Fluke multimeter calibrated to 200mV and connected to an Apogee insolation meter calibrated to 5W/m^2 per millivolt. The panel was set square to the sun and the meter was set vertically to record the horizontal insolation.

The plate temperature averaged 97.497°C and the insolation meter recorded the average horizontal insolation of QI of 801.13 W/ m^2. The equivalent Module insolation would be 1024.85 W/ m^2.

Using Equation 7.1.1.2 and equating measured input energy against the calculated energy provides an estimate for the value of emissivity of the system:

$$Q_t = \epsilon \Theta A T^4$$

$$1024.85 = \epsilon \times 5.670367 \times 10^{-8} \times 1 \times (97.497 + 273.2)^4$$

$$\epsilon = 0.9571 \quad say \ 0.96$$

The above comparison indicates that the solar insolation is comparable to the emitted energy plus losses of around 40 Watts. The fact that these numbers correlate closely, indicates that the emissivity value is indeed very high hence the value of 0.96 is assumed for the use for this device.

NB – The author has previously (2007/2008) devised a thermo-chemical process to produce a very high emissivity coating for heat engine cooling purposes.

7.1.2 Collector Flowrate Estimations

For this test, the collector glass cover is fitted and the system filled with water. The inlet and outlet tubes are connected to the motive evaporator and the system is monitored for the day. The evaporator and return line are not insulated, so as to create a heat sink to promote flow. The insolation reading and the collector T1 and T2 readings are recorded. The data is tabled and the mass flow is determined from the inlet and outlet temperatures during the most stable period of the day, i.e. when temperature and insolation changes are at a minimum, usually between 11am and 1pm, dependent on cloud and haze.

The heat capacity calculation is used:

$$Q_I = m C (T2 - T1)$$

$$\dot{m} = Q_I / C (T2 - T1) \qquad [Equation\ 7.1.2.1]$$

This thermal calculation returns the mass flow through the heater to achieve the measured temperature rise, assuming that all available input energy is converted to heat. From previous exercises we assume the emissivity to be around 0.96.

Data from 3 November 2017 is used for the example below and reproduced as Attachment 7 Table 7.1.2:

$$\dot{m} = Q_I / C\,(T2 - T1)$$

$$\dot{m} = (0.96 \times 869.7) / 4187(80.7 - 30.7)$$

$$\underline{\dot{m} = 0.00399\ kg/s}$$

This result is checked using the Fanning friction factor for a smooth tube and using the relative densities of the hot and cold legs, 570mm apart, to determine the motive pressure. It must be noted that the cold leg density remains fairly constant whilst the hot leg density reduces as it heats to temperature T2. The density at the hot leg is 972 kg/m^3 and that of the cold leg is 996 kg/m^3 – average density is 990 kg/m^3.

$$\Delta p = \Delta \rho \times gH$$

$$\Delta p = (996 - ((996+972)/2)) \times 9.81 \times 0.57$$

$$\underline{\Delta p = 67\ Pa}$$

In terms of differential head, this value is expressed in linear measure as:

$$h = \Delta p / \rho g$$

With the proviso that the same density is used as for the previous equation:

$$h = 67 / (990 \times 9.81)$$

$$\underline{h = 0.0069\ m}$$

The assumption is made that all pressure energy is exhausted by friction, i.e. the maximum flow is achieved:

$$h = h_f$$

Whether laminar or turbulent, a low velocity flow in a smooth bore tube on any side of the transition zone of a Moody diagram would suggest a Fanning factor of close to 0.009. For a tube of 14m, the expected flow velocity will be:

$$v = \sqrt{(h_f \times d \times g / (2 \times f_f \times L))}$$

$$v = \sqrt{(0.0069 \times 0.01 \times 9.81)/ (2 \times 0.009 \times 14)}$$

$$\underline{v = 0.0518 \text{ m/s}}$$

The equivalent mass flow will be:

$$\dot{m} = \rho_{ave} V$$

$$\dot{m} = 990 \times \pi/4 \times 0.01^2 \times 0.0518$$

$$\underline{\dot{m} = 0.00403 \text{ kg/s}}$$

This compares favourably with the mass flow that was arrived at using the heat flow equation, around 4g per second. It should be noted that this flow-rate does not take into account the presence of vapour bubbles that would affect the fluid calculation through both friction and buoyancy.

7.1.3 Hot Water Test of Collector and Motive Evaporator

The collector and motive evaporator assembly was completed and charged with distilled water up to the float switch closure level. The vapour outlet and pressure measurement ports were initially left open. Over a period of two solar days the collector inlet and outlet temperatures were measured, as well as the solar insolation values.

No insulation was fitted to the evaporator or the reticulation tubing in order to provide a heat sink to promote thermosiphon. During this period, T2 temperatures exceeding 99,5°C were recorded during horizontal insolation (I_H) values above 800W/ m2 and the system was seen to boil sporadically at atmospheric pressure during this time with vapour periodically venting from the open ports. See Attachment 7 Table 7.1.3.

The module insolation (I_M) input for this day, 6th October 2016, at Noon and horizontal insolation of 823 W/m^2 was calculated using the generally accepted solar positioning calculations as shown in Figure 7.1 below.

The Angle of Declination (δ) is firstly required to determine the angle of the sun due to the time of year and where DY is the day of the year counting from January 1st , using the empirical equation:

$$\delta = 23{,}45° \times \sin[360/345 \times (284 + D_Y)]$$

$$\delta = 23{,}45° \times \sin[1.0435(284 + 280)]$$

$$\underline{\delta = -17.57°}$$

Figure 7.1: Solar Insolation Angles and Orientation

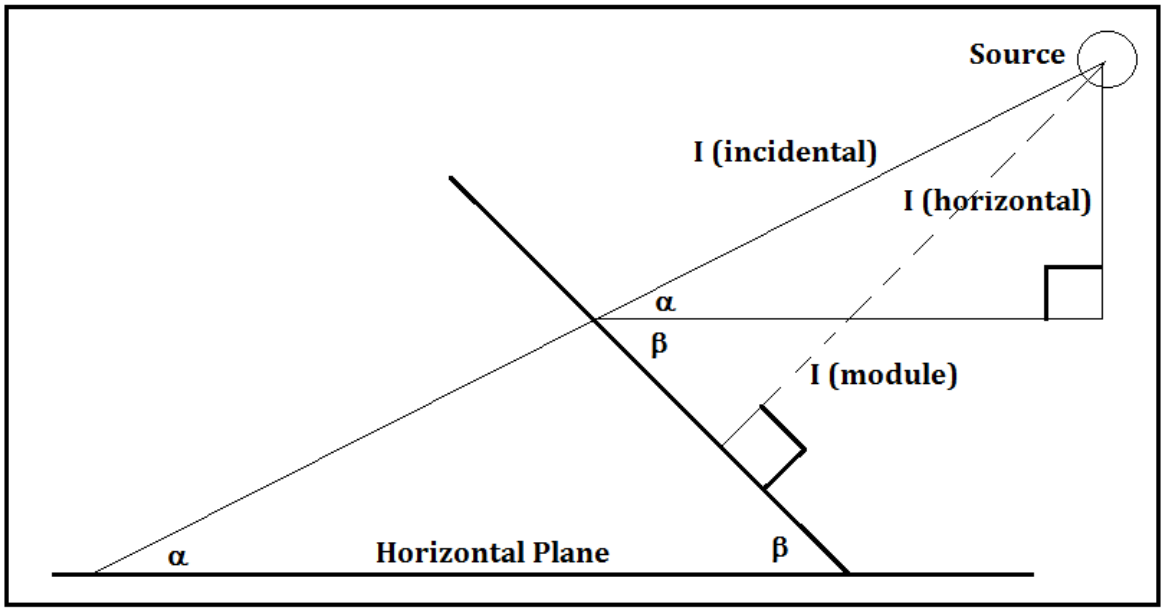

The incident angle of the sun (α) above the horizon is found using the above declination (δ) and the latitude of the test site (ϕ) at 24.41°N:

$$\alpha = 90 - \phi + \delta$$

$$\alpha = 90 - 24.41 - 17.57$$

$$\underline{\alpha = 48.02°}$$

Incidental Radiation (I_i) is found as the trigonometric ratio:

$$I_i = I_H / Sin\ \alpha$$

$$I_i = 823/Sin\ 48.02$$

$$\underline{I_i = 1\ 107\ W/m^2}$$

Finally, the Module Insolation is found as a function of the incident angle α and the panel angle β which is also 24° to match the latitude.

$$I_M = I_i \times Sin\ (\alpha + \beta)$$

$$I_M = 1\ 107\ Sin\ (48.02 + 24)$$

$$\underline{I_M = 1\ 053\ W/m^2}$$

Under these conditions (noon), a spot check of the heat absorbed according to the Boltzmann equation to predict the system maximum temperature, confirms previous assumptions of heat transfer:

$$Q_t = \epsilon\ \Theta\ A\ T^4$$

$$T^4 = Q_t / \epsilon\ \Theta\ A$$

$$T^4 = 1053 / (0.96 \times 5.670367 \times 10^{-8} \times 1)$$

T =372.94 K (99.74°C)

This figure correlates closely with the actual T2 water temperature measured at 99.5°C on an instrument resolution of 0.5°C per graduation.

Heat flow calculations under these conditions are complex, especially when using the full solar day and making corrections for Azimuth angles and Time Corrections to local time. For this reason all routine measurements from October 31st 2016 are made with the insolation measurement that is taken parallel with the plane of the panel at 24°, hence directly measuring the Module Insolation without the additional daily calculations.

7.1.4 Boil-off Testing

This test is a part of the start-up process for the system. It is done to reduce the amount of air in the system by expanding and dislodging the air trapped in the circuit and then to evacuate the wet air and vapours from the system. This test is also the first boiling and steam production and ensures pressure and vacuum integrity of the device. For this exercise the ports to the atmosphere are initially left open and then closed after the system is heated. The system is then evacuated with the vacuum pump until water is seen at the pump outlet. The pressure cannot be reduced much below vapour pressure at ambient temperature due to the large amounts of water vapour contaminating the vacuum pump oil charge.

The first reliable boil-off was achieved on test day, 6 October 2016. Temperature T2 was measured approaching 100°C by late morning and the motive evaporator was noted to vent hot vapour periodically at ambient pressure. The ports were closed and the internal pressure was reduced to around 40 kPa(abs). The result was a violent boiling which reduced to a steady boil after a short time. During the following hours the system was noted to be boiling constantly, producing an audible rattling sound. This test was repeated on 7th October 2016 with similar results. It is clear from the graph that the evacuation and subsequent boil-off cause erratic and constant variations in the flow and temperature, hence the analysis of boiling data is best done by using large sample averages. Note the significant temperature reduction once the flow and evaporation processes begin at around reading #310.

Figure 7.2: Plot of T2 temperature showing temperature excursions caused by flow oscillations from boiling in the heater outlet tube.

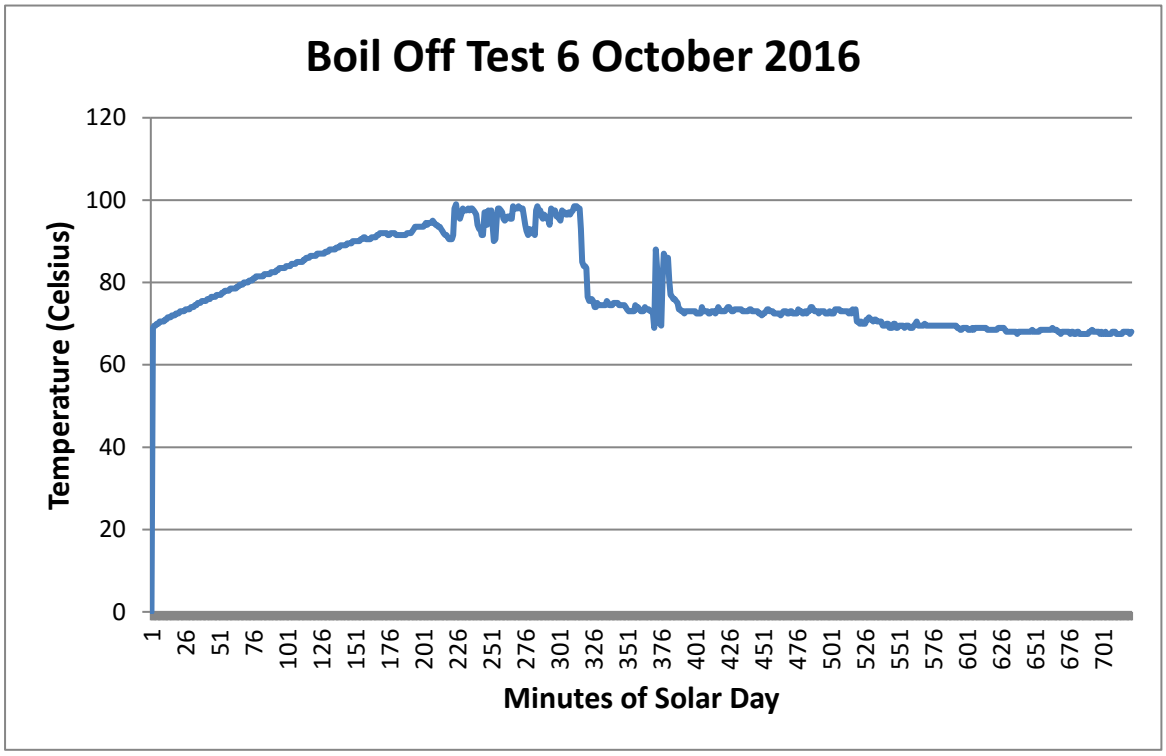

7.1.5 Condenser Capacity Test

This test was performed with each variant of collector design. For brevity, the results below reflect only the final results of November 2016.

The vapour outlet of the Motive Evaporator was connected to the ejector inlet. The ejector induction port was blanked and the ejector was attached to the condenser. The condensate outlet was connected back to the Motive Evaporator via a peristaltic pump and an in-line check valve. The pump electric circuit was wired via a stainless steel float valve and the system was then evacuated down to vapour pressure at an ambient temperature.

The above circuit effectively bypasses the Refrigeration Evaporator.

The system was noted to boil off continuously and the peristaltic feed pump was noted starting and stopping periodically to maintain the water balance, indicating continuous evaporation and condensation.

A method of measuring flow rates by timing the peristaltic pump proved to be erroneous as the peristaltic pump displacement is not constant due to a distortion of the peristaltic tube at low pressure, which alters the flow-rate per revolution. This means that it is not a true positive displacement pump. A better experimental flow rate check is timing the pump's stop/start operations as this is directly proportional to the change in the level of the evaporator which has a known internal diameter, amounting to 95g per operation and which was observed to start roughly every 5 minutes during peak insolation. The system achieved a steady state Rankine cycle with an estimated condensation rate of between 866g/h and 950g/h.

7.1.6 Refrigeration Evaporator Test

The Refrigeration Evaporator was initially tested against a vacuum pump in the workshop. A small leak caused several delays in testing this item while not permitting pressures below 24kPa (abs). The cylinder welds were eventually buttered over with silicone sealer and the pressure was reduced to 3kPa (abs) which was the best performance of the vacuum pump.

This pressure was held for 2 hours with an empty vessel and the exercise was repeated with a water-filled vessel which had been allowed to stand to stabilise to room temperature. The pressure decayed to over 4kPa (abs) but stabilised there and subsequent efforts to reduce the pressure to 3kPa (abs) were short lived. After several attempts, the vacuum pump oil was noticed to have become milky from moisture contamination.

The test was repeated outdoors at a temperature of 40 °C and a relative humidity of 55% and after some time it produced a visible moisture condensation on the condenser body with the vacuum pump being started repeatedly throughout the exercise.

7.2 ASSEMBLY AND PREPARATION FOR PRODUCTION TESTING

The system as developed above was slightly refined by improving insulation and curing some vacuum leaks. A windshield of corrugated cardboard sheeting was fitted to control air flow past the Refrigeration Evaporator and a calibrated collection vessel was attached to record the water production.

The data loggers were programmed for same-start and same-interval sampling and they were downloaded daily up to the start of production testing.

The system and the area were thoroughly cleaned and the area was cleared of all unrelated equipment and materials.

Routine daily tasks were established to download data and to do vacuum checks and corrections as well as the daily cleaning of the Collector glass.

CHAPTER 8

PRODUCTION TESTING

8.1 Test Procedures

The purpose of testing the device is ultimately to measure the amount of water that is collected in relation to the heat input and system constants. In order to understand the causes of any observed deficiencies in performance, it is essential to have tested the components individually and to know their physical limitations. For the purpose of the performance analysis and fault finding, the monitoring and recording of system parameters is done during each test day and the results are summarised and processed.

8.1.1 Climactic Comparison

Prior to the start of any prototype testing, some climactic comparison testing was done. The purpose of the test was to prove the instrumentation and data logging capabilities and establish a testing routine.

A cabinet was built from thermal insulating material to measure the basic atmospheric variables. The insulation material prevents data skewing from the solar heating of the walls. The cabinet was also naturally ventilated to allow a constant flow of sample air. The vents were covered with fine gauze to prevent insects and small animals nesting in the cabinet.

For a view of the cabinet see Photograph 8.1.

The instrumentation that was used was the Extech® RHT type data logging multi sensors, one Model RHT50 measuring barometric pressure, air temperature and relative humidity, with redundancy of air temperature and relative humidity measured by one Model RHT10. Data sheets on the ExTech® and other instruments used in this project are provided in Attachment 6.

Figure 8.1: Meteorological Instrument Cabinet

The first weather baseline test was started on Friday 14th June 2013 at 14h00 on the site at co-ordinates 24°24’35’’North and 56°39’21’’East.

The parameters measured were primarily Air Temperature (T_a) and Relative Humidity (RH). The loggers were set for 1500 readings at 10 minute intervals, a test of 13 full days from midnight of one day to midnight of the next, to coincide with the weather stations’ practise. The test included a redundancy of temperature and relative humidity instruments to determine the relative accuracy and repeatability of the sensors.

The above exercise indicated that, during the time of the test, the test site instrumentation produced similar trends to the local weather station although the absolute values differed considerably between the Sohar test site and the regional weather station data from Fujairah (93km North West) and Majis (12km North East). The temperature comparison used the daily averaged temperatures and showed the Sohar site to be hotter by several degrees than the two regional weather stations, yet the Sohar data was collected by two adjacent instruments which agree closely.

The trend from Fujairah was very different to the rest, probably due to the distance from the Sohar site and the mountainous terrain. The Majis trend tended to approximate the Sohar trend, albeit several degrees cooler.

It was reasoned that the Fujairah weather station is too distant and geographically too different to make any worthwhile comparisons. The Sohar humidity trend shows a good correlation with the Majis Weather Station and the absolute difference in Relative Humidity correlated with the temperature difference.

A second set of tests was conducted from Saturday 6th July, 2013 for twelve days from midnight to midnight, again to coincide with the weather station practise. The second test differed from the first in that the same instruments were used but the data logger cabinet was placed inside a ventilated cabinet similar to that which is used at the Majis weather station. The result of the second comparison test is shown in Figure 8.1 below.

Figure 8.2: Local Weather Comparison – July 2013

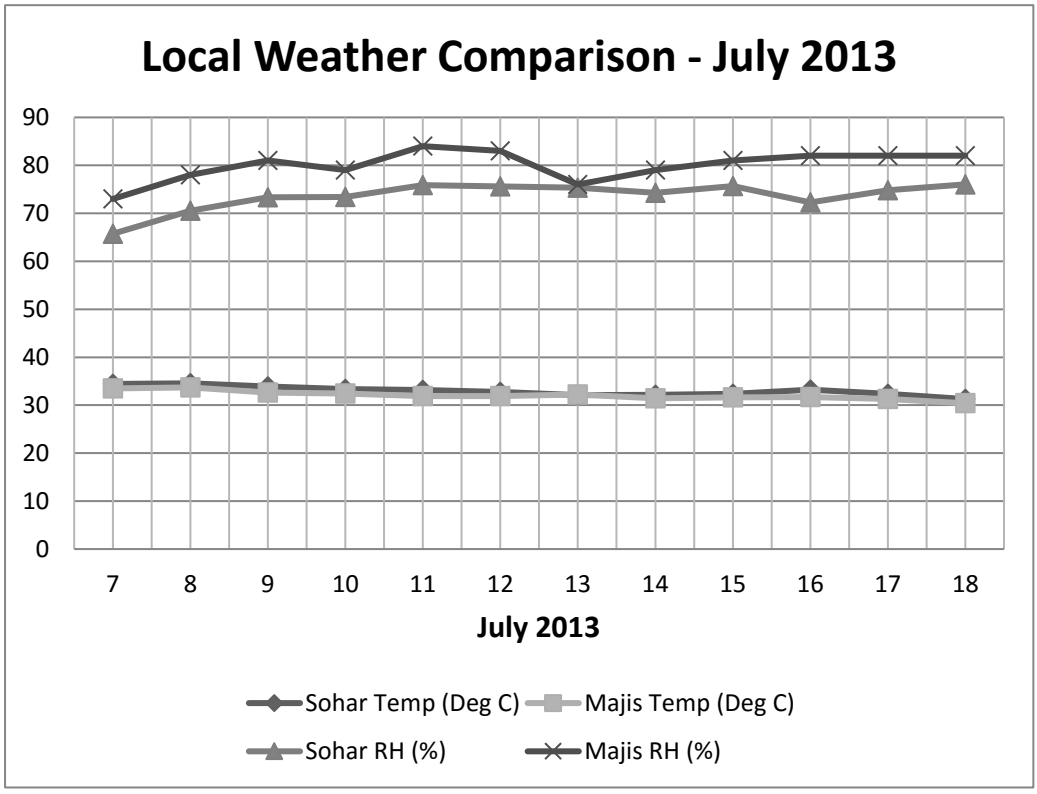

The results show a similar trend between the Sohar and the Majis locations and the change in the measurement technique has decreased the gap between the values.

The site temperature and humidity may well be different to those at Majis since the site is several kilometres inland whereas the Majis station is a few hundred metres from the seaport and only a few meters above sea level, adjacent to a seawater cooling water circulation canal.

In conclusion, our site measurement trends compare favourably with the trends that were presented by the local Majis weather station. Hence the local weather data may be used to establish a weather backdrop for the machine tests.

Routine weather testing on the site was started on Saturday 14th September 2013 after the acquisition of a voltage data logger which enabled readings to be taken of solar insolation.

8.2 TESTING IN THE SULTANATE OF OMAN

8.2.1 Whole System Start-up

The system was assembled during summertime 2016 according to the P&ID provided in Attachment 3, using the following methodology.

The water levels were adjusted using filtered and boiled water and the system was sealed.

The pressure was reduced using the vacuum pump and drawing from the coolest place, at the top of the hotwell.

Audible boiling was heard from the motive evaporator at pressures approaching 10 kPa (abs). This corresponds to the saturation point of water at the ambient temperature above 45°C.

The vacuum pump was stopped and started periodically to evacuate more air and to allow the heavier air to gravitate to the hotwell.

The contamination of the vacuum pump oil charge is inevitable and the oil was changed many times, eventually resorting to 20W50 motor oil for cost purposes.

8.2.2 Data Measurement - General

Data loggers were set up initially to read every 30 seconds, but later it was extended to read every 5 minutes for extended periods and data space saving.

Only daytime records are saved.

Instrumentation specifications are found in Attachment A6.

8.2.3 Temperature Measurement

The three relevant process temperature measurements are taken by means of a Type K thermocouple and the outputs were measured and logged by single channel USB data loggers from Lascar Electronics designated EL-USB-TC and calibrated to record 0 - 150°C. These are fitted to the outside of the vessels and tubing using aluminium tape and covered by an insulating pad that was taped in position with duct tape.

The three measurements are:

- Motive Evaporator Outlet Temperature T1
- Motive Evaporator Inlet Temperature T2
- Refrigeration Evaporator Temperature TR

8.2.4 Pressure Measurement

Pressure measurements are taken by using combination pressure transducer and transmitter units manufactured by SICK AG and designated PBT. The transducers are set up to measure 0 – 100 kPa across a range of 4 – 20 mA. The signal is recorded by another variant of the Lascar data logger range designated EL-USB-4. The reference voltage is provided by a 12V lead acid motorcycle battery that was connected to a voltage stabiliser and a 10W silicon solar panel.

The three pressure measurements of interest are:

- Motive Evaporator Steam Pressure PE
- Refrigeration Evaporator Steam Pressure PR
- Condenser Pressure PC

8.2.5 Solar Insolation

The radiation is measured using an instrument that was manufactured by Apogee Instruments USA which is marketed as Precision Pyranometer SP-110. The device reads all light radiation between 300nm and 1150nm. The output of 0 – 220mV is recorded using a millivolt 2 channel logger named a Track-It by Monarch Instrument Co. The instrument can measure up to 220mV, which equates to 1100 W/m2 of solar power.

8.2.6 Meteorological Measurements

Ambient Temperature, Barometric Pressure and Relative Humidity are all measured using either of the USB loggers designated RHT10 and RHT50 manufactured by ExTech Instrument, as described in Paragraph 8.1.1. The instrument is mounted in a shady area in a ventilated box as shown in Photograph 8.1.1.

8.2.7 History of Measurements

The major obstacle in obtaining useful results from the system is the required very low internal pressure, using water as the refrigerant. Even a very small air leak expands significantly to ruin the pressure profile and to coat the condensing surfaces. Many thousands of readings were taken which invariably show a vacuum decay and no sustained refrigeration effect. Many leaks were found and cured, leading to the replacement of several parts with new ones that were better equipped to seal against vacuum leak. Pressure testing of very small leaks is not effective and the best solution appears to be a vacuum decay test whilst methodically sealing each joint and potential leak until the decay rate is slowed. This exercise takes many hours.

The refrigeration evaporator pressure profile follows closely behind the motive pressure plot. The variance is around 2kPa. The two transducers were exchanged to prove a calibration error, but the profile differential persists, indicating that the readings are plausible.

8.2.8 Discussion of Results

8.2.8.1 Heat Exchange

The collected heat meets expectations when compared to the $1m^2$ collector aperture and the 1000W/m2 insolation generalisation. Figure 8.2 below shows two examples of how the calculated and measured heat values compare. Despite the excursions caused by surging flow, the daily averages are usually within around 7%.

8.2.8.2 Test vs Predicted

Performance of almost all aspects has met the expectation except for vacuum integrity. The fact that condensation could be produced with the assistance of the vacuum pump indicates that the refrigeration system is capable of reaching sub-dew-point temperatures. The occasional excursion below dew-point has caused the evaporator to show signs of surface rust near the base of the fins.

Ejector vacuum has not met with the expectations. The 2kPa depression is some way off the expected 5kPa required. Several variants of the ejector nozzle have been machined and tested without any marked improvement. The cleaning of the scale in the ejector and the stainless steel nozzle has helped and the use of an aluminium nozzle shows performance deterioration in a matter of days due to a white oxide build-up, possibly as a result of air ingress and oxygen induced corrosion.

At the elevated temperatures inside the evaporator, corrosion is a real problem. Chromed steel fittings have a life of around two months after which the chrome plating begins to lift from corrosion under the plating, the flakes of this corrosion block the collector's lower tube and prevents the valves from sealing off. Galvanised fittings have a lifetime of around three to four weeks until visible rust has coated the wetted parts and discoloured the water.

Figure 8.3: Comparison of Measured and Calculated Energy Inputs, 16 & 17 July 2017

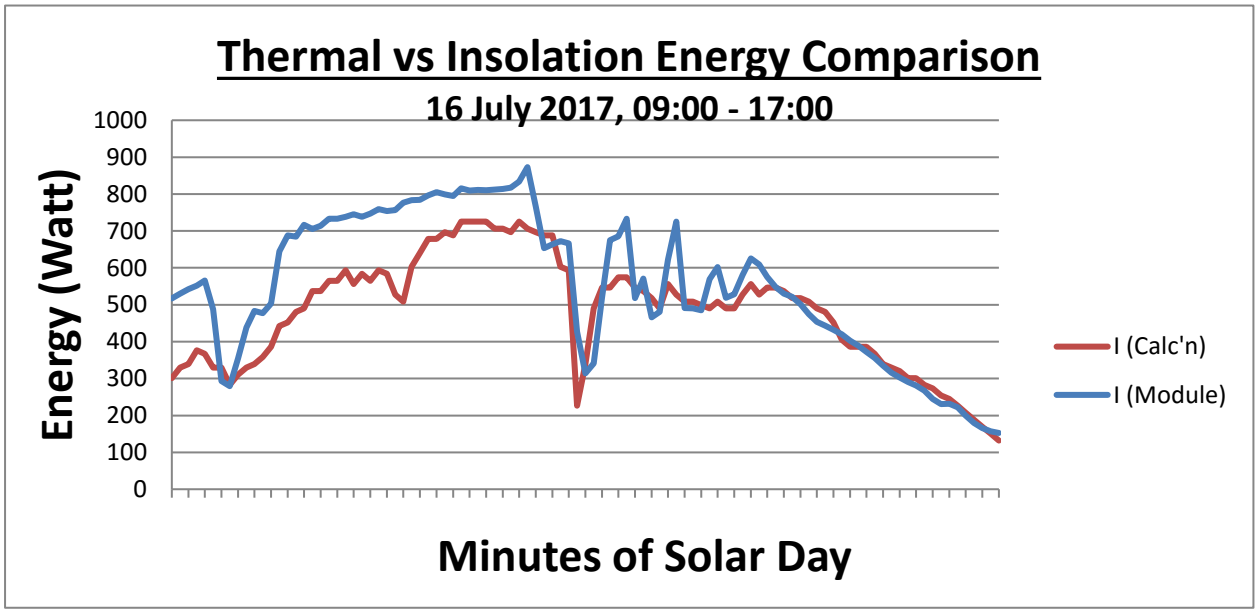

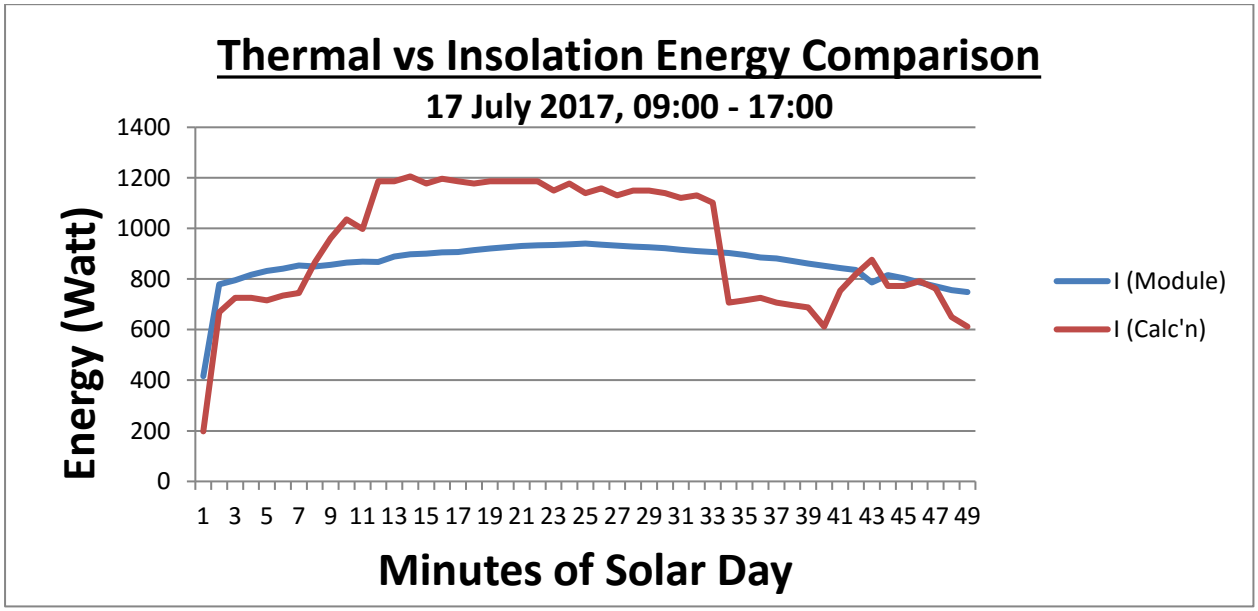

The condensation capacity appears to be more than adequate. The temperature profile across the Plenum shows a temperature drop of between 30 and 35 degrees, the radiator temperature drop reduces this temperature to around 7 degrees above ambient temperature.

8.2.8.3 Circulation Flowrate

Figure 8.4: Comparison between Calculated Flowrate and Derived Rate

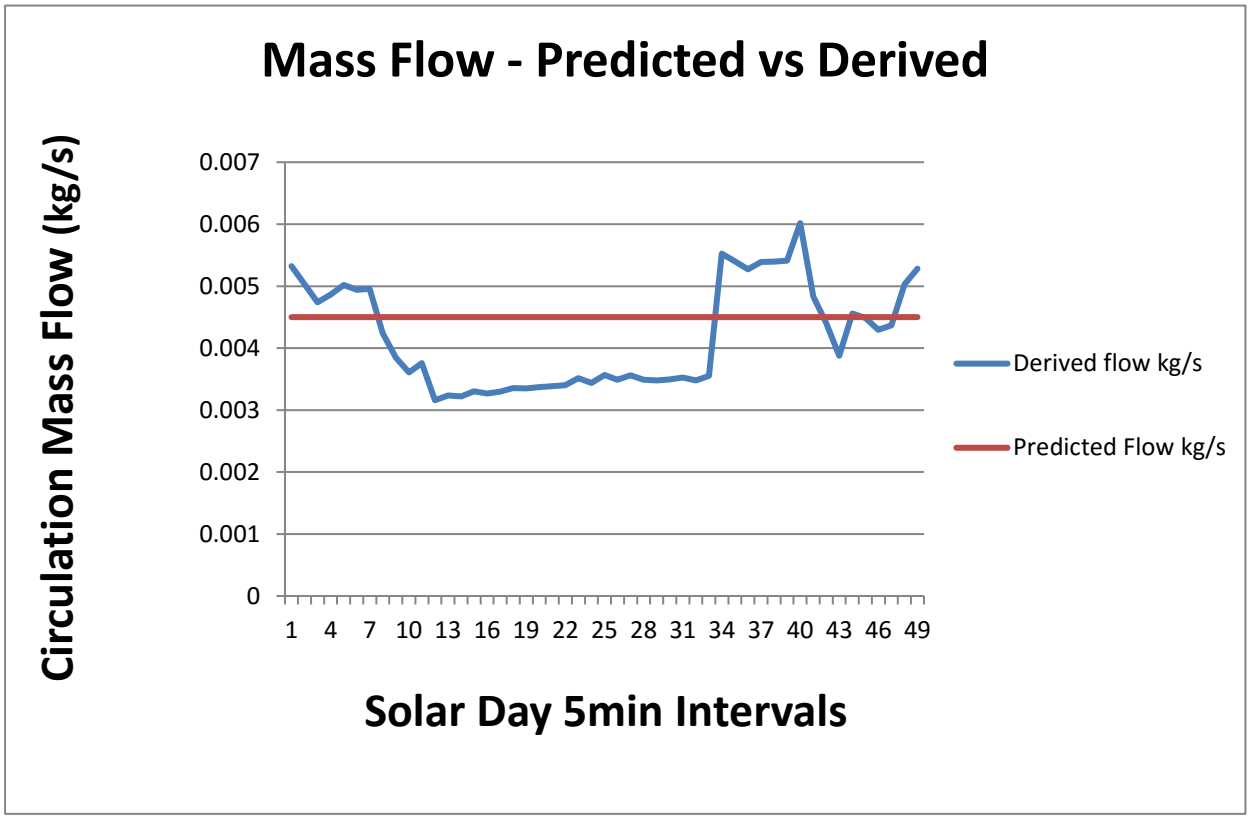

The plot above in Figure 8.3 shows the comparison between the calculated flow-rate using the differential pressure from heating and density change, corrected for friction in the heater as compared to the dynamic real measurement of temperature change and heat absorption equated to the measured heat input. The small sample above is indicative of the larger picture – although excursions due to vapour in the liquid flow cause surging and clouds and birds to have an effect on the heater, the long averages are very comparable and always a little lower for those reasons.

8.2.8.4 Terminal Temperature

As described previously in paragraph 7.1.1, the average stagnation temperature of the dry collector unit was measured at 97.5°C using the module radiation figure. The design model predicted 112°C at an emissivity of 0.8. Using an emissivity of 0.96, the predicted stagnation temperature matches the measured value.

8.2.8.5 Pressures – Actuals and Differentials

Pressure readings generally follow the Steam Tables with no anomalies seen. The steam produced is very wet and has no opportunity of gaining superheat under normal operation. For this reason the ejector feed tube is constantly draining condensate back to the evaporator, despite the insulation that is provided.

8.2.8.6 Refrigeration and COP

The refrigeration effect can hardly be noticed. This is due to several factors. The ejector is designed to discharge an extremely low density vapour in the order of 150 cubic metres per kilogram specific volume, in order to achieve the velocity dynamics that is required for a good vacuum performance. Across the duration of the project there have been very few occasions where the vacuum has been maintained under 10kPa (abs).

The sample occasions where the equipment managed to operate long enough to reduce the evaporator temperature to approach dew point, were mainly managed tests and usually with the aid of a vacuum pump to periodically remove air.

8.2.8.7 Water Harvest

The presence of water was seen on the occasions when dew point was reached. This was observed as a wetting of the shell of the evaporator rather than the fins and the formation had to be wiped off due to the thin film not developing enough to roll away by gravity.

CHAPTER 9

CONCLUSIONS

9.1 CHOICE OF WATER AS REFRIGERANT

Water as refrigerant has the attraction of a very large latent heat of evaporation. The extremely high specific volume at useful temperatures as well as the extremely low pressures required at those useful temperatures at the base of the hyperbola approaching absolute zero pressure, unfortunately outweigh any benefits to be gained and render the use of it impractical for this application.

9.2 ENERGY EFFICIENCY AND COMPARISONS

The system as monitored produced predictable performance in most aspects, with the exception of the vacuum performance and the direct effect of disappointing water production. The test results indicate only small losses in the collection of solar energy and generation of steam which is encouraging for other prospects of solar derived steam without very deep vacuum applications.

9.3 FUTURE DEVELOPMENTS FOR A WORKABLE SOLUTION

The system, as it has developed in the search for workable solutions, is at a point where it can be made more effective, reliable and water productive. In order to achieve this, the following additional work is required:

- The entire system should be made from a stainless steel material and treated for corrosion (pickled and passivated).

- The system scale should be much larger, say 50kW or larger. The problem with the small scale is the tiny parts of ejector and pumping systems that make precision dimensions difficult and clog up more readily than say a large ejector steam nozzle. The small scale is impractical for a water refrigerant.

- All joints should be seal welded since the rankine pressure jump is required to be a submersible pump built into the system with no external interfaces but for a vacuum tight cable gland.

- The system will need some form of vacuum ejector to remove incondensable gases. Despite the best seal achieved and long term vacuum integrity, there appears to be a source of gas which forms inside the hermetic envelope.

- The water produced was visibly clear. The author has on occasion tasted the water with no comment other than the test environment allowed some dust contamination due to the limestone desert environment. In order to produce fully potable water, future enhancements may well include a low pressure circulation system utilising a coarse filtration for dust and organics and followed by a charcoal filtration for dissolved contaminants. For full coverage against any harmful agent, the above circulating flow may be further enhanced by exposure to a UV light source to neutralise any bacterial content. The power requirement for these measures would be minimal due to low flow and low head circulation. Ultraviolet light sources are also available in very low wattage DC fluorescent tube form.

Despite all of the above, the modern trend to water harvesting is leaning in favour of the desiccant type systems which do not rely on refrigeration and which are highly energy efficient.

REFERENCES

1. Rosegrant, M W. World Water and Food to 2025 - Dealing with Scarcity. International Food Policy Research Institute. HD1691.R66 2002: 2002.
2. Unesco. Water, a Shared Responsibility. United Nations. UN-WWAP 2006/3: 2006.
3. UNICEF and WHO. Drinking Water Equity, Safety and Sustainability. WHO/UNICEF Joint Monitoring Programme (JMP). WA 675:2011
4. Unesco. Water, a Shared Responsibility. United Nations. UN-WWAP 2006/3: 2006.
5. El-Dessouky H et al. Evaluation of steam jet ejectors. Chemical Engineering and Processing. 2002; Vol 41: 551-561.
6. Nikolayev V S et al. Water Recovery from Dew. Journal of Hydrology. 1996; Vol 182: 20-23.
7. Beyens D et al. Comment on “The Moisture from the air as water resource in arid region: Hopes, doubts and facts” by Kogan and Trachtman. Journal of Arid Environments. 2006; Vol 67: 343.
8. Solar Water Supply. Article in Muscat Times, 13 January 2015
9. Pridasawas W., Lindqvist P. An exergy analysis of a solar-driven ejector refrigeration system. Solar Energy. 2004; Vol76: 369-379
10. Pridasawas W. Solar-Driven Refrigeration Systems with Focus on the Ejector Cycle. Stockholm: KTH: 2006
11. Kiliscarslan A., Muller N. A Comparative Study of Water as a Refrigerant with some Current Refrigerants. International Journal of Energy Research. 2005; Vol 29: 947-959.
12. Khurmi R S. A Textbook of Refrigeration and Air Conditioning. 8th Edition. New Delhi: Eurasia Publishing: 1999.
13. Zhengshu D et al. Ejector Performance of a Pump-less Ejector Refrigeration System Driven by Solar Thermal Energy. Paper presented at: IRACC 2012: Proceedings of the International Refrigeration and Air Conditioning Conference; 2012 Jul 16-19; Purdue USA; Purdue E-Pubs 2012. 2412/1-9.
14. Huang B J et al. Development of an ejector cooling system with thermal pumping effect. International Journal of Refrigeration. 2006; Vol 29: 476-484.

15. Huang B J et al. A Solar Ejector Cooling System using Refrigerant R141b. Solar Energy. 1998; Vol 64: 223-226.
16. Shen S. et al. Study of a Gas-liquid Ejector and its application to a Solar-powered Bi-ejector Refrigeration System. Applied Thermal Engineering. 2005; Vol 25: 2891-2902.
17. Elhub B et al. Review of ejector design parameters and geometry for refrigeration and air conditioning application. Paper presented at: RES 2015: Proceedings of the 8th International Conference on Renewable Sources; 2014 Apr 23-25; KL Malaysia; Kuala Lumpur: WSEAS 2014. 54-66.
18. Pereira PR et al. Experimental Results with a Variable Geometry Ejector using R600a as Working Fluid. International Journal of Refrigeration. 2014; Vol 46: 77-85.
19. Scott d. et al. CFD Simulations of a Supersonic Ejector for use in Refrigeration Applications. Paper presented at: International Refrigeration and Air Conditioning Conference; 2008 Jul 14-17; Purdue USA; 2159/1-8
20. Cassie A.B.D. et al. Wettability of porous surfaces. Transactions of the Faraday Society. 1944; 546 - 551
21. Wenzel R N. Resistance of solid surfaces to wetting by water. Industrial Chemical Engineering. 1936; Vol 28(8):988
22. Choi C et al. Wettability Effects on Heat Transfer, Two Phase Flow, Phase Change and Numerical Modelling. [Internet]: InTech; 2011 September. Available from: http://www.intechopen.com/books/two-phase-flow-phase-change-and-numerical-modelling/wettability-effects-on-heat-transfer.

ATTACHMENT 1

OVERVIEW OF COMMERCIAL WATER-FROM-AIR EQUIPMENT

Overview of Commercial Water-from-Air Equipment*

SMALL WATER FROM AIR DEVICES - COMMERCIAL OFFERINGS								
SUPPLIER	**MODEL**	**TECHNOLOGY**	**ENERGY** **Watts**	**SOURCE**	**OUTPUT** **kg/24hrs**	**PRICE** **USD**	**SALE**	**COMMENT**
1 - Watair	Air Juicer	Vapour Compression	0.495	Grid	24	999.00	Retail	Indoors model - office & domestic
2 - Shenzen FND	F20	Vapour Compression	0.400	Grid	20	1780.00	Import	5 Indoors models - office & domestic
3 - Air Solar Water	A2WH	Desiccant	0.200	Solar	1.5	2890.00	Retail	Outdoors unit. Can be mounted in series
4 - Planets Water UK	AWG-30H/O	Vapour Compression	0.450	Grid	30	Not Listed	-	Indoors model - office & domestic
5 - Water from Air	AW3	Vapour Compression	0.430	Grid	32	Not listed	-	Indoors model - office & domestic
6 - Ecoloblue	30E	Vapour Compression	0.450	Grid/Solar	30	799.00	Retail	Basic Indoors model - office & domestic
7 - Ecoloblue	30X	Vapour Compression	0.450	Grid/Solar	30	1299.00	Retail	Also Heats and Cools - office & domestic
8 - VICI Labs	Waterseer	Condensation	Various	Wind	39	134.00	Retail	Outdoors unit

* Brochures and partial specifications from various retail suppliers are attached for information

ATTACHMENT 2

PROCESS DIAGRAMS

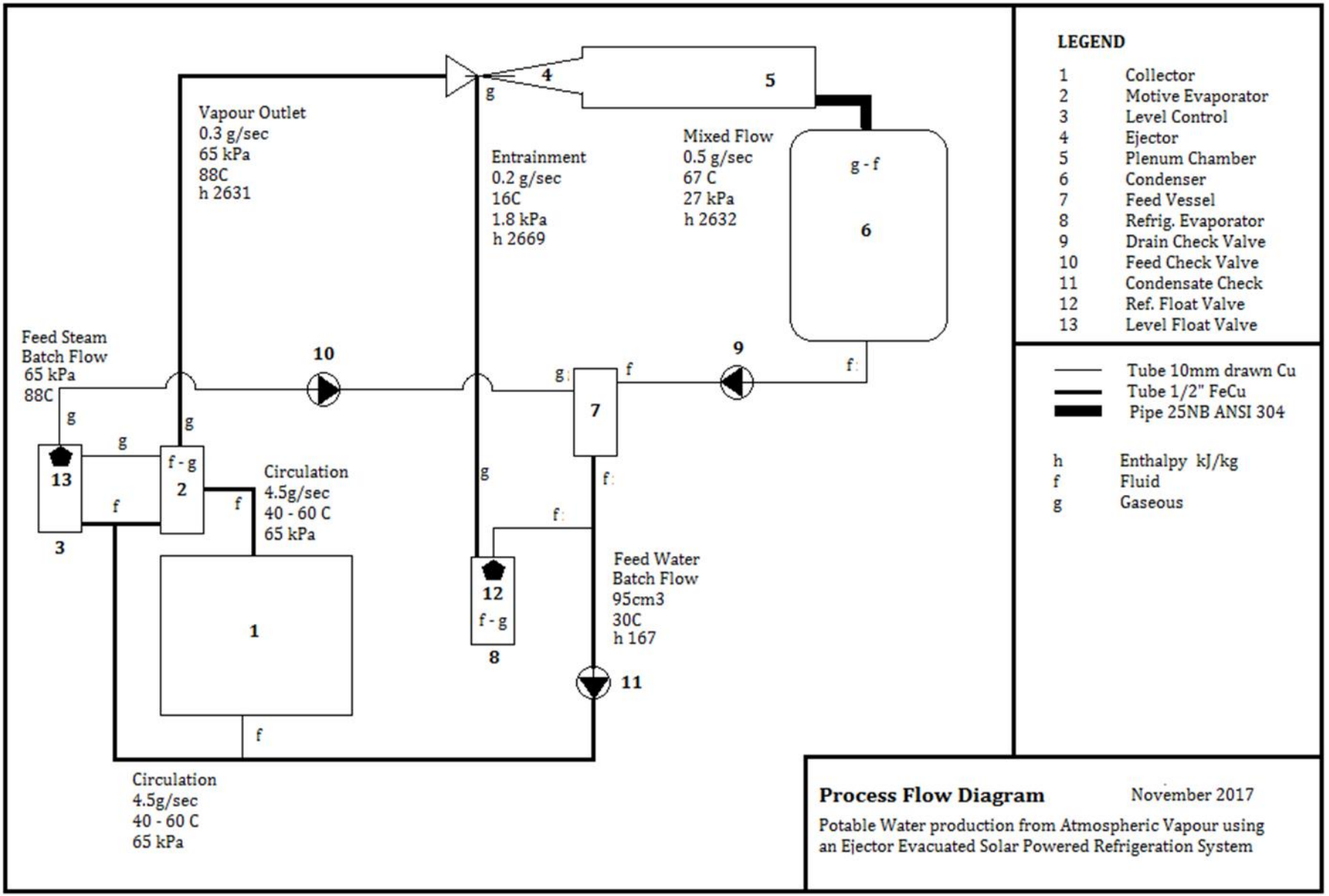
Vapour Outlet
0.3 g/sec
65 kPa
88C
h 2631
Entrainment
0.2 g/sec
16C
1.8 kPa
h 2669
Mixed Flow
0.5 g/sec
67 C
27 kPa
h 2632
Feed Steam
Batch Flow
65 kPa
88C
Circulation
4.5g/sec
40 - 60 C
65 kPa
Feed Water
Batch Flow
95cm3
30C
h 167
Circulation
4.5g/sec
40 - 60 C
65 kPa
1
2
3
4
5
6
7
8
9
10
11
12
13
g - f
f - g
LEGEND
1 Collector
2 Motive Evaporator
3 Level Control
4 Ejector
5 Plenum Chamber
6 Condenser
7 Feed Vessel
8 Refrig. Evaporator
9 Drain Check Valve
10 Feed Check Valve
11 Condensate Check
12 Ref. Float Valve
13 Level Float Valve
Tube 10mm drawn Cu
Tube 1/2" FeCu
Pipe 25NB ANSI 304
h Enthalpy kJ/kg
f Fluid
g Gaseous
Process Flow Diagram
November 2017
Potable Water production from Atmospheric Vapour using
an Ejector Evacuated Solar Powered Refrigeration System

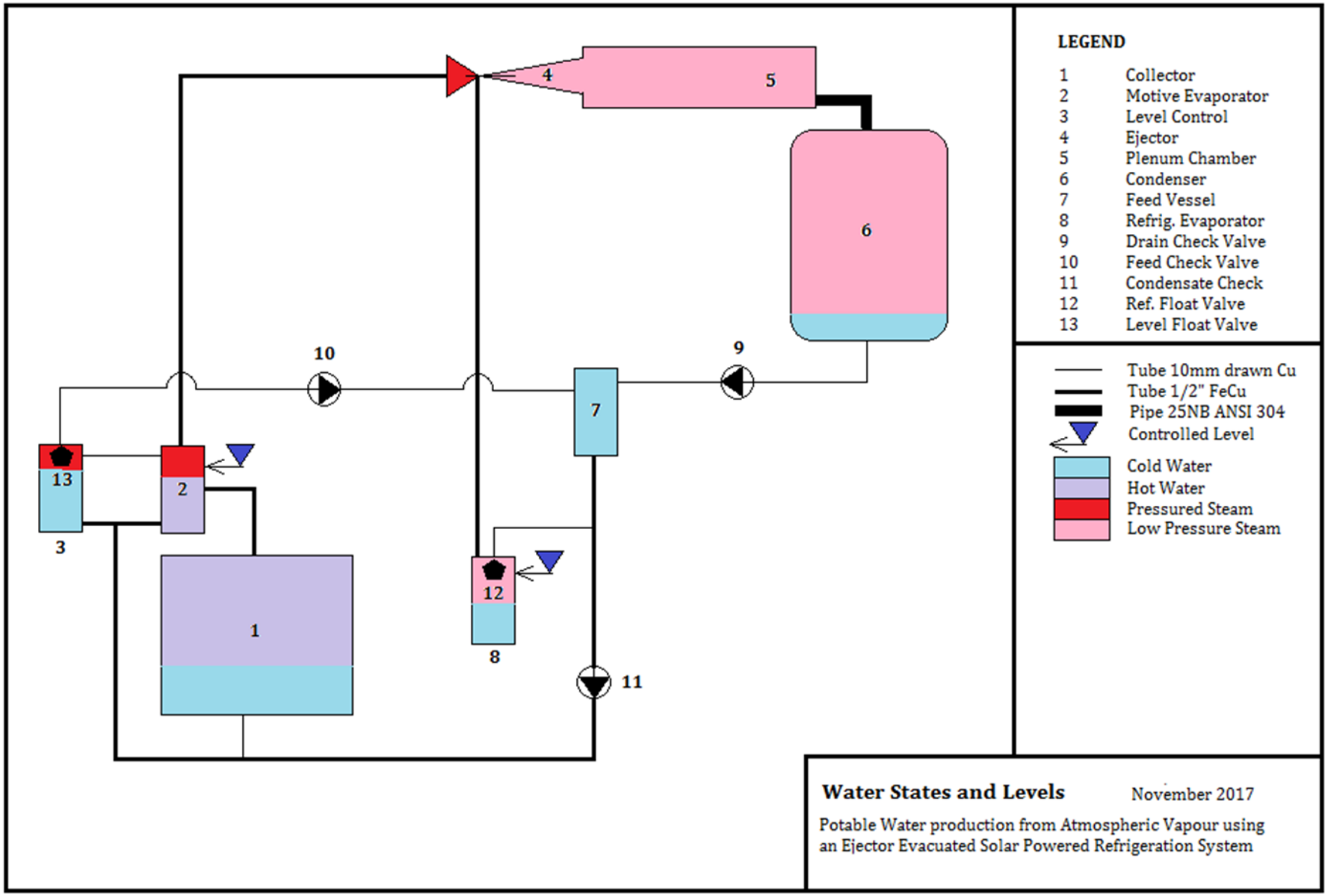
LEGEND
1 Collector
2 Motive Evaporator
3 Level Control
4 Ejector
5 Plenum Chamber
6 Condenser
7 Feed Vessel
8 Refrig. Evaporator
9 Drain Check Valve
10 Feed Check Valve
11 Condensate Check
12 Ref. Float Valve
13 Level Float Valve
Tube 10mm drawn Cu
Tube 1/2" FeCu
Pipe 25NB ANSI 304
Controlled Level
Cold Water
Hot Water
Pressured Steam
Low Pressure Steam
Water States and Levels
November 2017
Potable Water production from Atmospheric Vapour using an Ejector Evacuated Solar Powered Refrigeration System

ATTACHMENT 3

PIPING AND INSTRUMENTATION DIAGRAM

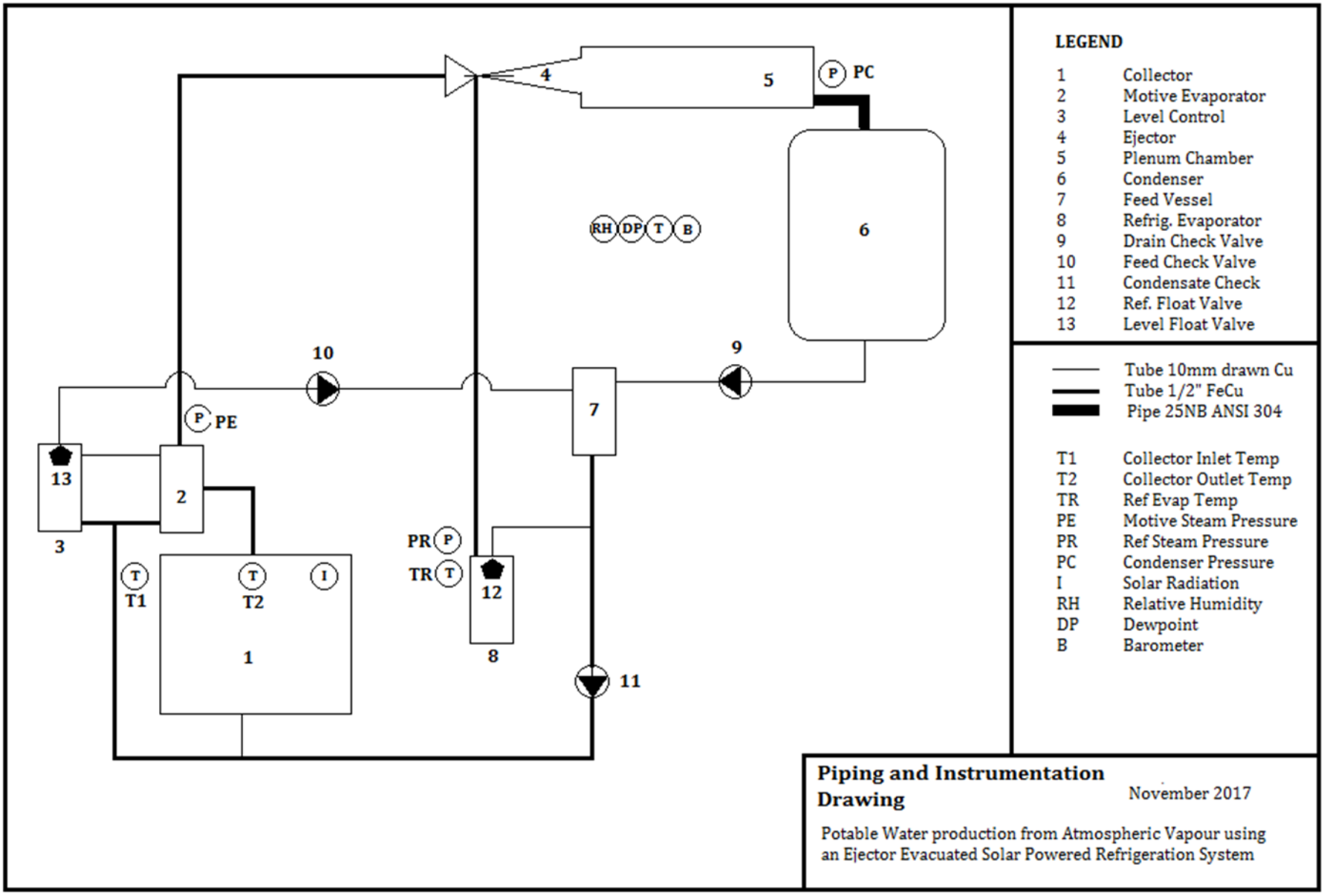

LEGEND

1	Collector
2	Motive Evaporator
3	Level Control
4	Ejector
5	Plenum Chamber
6	Condenser
7	Feed Vessel
8	Refrig. Evaporator
9	Drain Check Valve
10	Feed Check Valve
11	Condensate Check
12	Ref. Float Valve
13	Level Float Valve

Tube 10mm drawn Cu
Tube 1/2" FeCu
Pipe 25NB ANSI 304

T1	Collector Inlet Temp
T2	Collector Outlet Temp
TR	Ref Evap Temp
PE	Motive Steam Pressure
PR	Ref Steam Pressure
PC	Condenser Pressure
I	Solar Radiation
RH	Relative Humidity
DP	Dewpoint
B	Barometer

Piping and Instrumentation Drawing

November 2017

Potable Water production from Atmospheric Vapour using an Ejector Evacuated Solar Powered Refrigeration System

ATTACHMENT 4

COLLECTOR PLATE DESIGN AND CONSTRUCTION

Symbols and Constants

SYMBOL	QUANTITY	VALUE	UNITS
A	Exposed collection area of collector	-	m^2
A_c	Cross sectional area of collector plate	-	m^2
A_h	Total heat conduction area of plate	-	m^2
W	Width of collector plate	-	m
t_s	Thickness of collector plate	-	m
Q_1	Heat absorbed per tube	-	J/sec
k	Conductive heat transfer co-efficient	-	W/mK
ΔT	Temperature differential	-	K
z	Linear distance of heat conduction	-	m
L	Length of Collector Plate	-	m
N	Number of tube passes	-	ea
$\dot{m}$	Specific mass flow	-	kg/s
I	Solar Insolation	-	W/m^2
k_s	Conductive heat transfer co-efficient for Steel	36.35	W/mK
σ	Stefan-Boltzmann constant	5.676 E-8	W/m^2K^4
ϵ	Emissivity of black matt paint	0.8	No unit
K	Extinction coefficient for green glass	0.15	-/cm
Y	Glass thickness	-	cm
Re	Reynolds Number	-	No unit
v_t	Theoretical flow velocity	-	m/s
v_a	Actual flow velocity	-	m/s
P_f	Pressure loss due to friction	-	Pa
P_v	Dynamic pressure	-	Pa
f_D	DÁrcy friction factor	-	No unit
f_F	Fanning friction factor	-	No unit
Q_v	Volumetric flow rate	-	m^3/sec
ρ_{xx}	Water density at xxx condition	-	kg/m^3

Solar Collector Design

1.0 Introduction

The purpose of this collector is to heat a given quantity of water beyond boiling point at a given vapour pressure, to supply vapour to the ejector system and to recirculate and reheat the water that does not evaporate. This function is to be achieved at best cost and effectivity of the component.

To produce a cost effective collector with acceptable performance it is decided to use a Tube-on-Plate type collector. The tube nest is manufactured separately and attached to the collector plate by adhesion with a high conductivity bonding material **(1:60)**.

1.1 Description and Material Selection

For reasons of cost control, mild carbon steel is selected for the fabrications material of the collector plate. Copper tube is used for the collector tubing construction.

The housing is manufactured from commercially available extruded aluminium to be corrosion free, rigid and light. The insulation layer is mineral wool insulation and the cover is constructed from 6mm clear glass.

For the purpose of the prototype, the glass cover is a high quality toughened material which was salvaged from a breaker's yard. Normally a plain 'green glass' would be used where access to the unit is limited to adult, competent persons and the site is not prone to rapid weather variations of temperature or hail. The test installation is some 10m above ground and away from tampering by the public. The relevant safety precautions are observed when working with this material.

A foil coated reflective backing board of 10 mm fibre board is attached to contain the backing insulation. The backing board is soaked with enamel paint to render it weatherproof for the test duration.

The unit is intended for mounting at the flat roof of the test site. It is supported on two skids via four legs, all fabricated from extruded aluminium tubing and initially set up at an angle of 24 degrees above the horizon, which is the geographical latitude of the test site. Changes in angle and levelling are achieved by raising or lowering any of the legs by means of adjuster bolts on the extremities of the skids.

The area used for the absorber plate aperture is exactly 1m wide and 1m long which should collect around 1000 Joules of heat energy per second under normal conditions, in this region.

Basic dimensions and design and modelling guidelines are sourced from the publications as referenced in the Bibliography.

1.2 Position in the Process Flow Diagram

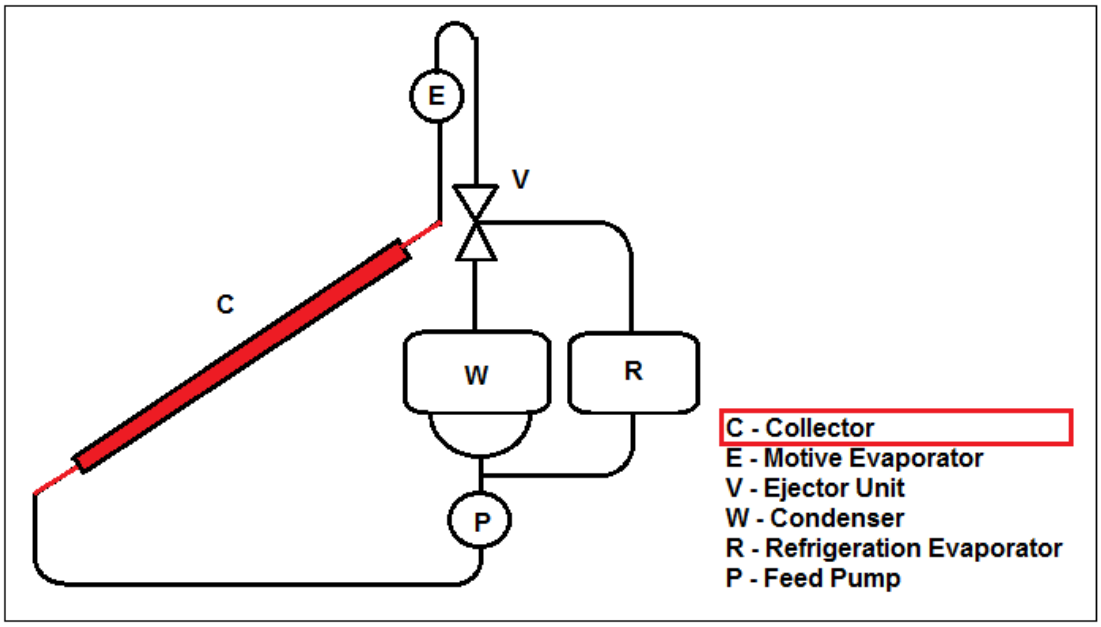

2.0 Physical Design

2.1 Stagnation Temperature

A solar collector which has a zero or stagnant cooling flow rate will rapidly heat up to the point where the energy rejected by the device is equal to the energy collected by the device. At this point a maximum or peak outlet temperature is attained. It is important to know the value of this stagnation temperature for the purpose of materials selection for high heat and pressure applications, especially where plastics and other fusible materials are potentially to be used. The International Standards Organisation (ISO) has a prescribed stagnation test method for commercially produced domestic solar heaters in Europe.

The flow rate of this heater design will be proportionally lower than a header type design due to the higher friction loss over one long tube. Similarly, the temperature reached will subsequently be higher on the first cycle due to the extended residence time. The energy effectivity of the two basic designs differs in that the single tube unit has a greater average differential temperature and subsequently reaches temperature in one heater flow cycle, so that under ideal circumstances, recirculation flow is the result only of evaporative cooling on the unevaporated (recirculating) flow mass.

The estimation of the stagnation temperature [2:437] is found using the radiation constant for sunshine, the Stefan Boltzmann constant of 5,670367 E-8 W/m^2K^4.

The surface of the heater is coated with a selective absorptive coating, emissivity co-efficient approximated at $\epsilon = 0.96$ **(2:443)**

For sunshine, the Insolation required to produce a given temperature is -

$$I = \epsilon \times \sigma \times T^4 \times A$$

Similarly,

$$T^4 = I / (\epsilon \times \sigma \times A)$$

$$T^4 = 1000 / (0.96 \times 5.670367\ E\text{-}8 \times 1)$$

$$\boldsymbol{T = 368.1\ K\ (94.9°C)}$$

This temperature assumes no energy loss through the glass.

The glass used is a medium quality material with Extinction Co-efficient of 0.1/cm. The range for glass is 0.05/cm for crystal quality and 0.25 for plain "green" window glass.

According to Bouguer's Law **(1:67)**, glass transmittance will be –

$$\tau_\alpha = e^{-Ky}$$

Hence, for a glass cover of 0.6cm -

$$\tau_\alpha = e^{-0.5 \times 0.6}$$

$$\boldsymbol{\tau_\alpha = 0.942\ or\ 94.2\ \%}$$

The equivalent stagnation temperature for a glass transmissivity of 94.2 % will be –

$$T^4 = (I \times \tau_\alpha) / (\epsilon \times \sigma \times A)$$

$$\boldsymbol{T = 362.6\ K\ (89.4°C)}$$

2.2 Heat Allocation per Tube

To determine the tube spacing across the collector, it is essential to note that the heat collected in the plate should conduct freely to the tube and that the heat absorbed per tube remains fairly constant. Initially, the conduction of heat to each tube needs to be estimated -

The cross-sectional heat conduction area of the collector plate A_c is –

$$A_c = W \times t_s$$

Where L is the width of the exposed collector plate and t is the plate thickness. The basic design requires a width of 1m and initially a standard plate of 2mm is selected.

$$A_c = 1 \times 0.002$$

$$\boldsymbol{A_c = 0.002\ m^2}$$

Heat is conducted into the tube from either side so that the feed area is doubled –

$$A_h = Ac \times 2$$

$$\boldsymbol{A_h = 0.004\ m^2}$$

The heat conducted per tube would be –

$$Q_1 = k \times A \times \Delta T / z_{mean}$$

The heat absorbed per tube would be –

$$Q_1 = I/N$$

The edges of the collector have half pitch spacing at either end so that N tube pitches at 2z spacing exactly equals L –

$$L = 2 \times z \times N$$

$$z = L / 2N$$

But, z expressed in this way is a maximum and $z_{min} = 0$ so that $z_{mean} = z/2$

Therefore, combining the above equations –

$$I/N = k \times A_h \times \Delta T \times N / L$$

$$I = k \times A_h \times \Delta T \times N^2 / L$$

From initial Insolation tests, assume I = 1000W/m^2 at a transmittance of 0.942 and conduction heat transfer co-efficient of 36.35 W/m^2K

For an ambient temperature estimated at 40°C and a stagnation temperature of 89.4°C and allotting equal temperature differentials for heat sourcing as heat sinking, ΔT will be estimated at (89.4 – 40)/2 or 24.7°C .

So that –

$$1000 \times 0.942 = 36.35 \times 0.004 \times 24.7 \times N^2/L$$

$$\boldsymbol{N = 16.2\ Tubes\ (say\ 16)}$$

The tube total length will be somewhat shorter than 16m; a 14m length is estimated.

The tube Pitch is then –

$$\boldsymbol{L/N = 1000/16 = 62.5mm}$$

2.3 Dynamic Flow Analysis

For a once-through design, water is to be heated from 40°C to say 90°C to yield a ΔT of around 50°C from a heat source of 1000 Joule/sec. For a generalized Specific Heat Capacity for water 4,187 k J / kg K, required water mass flow for the required heat absorption is –

$$\dot{m} = 1000/ (4187 \times 50) = \underline{\mathbf{0.00478\ (ave)\ kg/s}}$$

Volumetric flow is then -

$$0.00478/992.5 = \underline{\mathbf{4.88\ x^{-6}\ m\hat{}3/sec}}$$

Water density of 992.5kg/m^3 at 40°C and 965kg/m^3 at 90°C, average 978kg/m^3.

The heater is mounted such that the difference in elevation between hot and cold legs is 570mm.

Hot column pressure -

$$P_h = \rho_{ave} \times g \times h$$

$$P_h = 978 \times 9.81 \times 0.57$$

$$\mathbf{P_h = 5467\ Pa}$$

Cold Column Pressure –

$$P_c = \rho_c \times g \times h$$

$$P_c = 992.5 \times 9{,}81 \times 0.57$$

$$\mathbf{P_c = 5548\ Pa}$$

Motive Pressure $P_v = P_c - P_h$

$$\mathbf{P_v = 81\ Pa}$$

Theoretical maximum velocity $v_t^2 = 2 \times P_v / \rho_{ave}$

$$v_t^2 = 2 \times 81/978$$

$$\mathbf{v_t = 0.406\ m/s}$$

2.4 Friction Losses

Determine Reynolds number assuming tube internal diameter of 10mm –

$$Re = \rho_{ave} x\, v_t\, x\, d / \upsilon$$

$$Re = 978 \times 0.406 \times 0.01 / (0.451 \times 10^{-3})$$

$$\boldsymbol{Re = 8867}$$

NB - Flow is in the turbulent zone, Use Moody diagram[2:209] to determine Fanning friction factor

Fanning factor 0.009, whether turbulent or laminar for such a light flow in a smooth bore tube. Hence the friction pressure loss -

$$P_f = \rho_{ave} \times g\ (2 \times f_f \times L \times v_a^2 / dg)$$

$$P_f = \rho_{ave}\ (2 \times f_f \times L \times v_a^2 / d)$$

$$P_f = 978\ (2 \times 0.009 \times 14 \times v_a^2 / 0.01)$$

$$\boldsymbol{P_f = 24\ 645\ v_a^2 \quad Pa}$$

Assuming that all motive pressure energy is converted to friction loss –

$$P_f = P_v = 81\ Pa$$

$$\boldsymbol{v_a = 0.0573 \quad m/s}$$

This equates to a mass flow in 10mm tubing of $\mathbf{4.5 \times 10^{-6} m^3/s}$ which equals a mass flow of 0.0046kg/s which closely matches the thermal equation flow result.

2.5 Summary – Basic Design

Area = 1m x 1m of exposed plate 2.0mm thick

Tube are 10mm bore, 16 pitches at 62.5mm apart.

Tube os continuous and placed in a flat convoluted pattern.

Design flow is 4.6 g/sec or 4.5 cm^3/sec.

3.0 Sourcing and Construction

3.1 Sourcing of Materials

The various components of the heater were manufactured and supplied as follows

Glass Covers – Salvaged from shop front windows, supplied by Al Ouhi Aluminium and Carpentry of A's Sinaiah, Sohar. Two covers were sourced whilst material was available.

Frames – Frames with an internal aperture of 1m + - 1mm were manufactured by Sinaiah Extruded Aluminium Works of Sohar. Two frames were supplied. The rectangular tube legs and skids were also provided from this supplier.

Backing board – This was provided rough cut by Al Ouhi and finished by the author.

Collector plate and tube nest – This part was manufactured by Middle East Engineering and Marine Services at New Airport Industrial, Falaj Al Ouhi. The unit was deformed from welding and required some tweaking to make it work.

Insulation – Two 25mm sheets of medium density mineral wool insulation was provided by Cape East Contractors of Industrial Free Zone Sohar.

3.2 Construction

The unit was constructed as follows –

- The framework was assembled upside down on a flat floor (Photo 4.1).
- The collector plate was prepared and fitted inside the frame using 20mm slotted wooden blocks for spacing after drilling the inlet and outlet tube ports. (Photo 4.2)
- The back of the tube nest was coated with aluminium tape and the edges sealed with high temperature spray epoxy foam sealant. (Photo 4.3 and 4.4)
- The foam sealant was allowed to cure and then trimmed to make way for the mineral wool.
- The mineral wool was placed against the tube nest and securely taped in position. (Photo 4.5)
- The backing board was soaked with enamel paint for waterproofing. The inner surface was covered with heavy duty aluminium foil and the cover then placed in position and secured with self-tapping screws.
- The legs were trial fitted (Photo 4.6) and then the whole unit was moved to the test site on the flat rooftop.
- The leg assemblies were attached and the unit provisionally positioned and levelled.
- The top edge of the frame was lined with dual sided mirror tape and the glass cover fitted in position. Self-tapping screws were attached at the lower edge and sides as a safety precaution against the failure of the adhesive tape.

4.0 Testing and Development of the Collector

4.1 Development of the Heater Unit

The first unit was fabricated in May 2013 using a fibre board frame and plywood backing. This selection did not resist the weather, despite many attempts to weatherproof the unit. The heater core and glass were salvaged for use in a second unit. No useful test results were obtained from this unit, the measurements being inconsistent and falling well short of expected results.

The second heater fabricated in June 2014 used extruded aluminium for the frame, automotive window adhesive for the glass seal and a rigid backing of fibre board impregnated with highly thinned polyurethane varnish. This unit managed to withstand the test site conditions and allowed some substantial tests to be carried out.
Despite a healthy stagnation temperature, which is a result of a properly sealed and insulated frame, the thermo siphon outlet temperature remained significantly high due to low mass flow, which in turn produced heat absorption figures well below the design expectations. Forced flow tests using a calibrated pump showed that the heat absorption rate was well within expectations, indicating that collector plate area, weld areas and tube length were adequate. The unit was dismantled and it was discovered that the fabricator had used tubing of 8mm bore and not the design inside diameter of 10mm or the 3/8" imperial equivalent, a fact which was not obvious at the time of delivery. The result of this error caused the thermo siphon flow rate to be reduced and the rate of heat absorbed was below expectations. A further setback was the onset of corrosion in the carbon steel tubing due to the open system during testing, causing discolouration and silting of the tubing from corrosion products. The use of this heater was stopped on 28th September 2014 to prepare a third unit.

The third heater design variant was identical in most aspects with the exception of the tubing bore.

5.0 Bibliography

1. Kothari DP, Singal K C, Renewable Energy Sources and Emerging Technologies. 2nd Edition. Delhi: Asoke Ghosh; 2013.
2. Welty J R, Wicks C E, Wilson R E, Fundamentals of Momentum, Heat and Mass transfer. 3rd Edition. Wiley: New York; 1984.
3. Papalambros Y, Wilde D J, Principles of Optimal Design. 2nd Edition. Cambridge: Cambridge; 2003.

6.0 Photographs

Photo 4.1 Extruded Aluminium Frame

Photo 4.2 Wooden Cleats for Collector Frame Attachment

Photo 4.3 Tube Bonded to collector Plate

Photo 4.4 Edge Insulation Completed

Photo 4.5 Insulation Mat Fitted

Photo 4.6 Underside Completed with Skids

Photo 4.7 Rooftop Assembly in Progress

ATTACHMENT 5

TRANSCRIPT OF THE BASIC MODEL

TRANSCRIPT OF THE BASIC MODEL

CONTENT

Operational Model to Predict Performance

OPERATIONAL MODEL TO PREDICT PERFORMANCE

This model uses fixed constants obtained from the Design Model to predict OUTPUTS under conditions dictated by the environmental INPUT conditions

ENVIRONMENTAL INPUTS		**SCHEMATIC**	1					
Ambient Temperature	ta	**40**	C		Dry Bulb Temperature			
Barometric Pressure	Pb	**101.3**	kPa					
Insolation	I	**1000**	W/m^2		min expected 700W, max expected 1050W			
Relative Humidity	RH	**40**	%					
DERIVED INPUTS								
Condenser Pressure		7.3584405	kPa		8.07131	1730.63	233.426	Antoine Constants < 100C
				Calc	A	m	Tn	
Vapour Saturation Pressure	Pws	73.8204537	HPa		6.116441	7.591386	240.7263	
Vapour Pressure	Pw	29.5281815	HPa					
Dewpoint Temperature	Td	23.8277479	C					
Evaporator Internal Pressure	Pc	13.7982074	mmHg		a	b	c	
Evaporator Core Temperature	Tc	16.2505726	C		8.07131	1730.63	233.426	
Exceed Dewpoint	delta Td	-7.57717531	C	(-) = BELOW DEWPOINT				

PROCESS								
Steam Generation								
Gross Input Energy	I	1000	Joule/sec		**Solar Insolation**			
Emmissivity	eta	0.8	co-eff		assumption			
Boltzmann constant	theta	5.67E-08	co-eff		reference			
Collector Area	A	1	m^2		actual			
Stagnation Temp (Theoretical)	Ts	385.323941	Kelvin		Emitted Energy = Eta x Theta x Area x Abs Temp^4			
Stagnation Temperature	Ts	112.173941	Celsius		maximum achievable temperature with this design			
Losses (typical)					am	pm	median	
Glass					0.15	0.08	0.126667	
Radiation					0.06	0.1	0.073333	
Conduction					0.06	0.09	0.07	
Efficiency	Nc	0.775	co-eff	Flechion, Lazzarin				
Nett Heat Energy Absorbed		**775**	Joule/sec					
Predicted Outlet Temperature K	tA	**361.535893**	K					
Predicted Outlet Temperature C	tA	**88.3858926**	C					
Steam Properties								
Temperature	tA	88.3858926						
Dryness Fraction	xA	0.92	dry		A	B	C	D
Enthalpy of Steam	hA	2631.89819	kJ/kg	sat	-6.14342E-05	0.001589	-2.36418	2500.79
Latent Heat of Steam	L1	2261.82646	kJ/kg	saturated	-6.14342E-05	0.001589	-2.36418	2500.79
Entropy of Steam	SA	6.03603667	kJ/kg					

PROCESS			2					
Flash Vapour Generation								
Flash Water Temperature		16.2505726	C	dewpoint - 0.5C				
R Evaporator Pressure		1.83961012	kPa	Calc	8.07131	1730.63	233.426	Antoine < 100C
Enthalpy of Dry Vapour		2530.56792	kJ/kg	sat	-6.14342E-05	0.001589	-2.36418	2500.79
Latent Heat	hfgB	2462.52677	kJ/kg	saturated	-6.14342E-05	0.001589	-2.36418	2500.79
Enthalpy of fluid	hfB	68.0411475	kJ/kg					
Entropy of fluid	SfB	0.24923497	kJ/kg					
Entropy of Vapour	SfgB	8.56685648	kJ/kg					
Dryness of expanded vap		0.67548718	dry					
Enthalpy of Wet vapour		1684.40526	kJ/kg					

PROCESS										
Mixing and Compression										
ASSUME Nn =0.88, Ne = 0.65, Nc = 0.8, STEAM IS 92% DRY						Assumptions corrected during field trials				
		hB	1731.44641	kJ/kg						
For Nn =	0.88	hB'	1798.10441	kJ/kg						
Dryness at B'		xB'	0.70255612	dry						
For Ne =	0.65									
Enthalpy of vapour at D		hD	2089.93223	kJ/kg						
Dryness at D		xD	0.82106359	dry						
xE =	0.92									
Enthalpy at E		hE	2333.56578	kJ/kg						
Entropy at E		SE	8.13074293	kJ/kg						
Liquid Enthalpy at F		hfF	167.48	kJ/kg						
Latent Heat at F		hfgF	2404.83384	kJ/kg	saturated	-6.14342E-05	0.001589	-2.36418	2500.79	
Enthalpy at vapour F		hF	2572.31384	kJ/kg						
Entropy at fluid F		SfF	0.61347985	kJ/kg						
Entropy of Vapour F		SfgF	7.20269048	kJ/kg						
dryness at F		xF	1.04367432	dry						
Nc =	0.8									
Enthalpy at F'		hF'	2632.00086	kJ/kg						
Entrainment Ratio ms/me		E	1.37766816	Ratio						
Entrainment Ratio me/ms (inverse)		e	0.7258642	Ratio						
Mass of Motive Steam		mv	0.00029446	kg/sec						
Mass of Entrainment		me	0.00021374	kg/sec						
Enthalpy of Entrainment		hC	2669.21196	kJ/kg						
Heat Removed		Re	0.53472289	kJ/sec						
Enthalpy of flash water		hfG	167.48	kJ/kg						
COP			0.73685452	: : 1						

PROCESS				
Condensation				
Total heat added to system	1309.72289	Joule/sec		
Total mass flow to condenser	0.00050821	kg/sec		
Temperature of Mixture	67.0903914	C	8.07131	1730.63	233.426
Enthalpy of condensate	167480	Joule/kg		
Heat in Condensate	85.114233	Joule/sec		
Heat Rejection	1224.60865	Joule/sec		

PROCESS									
Ejector Operation									
Vapour Pressure	Pp		65.83308	kPa	Calc	8.07131	1730.63	233.426	
Isentropic Index	n		1.038498	Index					
Nozzle Efficiency	Nn		0.88	Assumed					
Target nozzle outlet P	Pe		7.10844	kPa					
Nozzle Outlet Velocity	**Mp2**		**3.767186**	Mach					
Entrainment Velocity	**Mpe**		**6.957805**	Mach					
Nozzle outlet - Critical	M*p2		3.370641	Mach					
Entrainment - Critical	M*e2		5.053857	Mach					
Shock zone - Critical	M*4		2.454498	Mach					
Shock zone upstream velocity	M4		5.048219	Mach					
Velocity after compression	M5		0.056361	Mach					
Pressure ratio across shock wave	P5/P4		27.37532	Ratio					
CP process	P2=P3=P4		7.10844	kPa					
Pressure at end of mixing zone	P5		27.37532	kPa					
Pressure ratio across divergence	Pc/P5		1.00132	Ratio					
System pressure before condenser	Pc		27.41147	kPa					
Compression Ratio	Pc/Pe		14.90069	Ratio	Choked > 1.8				
Vapour Gas Constant	Rp		461.526	kJ/kg					
Area of Throat	A1		3.46E-06	m^2					
Diameter of throat	**D1**		**0.0021**	**m**		**2mm**			
Area Ratio mixer to throat	A1/A3		0.068906	Ratio	A1/A3 Correlation				
Area of mixer	A3		5.03E-05	m^2					
Diameter of mixer	**D3**		**0.008**	**m**		**8mm**			
Area Ratio nozzle outlet to throat	A2/A1		3.628118	Ratio	A2/A1 Correlation				
Nozzle Outlet Area	A2		1.26E-05	m^2					
Nozzle Outlet Diameter	**D2**		**0.004**	**m**		**4mm**			

Design Model to Determine Physical Dimensions

DESIGN MODEL TO DETERMINE PHYSICAL DIMENSIONS									
			1						
Quantity or Property	**Symbol**	**Nature**	**Value**	**Unit**	**Ref**				
ENVIRONMENTAL INPUTS									
Ambient Temperature	ta	Input	30	C					
Barometric Pressure	Pb	Input	101.3	kPa					
Insolation	I	Input	887.5	W/m^2					
Relative Humidity	RH	Input	40	%					
PROCESS									
Steam Generation									
Emmissivity	eta	assumed	0.96	co-eff	reference				
Boltzmann constant	theta	constant	5.67E-08	co-eff	reference				
Collector Area	A	measured	1	m^2	actual				
Inlet Temperature	T1	given	35	C	assume feedwater stagnation				
Efficiency of Steam Generation	Nc	assumed	0.771830986	co-eff	Flechion, Lazzarin				
Nett Input Energy			**685**	Joule/sec	Prisadawas				
Predicted Stagnation Temperature K	tA	calc	**357.3327099**	K	Of dry plate				
Predicted Stagnation Temperature C	tA	calc	**84.13270993**	C	Of dry plate				
Predicted Stagnation Temperature K	tA	calc	**334.9294416**	K	Of steam				
Predicted Stagnation Temperature C	tA	calc	**61.77944161**	C	Of steam				
Steam Properties									
Nozzle Inlet - Condition A									
Temperature	tA	calc	61.77944161						
Dryness Fraction	xA	calc	0.92	dry	ASSUMED	A	B	C	D
Enthalpy of Steam	hA	calc	2604.982779	kJ/kg	sat	-6.143E-05	0.00158927	-2.36418	2500.79
Latent Heat of Steam	L1	calc	2346.312257	kJ/kg	saturated	-6.143E-05	0.00158927	-2.36418	2500.79
Entropy of Steam	SA	calc	6.648881197	kJ/kg					
PROCESS			2						
Entrainment, Mixing and Compression									
Nozzle Exit assuming Isentropic Expansion - Condition B and B'					Khurmi & Gupta pp405				
ASSUME Nn =0.88, Ne = 0.65, Nc = 0.8, STEAM IS 92% DRY									
	hB	calc	1872.750771	kJ/kg					
For Nn = 0.88	hB'	calc	1942.779337	kJ/kg					
Dryness at B'	xB'	calc	0.767485323	dry					
Steam before entrainment - Condition D									
For Ne = 0.65									
Enthalpy of vapour at D	hD	calc	2174.550542	kJ/kg					
Dryness at D	xD	calc	0.861032682	dry					
Mixture before Shock - Condition E									
xE = 0.92									
Enthalpy at E	hE	calc	2320.646878	kJ/kg					
Entropy at E	SE	calc	8.237922441	kJ/kg					
Condenser Inlet - Condition F									
Liquid Enthalpy at F	hfF	calc	125.61	kJ/kg					
Latent Heat at F	hfgF	calc	2429.63622	kJ/kg	saturated	-6.143E-05	0.00158927	-2.36418	2500.79
Enthalpy at vapour F	hF	calc	2555.24622						
Entropy at fluid F	SfF	calc	0.46010989	kJ/kg					
Entropy of Vapour F	SfgF	calc	7.658741298	kJ/kg					
dryness at F	xF	calc	1.015547105	dry					
Nc = 0.8									
Enthalpy at F'	hF'	calc	2613.896055	kJ/kg					
Entrainment Ratio ms/me	W	calc	2.33501824	Ratio					
Entrainment Ratio me/ms (inverse)	w	calc	0.428262179	Ratio					
Mass of Motive Steam	ms	calc	0.000291948	kg/sec					
Mass of Entrainment	me	calc	0.00012503	kg/sec					
Minimum Recirculation flow		calc	0.005148033	kg/sec					
Velocity in 10mm recirc tube		calc	0.065546796	m/sec					
Enthalpy of Entrainment	hC	calc	2661.784489	kJ/kg					
Heat Removed	Re	calc	0.317098081	kJ/sec					
Enthalpy of flash water	hfG	calc	125.61	kJ/kg					
COP		calc	0.438073541	: : 1					

PROCESS			3						
Flash Vapour Generation									
Flash Water Temperature		calc	9.857154006	C	condenser temp				
R Evaporator Pressure		calc	1.209394782	kPa	Calc	8.07131	1730.63	233.426	
Enthalpy of Dry Vapour		calc	2518.853398	kJ/kg	sat	-6.143E-05	0.00158927	-2.36418	2500.79
Latent Heat	hfgB	calc	2477.581494	kJ/kg	saturated	-6.143E-05	0.00158927	-2.36418	2500.79
Enthalpy of fluid	hfB	calc	41.27190382	kJ/kg					
Entropy of fluid	SfB	calc	0.151179135	kJ/kg					
Entropy of Vapour	SfgB	calc	8.789938376	kJ/kg					
Dryness of expanded vap		calc	0.739220434	dry					
Enthalpy of Wet vapour		calc	1852.478867	kJ/kg					

PROCESS								
Ejector Operation								
Vapour Pressure	Pp	calc	21.56519745	kPa	Calc	8.07131	1730.63	233.426
Isentropic Index	n	calc	1.037393425	Index				
Nozzle Efficiency	Nn	assumed	0.88	Assumed				
Target nozzle outlet P	Pe	target	3.993490463	kPa				
Nozzle Outlet Velocity	**Mp2**	**calc**	**3.330174698**	Mach				
Entrainment Velocity	**Mpe**	**calc**	**2.21450389**	Mach				
Nozzle outlet - Critical	M*p2	calc	3.058956381	Mach				
Entrainment - Critical	M*e2	calc	2.139190171	Mach				
Shock zone - Critical	M*4	calc	2.005589685	Mach				
Shock zone upstream velocity	M4	calc	5.123655539	Mach				
Velocity after compression	M5	calc	0.054779879	Mach				
Pressure ratio across shock wave	P5/P4	calc	28.14587311	Ratio				
CP process	P2=P3=P4	calc	3.993490463	kPa				
Pressure at end of mixing zone	P5	calc	28.14587311	kPa				
Pressure ratio across divergence	Pc/P5	calc	1.001245966	Ratio				
System pressure before condenser	Pc	calc	28.18094192	kPa				
Compression Ratio	Pc/Pe	calc	23.30168969	Ratio	Choked > 1.8			
Vapour Gas Constant	Rp	constant	461.526	kJ/kg				
Area of Throat	A1	calc	9.22736E-06	m^2				
Diameter of throat	**D1**	**calc**	**0.00342763**	**m**		**2.0mm**		
Area Ratio mixer to throat	A1/A3	calc	0.475393249	Ratio	A1/A3 Correlation			
Area of mixer	A3	calc	1.941E-05	m^2				
Diameter of mixer	**D3**	**calc**	**0.00497127**	**m**		**8.0mm**		
Area Ratio nozzle outlet to throat	A2/A1	calc	1.011097557	Ratio	A2/A1 Correlation			
Nozzle Outlet Area	A2	calc	9.32977E-06	m^2				
Nozzle Outlet Diameter	**D2**	**calc**	**0.003446596**	**m**		**4.0mm**		

PROCESS			4					
Condensation	Model Condenser capable of absorbing all heat without significant temp rise							
Total heat added to system		calc	1002.098081	Joule/sec				
Total mass flow to condenser		calc	0.000416978	kg/sec				
Enthalpy of condensate		calc	125610	Joule/kg				
Heat in Condensate		calc	52.37655307	Joule/sec				
Heat Rejection Rate		calc	949.7215283	Joule/sec				
Condenser Pressure		calc	4.231675277	kPa	Calc	8.07131	1730.63	233.426

Process									
Psychometry and Water Collection									
Vapour Saturation Pressure	Pws	calc	42.43490463	HPa		6.116441	7.591386	240.7263	
Vapour Pressure	Pw	calc	12.73047139	HPa					
Dewpoint Temperature Required	Td	calc	10.53674638	C					
Evaporator Internal Pressure Required	Pc	calc	1.209394782	kPa		a	b	c	
Evaporator Core Temperature	Tc	calc	9.857154006	C		8.07131	1730.63	233.426	
Maximum water production	mw	calc	0.000126134	kg/sec		-6.143E-05	0.00158927	-2.36418	2500.79
Water production/solar day	mw/SD	calc	2.724498224	kg/SD					
Exceed Dewpoint	delta Td	calc	-0.679592374	C	(-) = BELOW DEWPOINT				

Attachment 6

Instrumentation Data Sheets

EasyLog EL-USB-TC Thermocouple Logger

EL-USB-TC

K, J & T-Type Thermocouple Data Logger

- Compatible with K, J and T type thermocouples with miniature thermocouple plug connection
- Stores over 32,000 readings
- EasyLog software available as a free download
- Supplied with 1.5m K-type thermocouple probe with 0 to 200°C (32 to 392°F) measurement range
- Logging rates between 1 second and 12 hours
- Immediate and delayed logging start
- User-programmable alarm thresholds
- Status indication via red and green LEDs

This standalone data logger measures and stores more than 32,000 temperature readings from a J, K or T-type thermocouple at a resolution of 0.5°C (1°F). It comes supplied with a K-type thermocouple capable of measuring from 0 to +200°C (32 to +392°F).

Your application will determine which probe is most suitable based on temperature range, accuracy, form and price. A wide variety of alternative thermocouples are available. Please call Lascar for vendor recommendations.

The user can easily set up the logger and view downloaded data by plugging the data logger into a PC's USB port and using the free EasyLog software. Data can then be graphed, printed and exported to other applications for detailed analysis.

The data logger is supplied with a lithium metal battery which typically gives 2 years' logging life.

SPECIFICATIONS

Probe measurement range	0 to 200°C (32 to 392°F) K type (supplied) -200 to +1350°C (-328 to +2462°F) K type -200 to +1190°C (-328 to +2174°F) J type -200 to +390°C (-328 to +734°F) T type
Internal resolution	0.5°C (1°F)
Accuracy (overall error)	±1°C (±2°F) (data logger only - thermocouple error not included)
Logging rate	User selectable between 1 second & 12 hours
Operating temperature range	-10 to +40°C (-14 to +104°F) (data logger only)
Battery Life	2 years (at 25°C and 1 minute logging rate)
Readings	32,510
Dimensions	118 x 27 x 27mm (4.64 x 1.06 x 1.06")

ACCESSORIES

BAT 3V6 1/2AA	Replacement battery
K-TYPE PROBE 1M5	Replacement K-type thermocouple probe
EL-DataPad	Handheld datalogger programmer & collector

INCLUDED IN THE BOX

BAT 3V6 1/2AA	Battery
K-TYPE PROBE 1M5	K-type thermocouple probe
EL-USB WALL BRACKET	Mounting Bracket

CALIBRATION CERTIFICATES NOW AVAILABLE

Lascar now offers a Traceable Calibration Certificate Service on Temperature Data Loggers. Using reference equipment which has been calibrated by a UKAS/NIST accredited laboratory and using apparatus traceable to national or international standards. For more information, please see **www.lascarelectronics.com.**

SICK AG **Type PBT Pressure Transducer**

A GENUINELY TALENTED ALL-ROUNDER

Product description

The PBT is a universal electronic pressure transmitter used in general industrial applications for pressure measurement of liquid and gaseous fluids. Suitable for standard measuring applications in machine and plant engineering, pressure control systems, hydraulics, pneumatics, etc., it supports a wide variety of configurations. and can thus provide the perfect match for individual customer requirements. Its precise and rugged measurement technology, compact dimensions, and quick and simple installation set the PBT apart as a genuinely talented all-rounder.

At a glance

- Pressure measurement ranges from 0 bar ... 1 bar up to 0 bar ... 600 bar
- Relative, absolute, and ± measuring ranges
- Large number of process connections available
- No mechanical moving parts. Hence no wear, fatigue, or maintenance
- Circularly welded, hermetically sealed stainless steel membrane
- Output signal 4 mA ... 20 mA, 0 V ... 5 V or 0 V ... 10 V
- Electrical connection M12 x 1, angled plug (acc. to DIN 175301-803 A) or cable connection

Your benefits

- Compact size takes up less space
- Simple and cost-saving installation
- Available in a wide selection of configurations, enabling a perfect match to individual customer requirements
- Robust design enables higher reliability
- Excellent price/performance ratio

Additional information

→ www.sick.com/PBT

For more information, simply enter the link or scan the QR code and get direct access to technical data, CAD design models, operating instructions, software, application examples, and much more.

8013160/2017-08-02
Subject to change without notice

Detailed technical data

Features

Medium	Liquid, gaseous
Pressure units	Bar, MPa, psi and kg/cm²
Measuring ranges	
Gauge pressure	0 bar ... 1 bar up to bar ... 600 bar
Absolute pressure	0 bar ... 1 bar up to 0 bar ... 25 bar
Compound pressure	–1 bar ... 0 bar up to –1 bar ... +24 bar
Process temperature	0 °C ... +80 °C, –40 °C ... +100 °C optional
Analog signal output and ohmic load R_A	4 mA ... 20 mA, 2-wire ($R_A \leq (L^+ - 8\ V) / 0.02\ A\ [Ohm]$) 0 V ... 10 V, 3-wire ($R_A > 10$ kOhm) 0 V ... 5 V, 3-wire ($R_A > 5$ kOhm)

Performance

Non-linearity	≤ ± 0.5 % of span (Best Fit Straight Line, BFSL) according to IEC 61298-2 ≤ ± 0.25 % of span (Best Fit Straight Line, BFSL) according to IEC 61298-2 optional Adjusted in vertical mounting position with pressure connection facing downwards
Accuracy	≤ ± 0.5 % of the span (with non-linearity 0.25 %) ≤ ± 0,6 % of Span (with non-linearity 0.25 % and with signal output 0 ... 5 V) ≤ ± 1,0 % of Span (with non-linearity 0.5 %) Including non-linearity, hysteresis, zero point and full scale error (corresponds to error of measurement as per IEC 61298-2)
Adjustment accuracy of zero signal	≤ 0.15 % of span typ., ≤ 0.4 % of span max. (with non-linearity 0.25 %) ≤ 0.5 % of span typ., ≤ 0.8 % max. % of span (with non-linearity 0.5 %)
Hysteresis	≤ 0.16 % of the span
Non-repeatability	≤ 0.1 % of the span
Response time	< 4 ms
Signal noise	≤ 0.3 % of the span
Long-term drift/one-year stability	≤ 0.1 % of span to IEC 61298-2
Temperature error	≤ 1.0 % of span typ., ≤ 2.5 % of span max.
Rated temperature range	0 °C ... +80 °C
Service life	Minimum 100 Mio. life cycles

Mechanics/electronics

Process connection	See type code
Wetted parts	Pressure Connection: stainless steel 316L Pressure sensor: stainless steel 316L (for measurement ranges from 0 bar ... 10 bar rel stainless steel 13-8 PH)
Internal transmission fluid	Silicone oil (only with pressure ranges < 0 bar ... 10 bar and ≤ 0 bar abs ... 25 bar abs)
Pressure peak dampening	Through integrated pressure port 0.6 mm or 0.3 mm for process connection G ¼ according to DIN 3852-E (0.3 mm at and above 10 bar)
Pressure port	3.5 mm (standard)
Housing material	Stainless steel 316L
Electrical connection/enclosure rating	Round connector M12 x 1, 4-pin, IP67 [1] L-connector (DIN EN 175301-803 A), IP65 [1] Flying leads 2 m / 5 m, IP67 [1]
Supply voltage	8 V DC ... 35 V DC with output signal 4 mA ... 20 mA and 0 V ... 5 V 14 V DC ... 35 V DC with output signal 0 V ... 10 V [2]

[1] Enclosure rating IP per IEC 60529. The enclosure rating classes specified only apply when connected with female connectors that provide the corresponding enclosure rating.

[2] The pressure transmitter must be supplied with power by a limited energy circuit compliant with 9.3 of UL/EN/IEC 601010-1 or LPS to UL/EN/IEC 60950-1 or Class 2 to UL 1310/UL1585 (NEC or CEC). The power supply must be suitable for operation above 2,000 m if the pressure transmitter is used above this altitude.

EL-USB-4

4-20mA Current Loop Data Logger

- 4-20mA d.c. current loop measurement range
- Stores over 32,000 readings
- Logging rates between 1 second and 12 hours
- Connection via two screw terminals
- Immediate and delayed logging start
- User-programmable alarm thresholds
- Status indication via red and green LEDs
- EasyLog software available as a free download.

This stand-alone data logger measures and stores over 32,000 current loop readings over a 4-20mA d.c. range at a resolution of 0.05mA d.c.

The user can easily set up the logger and view downloaded data by plugging the data logger into a PC's USB port and using the available free downloadable EasyLog software. Data can then be graphed, printed and exported to other applications.

The data logger is delivered complete with a lithium metal battery, which gives three year's logging life. The data logger is also issued with a 4-20mA cap featuring a pair of screw terminals and measurement leads terminating in crocodile clips.

EL-WIN-USB

Lascar's EasyLog control software is available as a free download from www.easylogusb.com. Easy to install and use, the control software is compatible with 32-bit and 64-bit versions of Windows 7, 8 and 10. The software is used to set up the logger, download, graph and annotate data or export in Excel, PDF and jpeg formats.

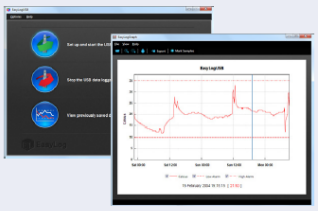

The software allows the following parameters to be configured:

- Logger name
- Logging rate (user selectable between 1 seconds and 12 hours)
- High and low alarms
- Immediate and delayed logging start

Download the latest version of the software free of charge from www.lascarelectronics.com/software/easylog-usb

SPECIFICATIONS

Measurement range	4 to 20mA d.c.
Internal resolution	0.05mA d.c.
Accuracy (overall error)	±1%
Logging rate	User selectable between 1 second & 12 hours
Operating temperature range	-35 to +80°C (-31 to +176°F)
Battery Life	3 years (at 25°C and 2 second logging rate)
Readings	32,510
Dimensions	98 x 26.8 x 26.8 mm (3.85 x 1.05 x 1.05")

ACCESSORIES

BAT 3V6 1/2AA	Replacement battery
USB-CAP-4-20	Replacement Cap

INCLUDED IN THE BOX

BAT 3V6 1/2AA	Battery
USB-CAP-4-20	**4-20mA Range** Cap
EL-USB WALL BRACKET	Mounting Bracket
EL-USB-LEADS	Measurement Leads

5.

Apogee Instruments Pyranometer SP-110

Silicon-cell Pyranometers | SP-100 and SP-200 Series

Accurate and stable global shortwave radiation measurement

Accurate, Stable Measurements
Calibration in controlled laboratory conditions is traceable to the World Radiometric Reference in Davos, Switzerland. Pyranometers are cosine-corrected with directional errors less than ± 5 % at a solar zenith angle of 75°. Long-term non-stability determined from multiple replicate pyranometers in accelerated aging tests and field conditions is less than 2 % per year.

Rugged, Self-cleaning Head
Patented domed shaped sensor head (diffuser and body) facilitate runoff of dew and rain to keep the diffuser clean and minimize errors caused by dust blocking the radiation path. Sensors are housed in a rugged anodized aluminum body and electronics are fully potted.

Heated Option
A heated pyranometer (SP-230 All-season) is available with a 0.2 W heater to keep water (liquid and frozen) off the sensor and minimize errors caused by dew, frost, rain, or snow blocking the optical path.

Output Options
Multiple analog output options are available including: 0 to 350 mV, 0 to 2.5 V, 0 to 5.0 V, and 4 to 20 mA ranges. The silicon-cell pyranometer is also available attached to a hand-held meter with digital readout.

Typical Applications
Applications include shortwave radiation measurement in agricultural, ecological, and hydrological weather networks and solar panel arrays.

6.

Monarch Track-It Voltage Logger

Track-It™
DC Voltage and Current Data Loggers

Description

The Track-It™ DC Voltage and Current Data Loggers are two channel battery powered stand alone compact data loggers that record up to 64,000 samples each of DC Voltage or Current data. Units are available in 4 DC voltage ranges or for DC current. The unit is easily set up using the included Track-It™ Software. Simply plug the logger into an open USB port on your PC and the software automatically identifies the logger. Configure the unit to start and stop recording at a predetermined time and date or only when an alarm condition is sensed. The sample storage rate can be set from 1 sample every 2 seconds up to 1 sample every 24 hours. The on board data storage is non-volatile so data will not be lost in the event of a depleted battery. The Track-It™ DC Voltage and Current Loggers

can also be used to record ambient temperature if one or neither input is being used. Information displayed on the LCD is also user programmable and can be sequenced by pressing the logger button. A multicolored LED indicator notifies the user of alarms, or general activity.

Features

- Push button or program to start recording
- Up to 64,000 samples per record
- 500mVDC, 1VDC, 5VDC, 10VDC, or 20mA
- +/- .5% accuracy
- Alarm set points
- Small compact size
- N.I.S.T. calibration available
- Integral USB interface (no custom cable!)
- Interactive software (included!)
- One year battery life (battery included!)
- Optional three year battery life
- High accuracy and repeatability
- Accurate internal clock (1 minute/year)
- Multiple user programmable displays

Typical Uses

- Industrial process
- Troubleshooting
- Productivity monitoring
- Remote indication

Ordering Information

Model	Description	Part Number
Analog 500mV Track-It	Logger with display, 500 mV module and standard battery	5396-0511
Analog 1V Track-It	Logger with display, 1 Volt module and standard battery	5396-0512
Analog 5V Track-It	Logger with display, 5 Volt module and standard battery	5396-0513
Analog 10V Track-It	Logger with display, 10 Volt module and standard battery	5396-0514
Analog 20mA Track-It	Logger with display, 20 mA module and standard battery	5396-0515
Analog 500mV Track-It LB	Logger with display, 500 mV module and long life battery	5396-0521
Analog 1V Track-It LB	Logger with display, 1 Volt module and long life battery	5396-0522
Analog 5V Track-It LB	Logger with display, 5 Volt module and long life battery	5396-0523
Analog 10V Track-It LB	Logger with display, 10 Volt module and long life battery	5396-0524
Analog 20mA Track-It LB	Logger with display, 20 mA module and long life battery	5396-0525
NIST Analog	Logger with NIST calibration certificate	5396-05-xxCAL

MONARCH INSTRUMENT

CE

ExTech **Temperature, RH and Dew-point Loggers**

EXTECH INSTRUMENTS

Experience the Extech Advantage

PRODUCT DATASHEET

Humidity and Temperature USB Datalogger

Records up to 16,000 readings for each parameter

Datalogs 16,000 Humidity and 16,000 Temperature readings with a user programmable sample rate

Features:

- Datalogs 32,000 readings (16,000 for each parameter: Humidity/Temperature)
- Dew point indication via Windows® software (included)
- RHT10-SW optional software to calculate Grains per Pound (grams per kilogram) to 1120GPP (160g/kg)
- Selectable data sampling rate: 2s, 5s, 10s, 30s, 1m, 5m, 10m, 30m, 1hr, 2hr, 3hr, 6hr, 12hr, 24hr
- User-programmable alarm thresholds for RH and Temperature
- Status Indication via Red/Yellow LED and Green LED
- Long battery life (approx. 1 year)
- Complete with 3.6V Lithium battery and Windows® 98, 2000, XP, Vista, 7, 8 and 10 compatible analysis software

Monitors Humidity and Temperature levels in warehouse, storage rooms, freezers, shipping vans, and water damage restoration

USB connector easily plugs into a computer for data analysis of Temperature and Humidity

Specifications	Range	Resolution	Accuracy (%rdg+digits)
Temperature	-40 to 158°F	0.1°F/°C	±1.8°F (14 to 104°F)
			±3.6°F (-40 to +14 and 104 to 158°F)
	-40 to 70°C		±1.0°C (-10 to 40°C)
			±2.0°C (-40 to -10 and +40 to 70°C)
Humidity	0 to 100%RH	0.1%RH	±3%RH
Datalogging interval	2 seconds to 24 hours		
Memory	Temperature: 16,000 points; Relative Humidity: 16,000 points		
Dimensions	5.1 x 1.1 x 0.98" (130 x 30 x 25mm)		
Weight	1oz (20g)		

Ordering Information:

RHT10 .....Humidity and Temperature USB Datalogger
RHT10-SW ....GPP (g/kg) Software for RHT10
42299 .....3.6V Lithium Batery (pkg of 2)

CE

www.extech.com

12/2/15 - R2

EXTECH INSTRUMENTS
A FLIR COMPANY

Experience the Extech Advantage

PRODUCT DATASHEET

Humidity/Temperature/Pressure Datalogger

Records Humidity, Temperature and Atmospheric Pressure

Datalogs up to 10,000 readings with a user programmable sample rate

Features:

- USB interface for easy set-up and data download
- Selectable Atmospheric Pressure Units: psi, hPa, kPa, and bar
- Selectable data sampling rate from 1 minute to 18 hours
- User-programmable Min/Max alarm thresholds
- Manual and Programmable start modes
- Status Indication via Red/Yellow LED and Green LED
- Long battery life
- Complete with 3.6V Lithium battery, mounting bracket, and Windows®98, 2000, XP, and Vista compatible analysis software

Monitors Humidity, Temperature and Air Pressure levels in clean rooms, warehouses, storage rooms, freezers, shipping vans, and water damage restoration

USB connector easily plugs into a computer for data analysis

Specifications	Range	Resolution	Accuracy (%rdg+digits)
Temperature	-40 to 158°F	0.1°F/°C	±1.8°F (14 to 104°F)
			±3.6°F (-40 to +14 and 104 to 158°F)
	-40 to 70°C		±1.0°C (-10 to 40°C)
			±2.0°C (-40 to -10 and +40 to 70°C)
Humidity	0 to 100%RH	0.1%RH	±3.5%RH
Air Pressure	13.7 to 15.2psi	0.1psi	
	950 to 1050hPa	0.1hPa	
	95 to 105kPa	0.1kPa	
	0.9 to 1.0bar	0.1bar	
Datalogging interval	1 minute to 18 hours		
Memory	10,000 points		
Dimensions	5.1 x 1.1 x 0.98" (130 x 30 x 25mm)		
Weight	1oz (20g)		

Ordering Information:

RHT50 .....Humidity/Temperature/Pressure Datalogger
42299 .....3.6V Lithium Batery (pkg of 2)

CE

www.extech.com

9/16/11 - R1

ATTACHMENT 7

TEST DATA IN ENGINEERING UNITS

TEST DATA IN ENGINEERING UNITS

Table 7.1.1 Emissivity Test

Date 5 October 2016
Sample Start 10:00
Sample End 13:15

T (plate)	Qi (Horizontal)	Qi (module)	Qt	Emissivity
C	Watt	Watt	Watt	
80.5	617.5	789.78	887.47	0.89
81	698.5	893.38	892.49	1.00
81.5	853	1090.99	897.54	1.22
81.5	667.5	853.73	897.54	0.95
82	489	625.43	902.62	0.69
82	695.5	889.54	902.62	0.99
82	789	1009.13	902.62	1.12
82.5	553.5	707.93	907.71	0.78
82.5	527	674.03	907.71	0.74
82.5	531.5	679.79	907.71	0.75
82.5	419.5	536.54	907.71	0.59
82	406	519.27	902.62	0.58
82.5	387.5	495.61	907.71	0.55
82.5	377	482.18	907.71	0.53
82.5	384	491.14	907.71	0.54
82.5	378.5	484.10	907.71	0.53
82	382	488.58	902.62	0.54
82	408	521.83	902.62	0.58
82	421.5	539.10	902.62	0.60
81.5	496.5	635.02	897.54	0.71
82	575	735.43	902.62	0.81
82	752.5	962.45	902.62	1.07
82.5	930	1189.47	907.71	1.31
83	923	1180.52	912.82	1.29
83	922	1179.24	912.82	1.29
83	783.5	1002.10	912.82	1.10
83.5	687	878.67	917.96	0.96
83.5	647	827.51	917.96	0.90
83.5	565.5	723.27	917.96	0.79
83.5	592	757.17	917.96	0.82

84	693.5	886.99	923.12	0.96
84.5	720.5	921.52	928.30	0.99
84.5	599.5	766.76	928.30	0.83
85	650.5	831.99	933.50	0.89
85	730	933.67	933.50	1.00
85	714	913.21	933.50	0.98
85.5	738.5	944.54	938.72	1.01
86	792	1012.97	943.97	1.07
86	959	1226.56	943.97	1.30
86	961	1229.12	943.97	1.30
86.5	911	1165.17	949.23	1.23
86.5	844.5	1080.12	949.23	1.14
87	985.5	1260.45	954.52	1.32
87.5	936.5	1197.78	959.83	1.25
88	748.5	957.33	965.17	0.99
88.5	700	895.30	970.52	0.92
89	563	720.08	975.90	0.74
89	570.5	729.67	975.90	0.75
89	648.5	829.43	975.90	0.85
89.5	842.5	1077.56	981.30	1.10
90	727.5	930.47	986.72	0.94
90	698.5	893.38	986.72	0.91
90	679.5	869.08	986.72	0.88
90	651.5	833.27	986.72	0.84
90	684.5	875.48	986.72	0.89
90.5	704.5	901.06	992.17	0.91
90.5	774	989.95	992.17	1.00
91	886	1133.19	997.63	1.14
91.5	863	1103.78	1003.12	1.10
92	783.5	1002.10	1008.64	0.99
92	899	1149.82	1008.64	1.14
92	952	1217.61	1008.64	1.21
92.5	942.5	1205.46	1014.17	1.19
93	926	1184.35	1019.73	1.16
93	937.5	1199.06	1019.73	1.18
94	884	1130.64	1030.91	1.10
94	770.5	985.47	1030.91	0.96
94.5	693	886.35	1036.54	0.86
94.5	848	1084.59	1036.54	1.05
95	935	1195.87	1042.19	1.15
95	926	1184.35	1042.19	1.14
95.5	923	1180.52	1047.86	1.13

96	919.5	1176.04	1053.56	1.12
96	917.5	1173.48	1053.56	1.11
96.5	914.5	1169.65	1059.28	1.10
96.5	910.5	1164.53	1059.28	1.10
97	907	1160.05	1065.02	1.09
97.5	902	1153.66	1070.78	1.08
98	897.5	1147.90	1076.57	1.07
98.5	894.5	1144.07	1082.38	1.06
98.5	890	1138.31	1082.38	1.05
99	885.5	1132.55	1088.22	1.04
99.5	883	1129.36	1094.08	1.03
99.5	880	1125.52	1094.08	1.03
100	875.5	1119.76	1099.96	1.02
100	842	1076.92	1099.96	0.98
100	832	1064.13	1099.96	0.97
100	862	1102.50	1099.96	1.00
100.5	859	1098.66	1105.87	0.99
101	856	1094.82	1111.80	0.98
101	854.5	1092.91	1111.80	0.98
101.5	850	1087.15	1117.75	0.97
101.5	849	1085.87	1117.75	0.97
102	847	1083.31	1123.73	0.96
102	847.5	1083.95	1123.73	0.96
102	846.5	1082.67	1123.73	0.96
102	848.5	1085.23	1123.73	0.97
102.5	848	1084.59	1129.73	0.96
102.5	848.5	1085.23	1129.73	0.96
103	846.5	1082.67	1135.76	0.95
102	846	1082.03	1123.73	0.96
101.5	845	1080.76	1117.75	0.97
101.5	831	1062.85	1117.75	0.95
101.5	836	1069.24	1117.75	0.96
100.5	835.5	1068.60	1105.87	0.97
100.5	840	1074.36	1105.87	0.97
102	841	1075.64	1123.73	0.96
105	841	1075.64	1160.10	0.93
105	840	1074.36	1160.10	0.93
102.5	837	1070.52	1129.73	0.95
101	834.5	1067.33	1111.80	0.96
100.5	834.5	1067.33	1105.87	0.97
102	835	1067.97	1123.73	0.95
104	836.5	1069.88	1147.88	0.93

104	839	1073.08	1147.88	0.93
104.5	838.5	1072.44	1153.98	0.93
104.5	815	1042.39	1153.98	0.90
104.5	816	1043.66	1153.98	0.90
103.5	798.5	1021.28	1141.81	0.89
103.5	801	1024.48	1141.81	0.90
103	819	1047.50	1135.76	0.92
100	805.5	1030.23	1099.96	0.94
103	807	1032.15	1135.76	0.91
103.5	825.5	1055.81	1141.81	0.92
103	841.5	1076.28	1135.76	0.95
104	837.5	1071.16	1147.88	0.93
103.5	838	1071.80	1141.81	0.94
103.5	834.5	1067.33	1141.81	0.93
103	833	1065.41	1135.76	0.94
102	833.5	1066.05	1123.73	0.95
98.5	832	1064.13	1082.38	0.98
97.5	835.5	1068.60	1070.78	1.00
96	844	1079.48	1053.56	1.02
103	848	1084.59	1135.76	0.95
104	847	1083.31	1147.88	0.94
103.5	842	1076.92	1141.81	0.94
103.5	842	1076.92	1141.81	0.94
103.5	822	1051.34	1141.81	0.92
104	805	1029.60	1147.88	0.90
103.5	796	1018.08	1141.81	0.89
104	794	1015.53	1147.88	0.88
103	762	974.60	1135.76	0.86
103	825.5	1055.81	1135.76	0.93
104	833	1065.41	1147.88	0.93
104.5	833.5	1066.05	1153.98	0.92
104	832.5	1064.77	1147.88	0.93
104	831	1062.85	1147.88	0.93
103	828	1059.01	1135.76	0.93
101	825	1055.18	1111.80	0.95
99	824	1053.90	1088.22	0.97
99	823.5	1053.26	1088.22	0.97
104	823.5	1053.26	1147.88	0.92
104.5	824.5	1054.54	1153.98	0.91
104	822	1051.34	1147.88	0.92
104.5	820	1048.78	1153.98	0.91
103.5	822.5	1051.98	1141.81	0.92

104	824	1053.90	1147.88	0.92
103.5	821.5	1050.70	1141.81	0.92
103	821	1050.06	1135.76	0.92
101.5	825.5	1055.81	1117.75	0.94
99.5	826	1056.45	1094.08	0.97
98.5	824	1053.90	1082.38	0.97
98	823.5	1053.26	1076.57	0.98
97.5	822	1051.34	1070.78	0.98
98	821	1050.06	1076.57	0.98
98	819	1047.50	1076.57	0.97
98	820.5	1049.42	1076.57	0.97
99.5	823.5	1053.26	1094.08	0.96
98.5	825	1055.18	1082.38	0.97
99	824	1053.90	1088.22	0.97
100.5	822.5	1051.98	1105.87	0.95
101	820.5	1049.42	1111.80	0.94
104	820	1048.78	1147.88	0.91
103.5	819.5	1048.14	1141.81	0.92
104	820	1048.78	1147.88	0.91
104	820.5	1049.42	1147.88	0.91
103.5	821	1050.06	1141.81	0.92
101.5	822.5	1051.98	1117.75	0.94
100	823.5	1053.26	1099.96	0.96
102	821.5	1050.70	1123.73	0.94
103	821.5	1050.70	1135.76	0.93
102	825	1055.18	1123.73	0.94
101.5	826	1056.45	1117.75	0.95
100.5	826.5	1057.09	1105.87	0.96
99	828.5	1059.65	1088.22	0.97
96.5	829	1060.29	1059.28	1.00
95.5	830	1061.57	1047.86	1.01
98.5	828.5	1059.65	1082.38	0.98
96	827.5	1058.37	1053.56	1.00
96.5	827	1057.73	1059.28	1.00
103.5	827	1057.73	1141.81	0.93
101	827.5	1058.37	1111.80	0.95
103.5	828	1059.01	1141.81	0.93
103	827	1057.73	1135.76	0.93
101.5	827	1057.73	1117.75	0.95
101	827.5	1058.37	1111.80	0.95
98.5	828	1059.01	1082.38	0.98
103.5	827.5	1058.37	1141.81	0.93

103	829.5	1060.93	1135.76	0.93
102	829.5	1060.93	1123.73	0.94
102.5	830.5	1062.21	1129.73	0.94
102.5	829.5	1060.93	1129.73	0.94
102.5	829	1060.29	1129.73	0.94
103	828	1059.01	1135.76	0.93
103	826.5	1057.09	1135.76	0.93
103	827	1057.73	1135.76	0.93
103.5	824.5	1054.54	1141.81	0.92
103	826	1056.45	1135.76	0.93
102.5	826	1056.45	1129.73	0.94
102.5	828	1059.01	1129.73	0.94
102	830	1061.57	1123.73	0.94
103	830	1061.57	1135.76	0.93
103.5	827.5	1058.37	1141.81	0.93
102.5	827.5	1058.37	1129.73	0.94
102	826	1056.45	1123.73	0.94
102	826	1056.45	1123.73	0.94
102	826	1056.45	1123.73	0.94
100	825.5	1055.81	1099.96	0.96
101.5	826.5	1057.09	1117.75	0.95
103.5	827	1057.73	1141.81	0.93
103	827.5	1058.37	1135.76	0.93
103	827	1057.73	1135.76	0.93
102	826.5	1057.09	1123.73	0.94
103	827	1057.73	1135.76	0.93
101	826.5	1057.09	1111.80	0.95
101.5	826.5	1057.09	1117.75	0.95
101.5	826	1056.45	1117.75	0.95
102	828	1059.01	1123.73	0.94
103.5	829.5	1060.93	1141.81	0.93
103.5	829	1060.29	1141.81	0.93
104	831	1062.85	1147.88	0.93
102.5	828.5	1059.65	1129.73	0.94
102.5	828.5	1059.65	1129.73	0.94
103	828	1059.01	1135.76	0.93
103	827	1057.73	1135.76	0.93
102.5	828.5	1059.65	1129.73	0.94
103	828.5	1059.65	1135.76	0.93
102.5	830	1061.57	1129.73	0.94
102.5	831	1062.85	1129.73	0.94
102	833	1065.41	1123.73	0.95

102.5	831.5	1063.49	1129.73	0.94
102.5	832	1064.13	1129.73	0.94
102.5	831.5	1063.49	1129.73	0.94
102	830.5	1062.21	1123.73	0.95
103	829.5	1060.93	1135.76	0.93
102.5	828.5	1059.65	1129.73	0.94
102	828.5	1059.65	1123.73	0.94
103.5	828	1059.01	1141.81	0.93
102	826	1056.45	1123.73	0.94
102.5	826	1056.45	1129.73	0.94
103	826	1056.45	1135.76	0.93
102.5	826	1056.45	1129.73	0.94
102.5	826.5	1057.09	1129.73	0.94
103	828	1059.01	1135.76	0.93
102.5	830	1061.57	1129.73	0.94
102	830.5	1062.21	1123.73	0.95
102	829.5	1060.93	1123.73	0.94
103	827	1057.73	1135.76	0.93
102.5	829.5	1060.93	1129.73	0.94
103	829.5	1060.93	1135.76	0.93
103.5	830.5	1062.21	1141.81	0.93
103.5	831	1062.85	1141.81	0.93
104	829.5	1060.93	1147.88	0.92
103	829	1060.29	1135.76	0.93
102.5	829.5	1060.93	1129.73	0.94
102.5	829	1060.29	1129.73	0.94
101.5	827	1057.73	1117.75	0.95
102.5	826.5	1057.09	1129.73	0.94
102.5	824.5	1054.54	1129.73	0.93
103.5	823.5	1053.26	1141.81	0.92
103.5	825	1055.18	1141.81	0.92
103.5	824	1053.90	1141.81	0.92
102.5	824.5	1054.54	1129.73	0.93
103.5	825.5	1055.81	1141.81	0.92
103	826	1056.45	1135.76	0.93
103	826	1056.45	1135.76	0.93
103	823.5	1053.26	1135.76	0.93
102.5	820	1048.78	1129.73	0.93
101.5	822.5	1051.98	1117.75	0.94
102	823.5	1053.26	1123.73	0.94
103.5	821	1050.06	1141.81	0.92
103	820.5	1049.42	1135.76	0.92

103	820	1048.78	1135.76	0.92
102.5	820.5	1049.42	1129.73	0.93
102	821.5	1050.70	1123.73	0.94
102	820.5	1049.42	1123.73	0.93
102	821	1050.06	1123.73	0.93
101.5	820.5	1049.42	1117.75	0.94
101.5	820	1048.78	1117.75	0.94
99.5	820.5	1049.42	1094.08	0.96
102.5	819	1047.50	1129.73	0.93
103	816.5	1044.30	1135.76	0.92
102.5	819	1047.50	1129.73	0.93
102	816	1043.66	1123.73	0.93
102.5	814.5	1041.75	1129.73	0.92
102	815.5	1043.02	1123.73	0.93
102	817	1044.94	1123.73	0.93
101	817	1044.94	1111.80	0.94
102	816	1043.66	1123.73	0.93
100.5	816	1043.66	1105.87	0.94
101.5	814	1041.11	1117.75	0.93
102	813	1039.83	1123.73	0.93
102	812.5	1039.19	1123.73	0.92
102	815.5	1043.02	1123.73	0.93
102	815	1042.39	1123.73	0.93
100	813	1039.83	1099.96	0.95
98.5	814	1041.11	1082.38	0.96
102	813.5	1040.47	1123.73	0.93
102	814	1041.11	1123.73	0.93
102	812	1038.55	1123.73	0.92
101	810	1035.99	1111.80	0.93
101	810.5	1036.63	1111.80	0.93
100.5	811.5	1037.91	1105.87	0.94
101.5	811.5	1037.91	1117.75	0.93
102	811	1037.27	1123.73	0.92
103	809	1034.71	1135.76	0.91
102.5	809	1034.71	1129.73	0.92
101	810.5	1036.63	1111.80	0.93
99.5	810.5	1036.63	1094.08	0.95
95.5	812	1038.55	1047.86	0.99
92.5	811.5	1037.91	1014.17	1.02
91	809	1034.71	997.63	1.04
101	808.5	1034.07	1111.80	0.93
102	806	1030.87	1123.73	0.92

102.5	805.5	1030.23	1129.73	0.91
103	806	1030.87	1135.76	0.91
103.5	807	1032.15	1141.81	0.90
101	806.5	1031.51	1111.80	0.93
98.5	806	1030.87	1082.38	0.95
94	806	1030.87	1030.91	1.00
92	806	1030.87	1008.64	1.02
91	804.5	1028.96	997.63	1.03
90	803.5	1027.68	986.72	1.04
88	801	1024.48	965.17	1.06
86.5	803.5	1027.68	949.23	1.08
85	804	1028.32	933.50	1.10
101	800.5	1023.84	1111.80	0.92
103.5	800	1023.20	1141.81	0.90
103	801	1024.48	1135.76	0.90
101.5	799.5	1022.56	1117.75	0.91
100	799.5	1022.56	1099.96	0.93
98	799	1021.92	1076.57	0.95
93	797.5	1020.00	1019.73	1.00
92	797	1019.36	1008.64	1.01
91	795.5	1017.44	997.63	1.02
87.5	795	1016.81	959.83	1.06
86.5	794	1015.53	949.23	1.07
85	792.5	1013.61	933.50	1.09
84	794.5	1016.17	923.12	1.10
83.5	792.5	1013.61	917.96	1.10
82.5	791	1011.69	907.71	1.11
82.5	789	1009.13	907.71	1.11
82.5	788.5	1008.49	907.71	1.11
81.5	790.5	1011.05	897.54	1.13
81	792	1012.97	892.49	1.13
80.5	789	1009.13	887.47	1.14
80	787.5	1007.21	882.46	1.14
96.5	790	1010.41	1059.28	0.95
101	790.5	1011.05	1111.80	0.91
101	791	1011.69	1111.80	0.91
100.5	788	1007.85	1105.87	0.91
100.5	788.5	1008.49	1105.87	0.91
100	786	1005.29	1099.96	0.91
99.5	787.5	1007.21	1094.08	0.92
99	788	1007.85	1088.22	0.93
97	786.5	1005.93	1065.02	0.94

94	786	1005.29	1030.91	0.98
92	784.5	1003.38	1008.64	0.99
101	782	1000.18	1111.80	0.90
101	784.5	1003.38	1111.80	0.90
101.5	784	1002.74	1117.75	0.90
101	784.5	1003.38	1111.80	0.90
98.5	783	1001.46	1082.38	0.93
96.5	783	1001.46	1059.28	0.95
94	782.5	1000.82	1030.91	0.97
91.5	783.5	1002.10	1003.12	1.00
90	780.5	998.26	986.72	1.01
89.5	783	1001.46	981.30	1.02
88	781.5	999.54	965.17	1.04
85.5	783.5	1002.10	938.72	1.07
86.5	784.5	1003.38	949.23	1.06
87.5	751	960.53	959.83	1.00
85	721.5	922.80	933.50	0.99
83.5	605	773.80	917.96	0.84
Averages				
T (plate)	**Qi (Horizontal)**	**Qi (module)**	**Qt**	**Emissivity**
97.50	**801.13**	**1024.65**	**1073.17**	**0.96**

Table 7.1.2 Flowrate Results

Date 3 November 2017
Sample Start 10:00
Sample End 14:00

I (module)	T1	T2	Mass flow
Watt	°C	°C	kg/s
778	26.5	60	0.005325
779	26.5	62	0.005031
796	26.5	65	0.00474
817	27	65.5	0.004866
832	27	65	0.00502
840.5	27.5	66.5	0.004941
854	27.5	67	0.004957
850	27.5	73.5	0.004237
856	28	79	0.003848
865	28	83	0.003606
869	28.5	81.5	0.003759
868	29	92	0.003159
889	29	92	0.003235
898.5	29	93	0.003219
901	29.5	92	0.003305
905	29.5	93	0.003268
906.5	30	93	0.003299
915	30	92.5	0.003357
920.5	30	93	0.00335
925.5	30.5	93.5	0.003368
931	30.5	93.5	0.003388
934	30.5	93.5	0.003399
935	31	92	0.003514
937	31	93.5	0.003437
940.5	31.5	92	0.003564
936.5	31.5	93	0.003491
932	31.5	91.5	0.003561
929	31.5	92.5	0.003492
925.5	31.5	92.5	0.003479
922	32	92.5	0.003494
915.5	32	91.5	0.003528
911	32	92	0.003481
906.5	32.5	91	0.003553
903.5	32.5	70	0.005524
895	32.5	70.5	0.0054

885.5	32.5	71	0.005273
882	33	70.5	0.005393
871	33	70	0.005397
861	33	69.5	0.005409
853	33	65.5	0.006018
843	33.5	73.5	0.004832
836.5	33.5	77	0.004409
786.5	33.5	80	0.003878
815.5	33.5	74.5	0.00456
802.5	33.5	74.5	0.004488
786.5	33.5	75.5	0.004294
771.5	33.5	74	0.004368
756.5	34	68.5	0.005028
749	34	66.5	0.005284
Averages			
I (module)	**T1**	**T2**	**Mass flow**
Watt	**°C**	**°C**	**kg/s**
869.7857143	**30.7755102**	**80.6938776**	**0.00418**

Table 7.1.3 Near-Boiling Temperature Readings

Date 5 October 2016
Sample Start 10:53:30
Sample End 11:04:30

Date and Time dd/mm/yyyy hh:mm:ss	Temperature C
05/10/2016 10:53:30	97
05/10/2016 10:54:00	96
05/10/2016 10:54:30	95.5
05/10/2016 10:55:00	95.5
05/10/2016 10:55:30	95.5
05/10/2016 10:56:00	94.5
05/10/2016 10:56:30	94.5
05/10/2016 10:57:00	96
05/10/2016 10:57:30	99
05/10/2016 10:58:00	99
05/10/2016 10:58:30	96.5
05/10/2016 10:59:00	95
05/10/2016 10:59:30	94.5
05/10/2016 11:00:00	96
05/10/2016 11:00:30	98
05/10/2016 11:01:00	98
05/10/2016 11:01:30	98.5
05/10/2016 11:02:00	98.5
05/10/2016 11:02:30	98.5
05/10/2016 11:03:00	97.5
05/10/2016 11:03:30	97.5
05/10/2016 11:04:00	97
05/10/2016 11:04:30	94